

# MEDICAL JOURNAL

香港醫學雜誌

The official publication of the  
Hong Kong Academy of Medicine and  
the Hong Kong Medical Association

22(3+4)

HONG KONG MEDICAL JOURNAL

香港醫學雜誌

Volume 22 Number 3 June 2016

## Research Fund for the Control of Infectious Diseases

### Research Dissemination Reports

### 控制傳染病研究基金

#### 研究成果報告

Respiratory Infectious Diseases  
呼吸道傳染病

Viral Hepatitis  
病毒性肝炎



# MEDICAL JOURNAL

香港醫學雜誌

**EDITOR-IN-CHIEF**

Ignatius TS Yu 余德新

**SENIOR EDITORS**

PT Cheung 張璧濤  
 Albert KK Chui 徐家強  
 Michael G Irwin  
 Martin CS Wong 黃至生  
 TW Wong 黃大偉

**EDITORS**

Gavin J Chan 陳慶釗  
 KL Chan 陳廣亮  
 KS Chan 陳健生  
 Henry LY Chan 陳力元  
 David VK Chao 周偉強  
 W Cheuk 卓華  
 TW Chiu 趙多和  
 Paul CL Choi 蔡祥龍  
 Stanley ST Choi 蔡兆堂  
 LW Chu 朱亮榮  
 Ellis KL Hon 韓錦倫  
 KW Huang 黃凱文  
 WK Hung 熊維嘉  
 Bonnie CH Kwan 關清霞  
 Alvin KH Kwok 郭坤豪  
 Paul BS Lai 賴寶山  
 Eric CH Lai 賴俊雄  
 CY Lam 林楚賢  
 Stephen TS Lam 林德深  
 Patrick CP Lau 劉志斌  
 Arthur CW Lau 劉俊穎  
 Keith KH Lau 劉廣洪  
 PY Lau 婁培友  
 Nelson LS Lee 李禮舜  
 Danny WH Lee 李偉雄  
 KY Leung 梁國賢  
 Danny TN Leung 梁子昂  
 Thomas WH Leung 梁慧康  
 WK Leung 梁惠強  
 Kenneth KW Li 李啟煌  
 David TL Liu 劉大立  
 Janice YC Lo 羅懿之  
 Herbert HF Loong 龍浩鋒  
 James KH Luk 陸嘉熙  
 Andrea OY Luk 陸安欣  
 Ada TW Ma 馬天慧  
 Arthur DP Mak 麥敦平  
 Henry KF Mak 麥嘉豐  
 Anthony CF Ng 吳志輝  
 Jacobus KF Ng 吳國夫  
 Hextan YS Ngan 顏婉嫦  
 Martin W Pak 白威  
 Edward CS So 蘇超駒  
 William YM Tang 鄧旭明  
 Kenneth KY Wong 黃格元  
 Patrick CY Woo 胡釗逸  
 Bryan PY Yan 甄秉言  
 TK Yau 游子覺  
 Kelvin KH Yiu 姚啟恒

**ADVISORS ON  
BIOSTATISTICS**

William B Goggins  
 Eddy KF Lam 林國輝

**ADVISOR ON CLINICAL  
EPIDEMIOLOGY**

Shelly LA Tse 謝立亞

**Research Fund for the Control of Infectious Diseases****Research Dissemination Reports****Editorial**

3

**RESPIRATORY INFECTIOUS DISEASES****Genetic characterisation of H9N2 influenza viruses in southern China**

4

*Y Guan, GJD Smith***Susceptibility of the upper respiratory tract to influenza virus infection following desialylation**

7

*J Nicholls, M Chan, D Kwong***Definition of the cellular interactome of the highly pathogenic avian influenza H5N1 virus: identification of human cellular regulators of viral entry, assembly, and egress**

10

*F Kien, HL Ma, R Bruzzone, LLM Poon, B Nal***A bioshield against influenza virus infection by commensal bacteria antiviral peptide**

13

*JD Huang, BJ Zheng, KY Yuen***Oral feeding of minocycline attenuates glial activation and reductions of tau and drebrin in response to systemically injected cytokines**

16

*DCH Poon, YS Ho, CF Lau, K Chiu, RCC Chang***Modulation of cell signalling by human coronavirus HKU1 S and M proteins**

22

*DY Jin, PCY Woo***Antibody-dependent enhancement of SARS coronavirus infection and its role in the pathogenesis of SARS**

25

*MS Yip, HL Leung, PH Li, CY Cheung, I Dutry, D Li, M Daëron, R Bruzzone, JSM Peiris, M Jaume*

**INTERNATIONAL EDITORIAL  
ADVISORY BOARD**

Sabaratnam Arulkumaran  
United Kingdom

Robert Atkins  
Australia

Peter Cameron  
Australia

Daniel KY Chan  
Australia

David Christiani  
United States

James Dickinson  
Canada

Willard Fee, Jr  
United States

Robert Hoffman  
United States

Sean Hughes  
United Kingdom

Arthur Kleinman  
United States

Xiaoping Luo  
China

William Rawlinson  
Australia

Jonathan Samet  
United States

Max Wintermark  
United States

Homer Yang  
Canada

Matthew Yung  
United Kingdom

---

**VIRAL HEPATITIS**

---

**Structure-based discovery and development of natural products as  
Type II JAK2 inhibitors for the treatment of hepatitis C** 32  
*EDL Ma, CH Leung, P Chiu, YC Cheng*

**Functional characterisation of hepatitis B viral X protein/microRNA-21  
interaction in HBV-associated hepatocellular carcinoma** 37  
*CH Li, SC Chow, DL Yin, TB Ng, YC Chen*

**Gender disparity of hepatocellular carcinoma: role of hepatitis B virus  
X protein and androgen receptor** 43  
*YT Chiu, IOL Ng*

**Author index & Disclaimer** 48

---

**MANAGING EDITOR**

Yvonne Kwok 郭佩賢

**DEPUTY MANAGING EDITOR**

Betty Lau 劉薇薇

**ASSISTANT MANAGING EDITOR**

Warren Chan 陳俊華

## Editorial

Dissemination reports are concise informative reports of health-related research supported by funds administered by the Food and Health Bureau, for example, the *Research Fund for the Control of Infectious Diseases* (which was consolidated into the *Health and Medical Research Fund* in December 2011). In this edition, 10 dissemination reports of projects related to respiratory infectious diseases and viral hepatitis are presented. In particular, three projects are highlighted due to their potentially significant findings, impact on healthcare delivery and practice, and/or contribution to health policy formulation in Hong Kong.

The threat from zoonotic transmission of avian influenza is ever present. H9N2 influenza viruses have become enzootic in terrestrial poultry populations around the world. Guan and Smith<sup>1</sup> conducted extensive surveillance of poultry in China and Hong Kong to characterise the H9N2 viruses found in poultry in southern China and the extent of their reassortment with other influenza viruses, particularly the highly pathogenic H5N1 viruses. They found that the poultry system in southern China allows H9N2 viruses to develop in multiple ways with mixing among species and the opportunity to transmit to humans. To prevent these developments leading to public health problems like those caused by the highly pathogenic H5N1 viruses, the authors advise better separation of birds within the poultry farming and marketing systems.

The specificity of influenza virus for a particular host cell is mediated by the interaction of haemagglutinin, a viral cell surface glycoprotein with host cell glycoconjugate receptors that contain

terminal sialic acid residues. A new pharmaceutical agent (sialidase) effectively degrades receptor sialic acid for both human and avian influenza and potentially confers protection against a broad range of influenza viruses. Nicholls et al<sup>2</sup> tested the presence of infection of human upper and lower respiratory tract tissue after sialidase treatment with avian and human viruses. Both prophylactic and therapeutic sialidase treatment was able to prevent infection by avian and human influenza viruses. Sialidase therapy offers a potentially useful clinical option and is now in phase II clinical trial.

Hepatitis C is a highly infectious disease that imposes a high health, social, and financial burden. Ma et al<sup>3</sup> constructed a new platform for the virtual screening of Janus kinase 2 (JAK2) Type II inhibitors and utilised it to identify amentoflavone as a lead scaffold for the development of new inhibitors. Novel natural inhibitors were developed and showed anti-JAK2 activity and antiviral activity in cellular systems. The compounds potentially represent a novel therapeutic approach to the treatment of hepatitis C, and may supplement existing regimens for hard-to-treat hepatitis C virus genotypes in Hong Kong.

We hope you will enjoy this selection of research dissemination reports. Electronic copies of these dissemination reports and the corresponding full reports can be downloaded individually from the Research Fund Secretariat website (<http://www.fhb.gov.hk/grants>). Researchers interested in the funds administered by the Food and Health Bureau also may visit the website for detailed information about application procedures.

### Supplement co-editors



Dr Edmond SK Ma  
Consultant  
(Research Office)  
Food and Health Bureau



Dr Richard A. Collins  
Scientific Review Director  
(Research Office)  
Food and Health Bureau

### References

1. Guan Y, Smith GJ. Genetic characterisation of H9N2 influenza viruses in southern China. *Hong Kong Med J* 2016;22(Suppl 4):4-6.
2. Nicholls J, Chan M, Kwong D. Susceptibility of the upper respiratory tract to influenza virus infection following desialylation. *Hong Kong Med J* 2016;22(Suppl 4):7-9.
3. Ma ED, Leung CH, Chiu P, Cheng YC. Structure-based discovery and development of natural products as Type II JAK2 inhibitors for the treatment of hepatitis C. *Hong Kong Med J* 2016;22(Suppl 4):32-6.

# Genetic characterisation of H9N2 influenza viruses in southern China

Y Guan \*, GJD Smith

## KEY MESSAGES

1. Two lineages of H9N2 influenza virus continue to be enzootic in terrestrial poultry. In China, one lineage is predominately found in quail (G1-like), and the other (Ck/Bei or Y280-like) in chickens.
2. Both lineages of H9N2 influenza viruses have undergone a series of reassortments with H5N1 and other influenza viruses in southern China.
3. Genetic characterisation of the H9N2 viruses suggests that all have the potential to infect

humans.

Hong Kong Med J 2016;22(Suppl 4):S4-6

RFCID project number: 06060722

Y Guan \*, GJD Smith

State Key Laboratory of Emerging Infectious Diseases, Department of Microbiology, The University of Hong Kong

\* Principal applicant and corresponding author: yguan@hkucc.hku.hk

## Introduction

H9N2 influenza viruses have become enzootic in terrestrial poultry populations from Egypt and the Middle East, across South, South East and East Asia.<sup>1</sup> H9N2 viruses have sporadically infected humans and swine and have provided segments, through reassortment, to the Asian highly pathogenic H5Nx viruses.<sup>2</sup> Two main lineages are found in these viruses, the widely distributed G1 lineage and the Ck/Bei or Y280-like lineage found in East Asia, particularly China.<sup>1,3,4</sup> Chickens are the primary hosts for these viruses, but they are also found in minor poultry, especially in the case of G1-like viruses in China.<sup>3,4</sup> In this study we sought to characterise the H9N2 viruses found in poultry in southern China and the extent of their reassortment with other influenza viruses, particularly the highly pathogenic H5N1 viruses.

## Results

This study was conducted from October 2006 to September 2008. H9N2 viruses were isolated from samples collected from chickens, ducks, and minor poultry from 2000 to 2005 in several provinces of southern China and from 2005 to 2007 in Hong Kong. The surveillance data provided 47 225 chicken samples, 49 150 duck samples, and 11 526 samples from quail and other minor poultry in provinces of southern China, as well as 30 770 chicken samples and 3422 samples from minor poultry in Hong Kong.

### Prevalence of H9N2 viruses

From all the samples collected, 1189 (2.5%) of chicken samples, 89 (0.2%) of duck samples, and 938 (8.6%) of minor poultry samples from provinces

of southern China were positive for H9 influenza viruses.<sup>3,4</sup> Among the minor poultry, quail had an unusually high prevalence of H9 influenza viruses, with 610 (13.3%) of 4601 quail samples positive.<sup>3</sup> Of the Hong Kong samples, 845 (2.7%) from chicken and 22 (0.6%) from minor poultry were positive for H9 influenza viruses.<sup>5</sup>

Chicken isolates came primarily from oropharyngeal samples, with isolates from cloacal or faecal samples decreasing over time.<sup>4</sup> In quail and other minor poultry, oropharyngeal samples accounted for over 90% of the isolates.<sup>3,4</sup> In Hong Kong, the ability to take oropharyngeal samples was limited and most isolates were from drinking water or cloacal/faecal samples.<sup>5</sup>

While H9 isolates could be isolated year round, the isolation rate in the summer months was generally lower.<sup>3,4,5</sup> In total, 73 quail, 84 other minor poultry, 139 chicken, and 15 duck H9N2 isolates were selected and subjected to full genome sequencing, with at least one isolate being taken from each positive sampling occasion.<sup>3,4,5</sup>

### Phylogenetic analysis

In the haemagglutinin (HA) gene phylogeny, approximately half of the quail viruses were part of the G1-like viruses, whereas the others were spread within two subgroups (1 and 2) of the Ck/Bei-like lineage.<sup>3</sup> Subgroup 1 had A/Quail/Shantou/243/2000 (ST243) as an early virus and subgroup 2 was part of a much larger sub-clade containing A/duck/Hong Kong/Y280/1997 (Y280).<sup>3</sup> Minor poultry viruses also fell into both these subgroups of the Ck/Bei lineage with subgroup 1 being almost exclusively from minor poultry viruses.<sup>3,4</sup> Chicken viruses were mainly part of subgroup 2 of the Ck/Bei-like lineage

and two duck viruses were from the Korean Y439-like lineage.<sup>4</sup> Viruses from both chickens and minor poultry in Hong Kong were part of the subgroup 2 (Y280-like) except for one chicken virus from the G1 lineage. The neuraminidase (NA) gene phylogeny showed that G1-like viruses remained predominantly within a consistent sub-clade and the NA of the Ck/Bei lineage poultry viruses from southern China also fell into two subgroups within that lineage, with one of them containing mostly minor poultry viruses.<sup>3,4</sup> A smaller proportion of viruses were in sub-clades with virus from eastern and northern China. All but one of the Hong Kong viruses were part of the same Ck/Bei lineage subgroup.<sup>5</sup>

### Antigenic analysis

Antigenic analysis was conducted using monoclonal antibodies raised against A/Quail/Hong Kong/G1/1997 (G1), A/duck/Hong Kong/Y280/1997 (Y280), and A/chicken/Hong Kong/G9/1997 (G9) in a haemagglutinin inhibition (HI) assay. A numerical analysis of the HI titres was conducted to provide a graphical overview of the patterns of antigenic changes. There were four different antigenic groups. Two corresponded to the G1-like viruses, primarily from quail, with one group associated with the prototype G1 virus and a smaller group showing an antigenic shift relative to the G1 virus. These viruses formed a sub-clade within the G1-like viruses.<sup>3</sup> Of the Ck/Bei- or Y280-like viruses a distinct sub-clade of mostly minor poultry viruses formed one antigenic group, with the bulk of the chicken and duck viruses forming the other antigenic group.<sup>3,4</sup>

### Genotyping

Reassortment, and classification of genotypes, among the H9N2 viruses were examined by tracking the phylogenetic origins of the segments. G1-like viruses were designated to have A-series genotypes and those from the Ck/Bei-like lineage were designated to have B-series genotypes, while two duck viruses were from the Korean Y439-like genotype.<sup>3,4</sup> The prototype G1 virus was designated to have genotype A0 and this persisted until 2002. Genotypes A1 and A2 had the NS segment and M (for A2) from the Ck-Bei lineage, indicating reassortment among the H9N2 major lineages. Genotype A3, which appeared in 2002, incorporated a PA segment of H5N1 origin and persisted and predominated during this study. A subset of viruses from this genotype showed antigenic drift. A transient genotype, A4, further incorporating a PB1 segment of unknown avian origin appeared in 2005.

The Ck-Bei-like lineage displayed a far greater variety of genotypes, whether or not the viruses came from minor poultry or chickens and ducks. This indicated extensive reassortment with other wild bird and poultry viruses, including the G1-like

viruses in quail and contemporary H5N1 viruses as well as with duck and aquatic bird viruses. Thirty B-series genotypes were reported in total, with only a few genotypes persisting for several years.<sup>3,4</sup> Fewer genotypes were observed in viruses from ducks, which is consistent with the trend for the H9N2 viruses to be found predominately in chickens and minor poultry.

### Molecular characterisation

The connecting peptides at the HA1/HA2 cleavage site (residues -1 to -4 of HA1) were predominately R-S-S-R.<sup>3,4</sup> Korean lineage and early viruses did not have the R at -4 of HA1. A few viruses had amino acids other than Ser at positions -2 and -3 and R was occasionally replaced by K at both positions -1 and -4.<sup>4</sup> One virus had an additional R at position -2, but this virus was not highly pathogenic in chickens.<sup>3</sup> Residues in the receptor binding sites positions 226 and 228 (H3 numbering) that are characteristic of avian (2-3) or human (2-6) receptor binding were predominately L (more human-like) and G (avian-like), respectively.<sup>3,4</sup> L226 predominated in the later viruses, which were infrequently isolated from ducks and more commonly isolated from oropharyngeal samples. Deletions of 2, 3, or 6 amino acids were found in the stalk regions of the NA proteins of several viruses.<sup>3,4</sup>

### Discussion

Viruses from the two major H9N2 lineages continue to circulate in southern China. The Ck/Bei-like lineage is predominant and is found primarily in chickens. In China, the G1-like lineage viruses were found mainly in quail, with few isolated from other minor poultry or chickens and ducks. This is in contrast with the situation in the Middle East and South Asia, where G1 viruses are prevalent and primarily isolated from chickens.<sup>1</sup> In southern China, the G1-like lineage viruses were relatively stable with respect to their genotypes, indicating limited reassortment with other viruses. This could be due to their more restricted prevalence in southern China and that quail, in particular, are more isolated from other birds in the poultry farming and marketing system. Evidence of antigenic drift in the quail G1-like viruses was found, which might be indicative of host selection pressure.

Ck/Bei-like viruses were more prevalent in southern China and predominately isolated from chickens. This lineage is not seen outside East Asia. A large number of genotypes were detected for viruses of this lineage indicating that they were readily able to reassort with viruses in the chicken or duck populations. However many of the genotypes were only transient. There were interchanges of segments with H5N1 viruses as well as viruses from

ducks and unknown birds. The interaction with H5N1 viruses raises the possibility of altering the way these highly pathogenic can be transmitted to humans. As with the G1-like viruses, two antigenic groups were detected. One group contained viruses mostly from quail and other minor poultry and was phylogenetically distinct from the other, predominately chicken, Ck/Bei-like viruses.

Overall, the H9N2 viruses from southern China and Hong Kong show patterns of both limited isolation and mixing within the poultry system. Quail and minor poultry are relatively more isolated in the farming and marketing system and were shown to host stable lineages of viruses. Ck/Bei-like viruses showed less stable lineages and had a greater level of exchange of segments with viruses from poultry and other birds. Therefore the poultry system in southern China allows H9N2 viruses to develop in multiple ways with mixing among species and the opportunity to transmit to humans.<sup>2</sup> To prevent these developments leading to public health problems like those caused by the highly pathogenic H5N1 viruses, better separation of birds within the poultry farming and marketing systems is advisable.

## Acknowledgements

This study was supported by the Research Fund for the Control of Infectious Diseases, Food and Health Bureau, Hong Kong SAR Government (#06060722), the Li Ka Shing Foundation, and the Ellison Foundation.

## References

1. Fusaro A, Monne I, Salviato A, et al. Phylogeography and evolutionary history of reassortant H9N2 viruses with potential human health implications. *J Virol* 2011;85:8413-21.
2. Lin YP, Shaw M, Gregory V, et al. Avian-to-human transmission of H9N2 subtype influenza A viruses: relationship between H9N2 and H5N1 human isolates. *Proc Natl Acad Sci U S A* 2000;97:9654-8.
3. Xu KM, Li KS, Smith GJ, et al. Evolution and molecular epidemiology of H9N2 influenza A viruses from quail in southern China, 2000 to 2005. *J Virol* 2007;81:2635-45.
4. Xu KM, Smith GJ, Bahl J, et al. The genesis and evolution of H9N2 influenza viruses in poultry from southern China, 2000 to 2005. *J Virol* 2007;81:10389-401.
5. Chu YC, Cheung CL, Hung Leung CY, et al. Continuing evolution of H9N2 influenza viruses endemic in poultry in southern China. *Influenza Other Respir Viruses* 2011;5(Suppl 1):68-71.

# Susceptibility of the upper respiratory tract to influenza virus infection following desialylation

J Nicholls \*, M Chan, D Kwong

## KEY MESSAGES

1. In general, human and swine viruses bind to host respiratory tract surface molecules that have an  $\alpha$ 2-6 linkage between sialic acid (Sia) and adjacent sugar molecules. Avian viruses preferentially bind to host receptors with an  $\alpha$ 2-3 linkage. Information on controlling influenza virus infection by removing Sia from the host surface is limited.
2. Lectin histochemistry was used to identify the Sia $\alpha$ 2-6 and Sia $\alpha$ 2-3 linkage and this lectin binding was re-examined after topical (surface) sialidase treatment. The presence of sialylated glycans in tissues was analysed using mass spectrometry. The presence of infection of human upper and lower respiratory tract tissue was tested after sialidase treatment with avian and human viruses.
3. There was a diffuse expression of Sia $\alpha$ 2-6 throughout the upper and lower respiratory tract. Sia $\alpha$ 2-3 varied according to site with more

N-linked Sia $\alpha$ 2-3 glycans in the upper respiratory tract and more O-linked glycans in the lower respiratory tract. Sialidase treatment was able to remove both types of glycans. Unexpectedly, the effect of desialylation was not the same in all cell lines tested.

4. Both prophylactic as well as therapeutic sialidase treatment was able to prevent infection with avian and human influenza viruses. Sialidase therapy offers a potentially useful clinical option and is now in phase II clinical trial.

Hong Kong Med J 2016;22(Suppl 4):S7-9  
 RFCID project number: 08070842

<sup>1</sup> J Nicholls, <sup>2</sup> M Chan, <sup>3</sup> D Kwong

The University of Hong Kong:

<sup>1</sup> Department of Pathology

<sup>2</sup> Department of Microbiology

<sup>3</sup> Department of Clinical Oncology

\* Principal applicant and corresponding author: nicholls@pathology.hku.hk

## Introduction

The specificity of influenza for a particular host is mediated by the interaction of haemagglutinin (HA), a viral cell surface glycoprotein with host glycoconjugate receptors that contain terminal sialic acid (Sia) residues. The HA of influenza A strains that infect humans attaches preferentially to cells with Sia linked  $\alpha$ 2-6 residues to galactose, whereas avian strains preferentially bind Sia linked  $\alpha$ 2-3 to galactose.<sup>1</sup> As an example, the H5N1 viruses of the bird flu outbreak in Hong Kong in 1997 had an affinity for binding to avian  $\alpha$ 2-3 linked Sia.

On the basis of binding by the lectin, *Maackia amurensis agglutinin* (MAA), Sia $\alpha$ 2-3 (and thus H5N1 infection) appears to be restricted mainly to the human lower respiratory tract, whereas by *Sambucus nigra agglutinin* (SNA) binding, Sia $\alpha$ 2-6 linkages in both the upper and lower respiratory tract have been identified. This presumed inability of the H5N1 virus to establish infection in the upper respiratory tract has significant clinical and epidemiological implications. For example, H5N1 transmission is unlikely to occur via droplets or ingestion, and will likely require aerosol transmission to reach the lower respiratory epithelium.

Previously we used different isoforms of the

lectin MAA and demonstrated that MAA2 (which binds O-linked Sia $\alpha$ 2-3) had limited binding in the upper respiratory tract, but there was widespread binding of MAA-I (which binds N-linked Sia $\alpha$ 2-3) in the nasopharynx, adenoid and trachea of adults and children.<sup>2</sup> We further went on to demonstrate that H5N1 viruses with only Sia $\alpha$ 2-3 binding specificity could replicate in the upper respiratory tract of humans.<sup>3</sup> There was widespread binding of MAA-I—the lectin that identifies Sia $\alpha$ 2-3Gal—a binding preference of H5 viruses. This isoform of MAA did detect non-Sia termini such as sulphated galactose.

A new pharmaceutical agent—DAS181—utilises the *Aspergillus viscosus* sialidase coupled together with an epithelial cell anchoring domain.<sup>4</sup> This fusion protein effectively degraded receptor Sia for both human and avian influenzas and potentially conferred protection against a broad range of influenza viruses. As MAA-I identified non-Sia residues, fresh tissues were also submitted for mass spectrometric analysis to determine residual glycoprotein profiles following DAS181 treatment.

If Sia are the sole receptors for influenza virus infection, then we proposed there would be an absence of influenza virus (IFV) infection as

determined by 50% tissue culture infectious dose (TCID<sub>50</sub>), enzyme-linked immunosorbent assay and immunohistochemistry following pre-incubation of normal upper respiratory tract tissues with neuraminidase (NA) and DAS181. Nonetheless, two reports have suggested that influenza virus infection may occur in the absence of NA, although these have been mainly confined to non-human or tumour cell lines. This warrants investigation of the alternate receptor hypothesis by exploring whether tissues can still be infected by influenza viruses despite NA or DAS181 treatment.

## Methods

This study was conducted from January 2009 to December 2010. Fresh biopsies were obtained from the normal nasopharynx and bronchus of individuals screened for nasopharyngeal carcinoma, and from healthy volunteers under a study approved by the Institutional Review Board of The University of Hong Kong and Hospital Authority (Hong Kong West). Lung tissue excised for pulmonary malignancy or other surgical procedures was also obtained.

Viruses used included A/HongKong/54/98 (H1N1), A/Hong Kong/1174/99 (H3N2), A/Qu/HK/G1/97 (H9N2), A/Dk/HK/Y280/97 (H9N2), A/Hong Kong/213/03 (H5N1), A/Vietnam/3046/04 (H5N1).

Infection was carried out using the viruses at a titre of  $1 \times 10^6$  TCID<sub>50</sub>/ml, and ultraviolet light inactivated viruses as controls. Following incubation of the tissue fragments with the virus, the supernatant was removed and replaced with fresh medium. The tissue fragments of each biopsy were incubated at 37°C for 48 hours at which time they were fixed in 10% neutral buffered formalin and processed for influenza nucleoprotein immunohistochemistry

## Lectin binding profiles

Sections were microwaved in 10 mM citrate buffer pH 6.0 at 95°C for 15 minutes then blocked with 3% H<sub>2</sub>O<sub>2</sub> in TBS for 12 minutes and with avidin / biotin blocking kit (Vector Labs). They were then incubated with biotinylated MAA-I and MAA-II (Vector Labs) and horseradish peroxidase (HRP)-labelled SNA and LFA (EY Labs) for 1 hour at room temperature, blocked with 1% bovine serum albumin for 10 minutes at room temperature, and then incubated with strep-ABC complex (Dako Cytomation, K-0377) diluted 1/100 for 30 minutes at room temperature.

## Neuraminidase and DAS181 treatment

Fresh and paraffin-embedded tissues were incubated with three different neuraminidases from Glyko (Glyko S – Sia $\alpha$ 2,3 specific; Glyko N – Sia $\alpha$ 2,3 and Sia $\alpha$ 2,8 specific and Glyko A – Sia $\alpha$ 2,3 and Sia $\alpha$ 2,6 specific) as well as DAS181 obtained from NexBio

pharmaceuticals. Incubation was performed at 37°C for 2 hours before influenza virus infection or lectin binding assessment.

## Mass spectrometric analysis

Frozen bronchus and lung tissue biopsies before and after DAS181 treatment were washed with PBS to remove any excreted mucus. Glycoproteins were solubilised from the tissues by homogenisation in a detergent extraction buffer. Extracted glycoproteins were reduced and carboxymethylated prior to tryptic protease digestion. N-linked glycans were enzymatically cleaved from the peptide backbone by digestion with peptide N-glycosidase F and subsequently purified on a Sep-Pak C18 reverse-phase cartridge. O-glycans were chemically released from glycopeptides by reductive elimination. GC-MS linkage data were performed on glycan samples both before and after digestion with linkage specific sialidases ( $\alpha$ 2-3 specific from *Streptococcus pneumoniae* and  $\alpha$ 2-3, 6, 8,9 specific from *Arthrobacter ureafaciens*). MALDI-TOF MS profiles of permethylated glycans after sialidase digestion were recorded to assess the degree of desialylation.

## Results

Sialidase treatment using Glyko A sialidase (which cleaves both  $\alpha$ 2-3 and  $\alpha$ 2-6 Sia) was able to remove binding of SNA and MAA to the epithelium, and this was more prominent in tissues from the bronchus and lung.

Using fresh bronchial and tracheal biopsies, the dosage of DAS181 necessary to lead to desialylation was determined. A concentration of 5  $\mu$ g/cm<sup>2</sup> was suitable to remove Sia from the surface epithelium, as shown by a decrease in SNA binding compared with the control. As DAS181 was not internalised there was no change in the intracellular Sia that remained in the goblet cells. Ten minutes exposure to DAS181 was sufficient to lead to significant desialylation at 10  $\mu$ g/cm<sup>2</sup>, although by 30 minutes there was an equal level of desialylation at both 5  $\mu$ g/cm<sup>2</sup> and 10  $\mu$ g/cm<sup>2</sup>. After a single treatment there was desialylation up to 48 hours with increased intracellular binding of SNA seen in bronchial epithelium associated with weak binding to the epithelium at 72 hours. This finding was in accord with an in vitro human airway epithelium finding; DAS181 at 5-10  $\mu$ g/cm<sup>2</sup> was able to stop lectin binding indicating removal of extracellular Sia, and this effect lasted for 72 hours.

Accordingly, if Sia was the sole receptor for influenza, then removal of the Sia from glycans should diminish infection with influenza. Because H5N1 is associated with a higher mortality than seasonal influenza, we initially focused on the prophylactic and therapeutic effect of DAS181 in H5N1 infection. After 2 hours incubation with DAS181, there was a

reduced binding of SNA and MAA and increased binding with PNA (which detects the exposed galactose). In a repeat experiment of the previously published mass spectrometric analysis, there was reduced sialylation after 2 hours incubation of lung tissues with DAS181. Infection experiments with H5N1 showed that control tissues had positive influenza nucleoprotein cells in the tissue sections indicating infection and this was reduced by a single dose of DAS181. Continuous exposure to DAS181 significantly abolished infection. When influenza M-gene analysis was performed, control H1N1, H3N2 and H5N1 tissues showed increased gene expression that was abolished after DAS181 treatment.

During the duration of the project, a new pandemic virus H1N1pdm emerged. We studied whether DAS181 would be able to abolish this infection. Pre-treatment with DAS181 prevented influenza virus replication as demonstrated by TCID<sub>50</sub> and influenza M gene analysis.

## Discussion

This project aimed to investigate interaction of the HA of different influenza viruses with the Sia present on the respiratory epithelium and how interfering with this interaction could affect influenza replication in the normal respiratory tract. We demonstrated that sialidase therapy was able to reduce lectin binding to epithelia from various sources (ie removal of both  $\alpha$ 2-3 and  $\alpha$ 2-6 linked glycans) and confirmed that different isoforms of the lectin *Maackia amurensis* should be used for detecting  $\alpha$ 2-3 type glycans. We then demonstrated that a single dose of DAS181 was sufficient for desialylation and that the effect of desialylation could last for up to 3 days and that ciliated epithelial cells were the preferred target for desialylation in the bronchial epithelium. In addition, DAS181 treatment was able to effectively block H5N1 and other seasonal virus infection in *ex vivo* tissue.

Overall, Sia was the main receptor for influenza, and removal of this Sia would be sufficient

to abolish influenza virus infection. Nonetheless, how our findings correlate with findings in other studies in which influenza infection occurred in the presence of desialylation remained unclear. We therefore tested the effects of DAS181 on a wider range of influenza viruses (including H7N7 viruses, H1N1pdm, H3N2, H5N1 and H1N1 viruses) and used MDCK cells and CHO cells. As expected, DAS181 treatment markedly reduced infection in CHO cells with all viruses tested, but in MDCK cells despite DAS181 treatment there was still definite evidence of infection with most H5N1 viruses—A/Vietnam/3046/04 (H5N1) and A/HongKong/54/98 (H1N1). The two possibilities (which are not mutually exclusive) are (1) there are glycans present on MDCK cells that are not present on CHO cells and are resistant to sialidase treatment and (2) these two viruses have distinct binding profiles that allow binding to non-Sia glycans.

## Acknowledgements

This study was supported by the Research Fund for Control of Infectious Diseases, Food and Health Bureau, Hong Kong SAR Government (#08070842). We thank Nex Bio for the supply of sialidase for use in *ex vivo* tissues.

## References

1. Rogers GN, Paulson JC. Receptor determinants of human and animal influenza virus isolates: differences in receptor specificity of the H3 hemagglutinin based on species of origin. *Virology* 1983;127:361-73.
2. Nicholls JM, Bourne AJ, Chen H, Guan Y, Peiris JS. Sialic acid receptor detection in the human respiratory tract: evidence for widespread distribution of potential binding sites for human and avian influenza viruses. *Respir Res* 2007;8:73.
3. Nicholls JM, Chan MC, Chan WY, et al. Tropism of avian influenza A (H5N1) in the upper and lower respiratory tract. *Nat Med* 2007;13:147-9.
4. Malakhov MP, Aschenbrenner LM, Smee DE, et al. Sialidase fusion protein as a novel broad-spectrum inhibitor of influenza virus infection. *Antimicrob Agents Chemother* 2006;50:1470-9.

# Definition of the cellular interactome of the highly pathogenic avian influenza H5N1 virus: identification of human cellular regulators of viral entry, assembly, and egress

F Kien \*, HL Ma, R Bruzzone, LLM Poon, B Nal †

## KEY MESSAGES

1. Novel H5N1-human host protein-protein interactions were identified using a genome-wide yeast two-hybrid screen.
2. Annexin A6 interacts with the cytoplasmic tail of influenza A M2 protein.
3. Annexin A6 negatively regulates influenza A infection.
4. Annexin A6 impairs influenza A virus budding and release.

Hong Kong Med J 2016;22(Suppl 4):S10-2

RFCID project number: 09080892

<sup>1,2,3</sup> F Kien, <sup>1,4</sup> HL Ma, <sup>1,5</sup> R Bruzzone, <sup>3</sup> LLM Poon, <sup>1,6</sup> B Nal

<sup>1</sup> HKU-Pasteur Research Pole, Hong Kong

<sup>2</sup> Ksilink, French-German Advanced Translational Centre, Strasbourg, France

<sup>3</sup> Centre of Influenza Research, School of Public Health, LKS Faculty of Medicine, The University of Hong Kong, Hong Kong SAR, China

<sup>4</sup> Emory University Vaccine Research Center, Atlanta, Georgia, USA

<sup>5</sup> Department of Cell Biology and Infection, Institut Pasteur, Paris, France

<sup>6</sup> Brunel University London, Division of Biosciences, College of Health and Life Sciences, Uxbridge, United Kingdom

\* Principal applicant: francois.kien@ksilink.com

† Corresponding author: beatrice.nal-rogier@brunel.ac.uk

## Introduction

Influenza A virus causes acute infection of the respiratory tract in humans. H1N1 and H3N2 viral strains are responsible for seasonal epidemics. Symptoms include fever, headache, chills, myalgia, dry cough and sore throat. Influenza is usually a self-limiting disease with recovery within a week in healthy individuals. Nonetheless, risk of serious illness affects young children, the elderly and patients with underlying health conditions. Due to antigenic variation of the virus, vaccination only enables incomplete protection. Circulation of influenza viruses in the animal reservoir causes additional threat. Because of rapid adaptation of viruses to environmental pressures, drugs directed against viral components are likely to induce selection of drug-resistant strains.<sup>1</sup> Our strategy is to characterise cellular pathways used by viruses in the human host and identify potential novel cellular targets for drug development.

The spread of H5N1 avian influenza in South East Asia in the mid 2000s, its extreme virulence in poultry and the threat of a deadly pandemic in humans prompted us to work on this virus. We used a yeast-two hybrid approach to screen the entire human genome for factors that interact with H5N1 viral structural proteins. We had previously successfully used this technology for virus-host interaction studies on the severe acute respiratory syndrome coronavirus.<sup>2,3</sup> Six highly relevant

interactions were identified for H5, M1, and M2. Pilot biochemical confirmation of interactions and gene silencing studies prompted us to primarily focus on human annexin A6 (AnxA6). The yeast-two hybrid assay had revealed that AnxA6 binds the cytosolic tail of the viral M2 proton channel.

M2 is an essential protein for the virus. It has a proton channel activity with key roles during virus entry and uncoating, transport of viral haemagglutinin to the cell surface and assembly, budding and release of progeny virions at the surface of infected cells.<sup>4</sup> There, M2 is known to accumulate at the edges of cholesterol-enriched viral budding platforms and induce a negative membrane curvature at the neck of the bud, responsible for scission and release of viral particles.<sup>5</sup>

AnxA6 belongs to the annexin family of human proteins. It plays important roles in membrane trafficking and cell signalling in mammalian cells. Its overexpression has been shown to cause accumulation of cholesterol in late endosomes and alter transport and recycling of cellular cargos.<sup>6</sup>

In this study we confirmed interaction between influenza M2 and human AnxA6 and demonstrated that AnxA6 restricts release of progeny viruses from infected cells.

## Methods

This study was conducted from October 2009 to September 2011. To confirm the interaction

identified in yeast (Hybrigenics, Paris, France), both biochemical and microscopy assays were performed. To determine whether AnxA6 is essential for infection both AnxA6 depletion and AnxA6 overexpression studies were analysed. Steps of virus life cycle regulated by AnxA6 were identified using a comprehensive and systematic dissection of the viral life cycle. Impact of AnxA6 expression modulation on infection was studied using the previously mentioned AnxA6 depletion and overexpression protocols together with virus life cycle step-specific assays such as transmission electron microscopy to study virus budding and morphology.

## Results

We hypothesised that cellular factors interacting with influenza M2 54-residue cytoplasmic tail (CT) could either help or restrict processes involving M2. We identified a novel interaction between the M2 CT of a highly pathogenic avian influenza strain (H5N1) and human AnxA6 in yeast. This interaction was confirmed *in vitro* using GST pull-down assay with M2 CT of the laboratory adapted influenza strain A/WSN/33 (H1N1). We found that a GST-M2 CT fusion protein interacts and pulls down AnxA6 from total human cell lysate, demonstrating that this interaction is not an artefact observed in the yeast system and the interaction is shared among different viral subtypes. Physical interaction was further confirmed in human virus-infected cells using a reciprocal co-immunoprecipitation assay of recombinant myc-AnxA6 and viral M2 protein. Co-localisation studies using confocal fluorescent microscopy showed a partial co-localisation of viral M2 and recombinant GFP-AnxA6 in distinct puncta-like areas at or close to the plasma membrane of virus-infected human cells, suggesting that this interaction occurs close to the virus assembly and budding site.

To define the role and impact of M2-AnxA6 interaction on the viral replication cycle, we used two complementary approaches and studied the effect of AnxA6 depletion or overexpression on the production of viral particles. AnxA6 depletion significantly increased virus production, while overexpression reduced the titre of virus progeny, suggesting a negative regulatory role for AnxA6 during influenza A virus infection. This was observed with different virus strains and subtypes of human seasonal influenza viruses, A/WSN/33 (H1N1), A/HK/1/68 (H3N2), and A/HK/54/98 (H1N1), suggesting a common hijacked cellular pathway by influenza A viruses.

Using AnxA6 depletion or overexpression protocols combined with virus life cycle step-specific assay, we showed that AnxA6 does not affect virus binding and entry, vRNA replication and viral mRNA transcription, viral polymerase complex

activity or NP nuclear export. On the contrary, we demonstrated that AnxA6 negatively modulates influenza virus infection by affecting virus budding as indicated by a drop in progeny virus PFU titre in supernatants and an increased number of virions at the cell surface of cells overexpressing AnxA6, which exhibit an elongated rather than spherical shape. This was observed by a semi-quantitative analysis of virus budding and morphology by transmission electron microscopy. These results demonstrate that AnxA6 overexpression results in defects in virus budding and release of infectious viral particles.

## Discussion

This work identified AnxA6 as a novel cellular regulator that impairs virus budding and release stages of the lifecycle of influenza A virus. We proposed that AnxA6 acts as a restricting factor of influenza virus budding either by interacting with M2, which is able to mediate membrane scission,<sup>5</sup> or by modulating cellular components such as cortical actin and cholesterol<sup>7</sup> involved in viral budding, or both. Use of a recombinant mutant WSN influenza virus lacking M2 suggested that regulation of influenza virus production by AnxA6 is dependent on M2 and its interaction with AnxA6; this work has been published.<sup>8</sup> Since then inhibition of influenza A virus production by AnxA6 has been further confirmed, and this effect linked to deregulation of cholesterol transport by AnxA6.<sup>9</sup>

Our study has enhanced the understanding of cellular factors requirements for influenza A virus assembly and budding and underscores the unique budding strategy implemented by this virus. Nevertheless, the detailed molecular mechanism underlying this AnxA6-mediated negative modulation of influenza virus budding awaits further investigation. It will be important to determine the functional correlation between M2-AnxA6 interaction and the defective viral budding phenotype. This research will help to delineate new strategies for the rational design of antiviral molecules.

## Acknowledgements

This study was supported by the Research Fund for the Control of Infectious Diseases, Food and Health Bureau, Hong Kong SAR Government (#09080892), University Grants Committee Area of Excellence Scheme (AoE/M-12/-06), French Ministry of Health, RESPARI Pasteur network, and the Li Ka Shing Foundation. We thank Dr Carlos Enrich (Departament de Biologia Celular, Facultat de Medicina, Universitat de Barcelona, Spain) for expert advice and helpful discussions and all the staff from HKU-Pasteur Research Pole for stimulating discussions. We acknowledge the Core Imaging

Facility and Electron Microscopy Unit of the Faculty of Medicine of the University of Hong Kong.

### References

1. de Jong MD, Tran TT, Truong HK, et al. Oseltamivir resistance during treatment of influenza A (H5N1) infection. *N Engl J Med* 2005;353:2667-72.
2. Teoh KT, Siu YL, Chan WL, et al. The SARS coronavirus E protein interacts with PALS1 and alters tight junction formation and epithelial morphogenesis. *Mol Biol Cell* 2010;21:3838-52.
3. Millet JK, Kien F, Cheung CY, et al. Ezrin interacts with the SARS coronavirus Spike protein and restrains infection at the entry stage. *PLoS One* 2012;7:e49566.
4. Kien F, Ma H, Diaz Gaisenband S, Nal B. Viroporins: differential functions at late stages of viral life cycles. Kishore U, Nayak A, editors. *Microbial pathogenesis: infection and immunity*. Landes Bioscience and Springer Science & Business Media; 2013:25.
5. Rossman JS, Lamb RA. Influenza virus assembly and budding. *Virology* 2011;411:229-36.
6. García-Melero A, Reverter M, Hoque M, et al. Annexin A6 and late endosomal cholesterol modulate integrin recycling and cell migration. *J Biol Chem* 2016;291:1320-35.
7. Enrich C, Rentero C, de Muga SV, et al. Annexin A6-Linking Ca(2+) signaling with cholesterol transport. *Biochim Biophys Acta* 2011;1813:935-47.
8. Ma H, Kien F, Manière M, et al. Human annexin A6 interacts with influenza A virus protein M2 and negatively modulates infection. *J Virol* 2012;86:1789-801.
9. Musiol A, Gran S, Ehrhardt C, et al. Annexin A6-balanced late endosomal cholesterol controls influenza A replication and propagation. *MBio* 2013;4:e00608-13.

# A bioshield against influenza virus infection by commensal bacteria secreting antiviral peptide

JD Huang \*, BJ Zheng, KY Yuen

## KEY MESSAGE

A commensal bacterial strain was engineered to express and secrete antiviral peptide against influenza A virus.

Hong Kong Med J 2016;22(Suppl 4):S13-5

RFCID project number: 08070592

<sup>1</sup> JD Huang, <sup>2</sup> BJ Zheng, <sup>2</sup> KY Yuen

<sup>1</sup> Department of Biochemistry, The University of Hong Kong

<sup>2</sup> Department of Microbiology, The University of Hong Kong

\* Principal applicant and corresponding author: jdhuang@hku.hk

## Introduction

Avian influenza is caused by influenza viruses such as the influenza A virus. In 1997 in Hong Kong, the avian influenza viruses were found to cross the species barrier to infect human beings and cause respiratory illness and death. H5N1 viruses later re-emerged in Asia with human cases of infection, of which more than 50% were fatal.

We proposed to genetically engineer naturally occurring bacteria to provide protection against influenza A virus infection by secreting a peptide that interferes with viral attachment. Introduction and colonisation of these genetically modified bacteria in the oral mucosa and respiratory tract would provide a natural bioshield for uninfected individuals and protection against influenza A virus.

## Methods

This study was conducted from December 2008 to May 2011. In order for the bioshield to be successful, there should be (1) continuous expression and secretion of a potent antiviral peptide at a high level; (2) colonisation of the genetically modified microbes on the mucosal surface of the respiratory tract for prolonged periods to block infection by influenza A virus; and (3) no pathology in the colonised host caused by the genetically engineered bacteria. Similar strategies have been used to protect animals against HIV,<sup>1</sup> *Candida albicans*,<sup>2</sup> and *Streptococcus mutans*.<sup>3</sup> The technology and 'bio-bricks' necessary for building an anti-H5N1 bacterium strain are all available as follows:

(1) Bacterial strains that colonise the respiratory tract: unlike immunisation in which the bacteria need to exist only for a limited period, antiviral peptide has to be present continuously in the secretions of the upper airway when the patient is challenged by the influenza virus. This can only happen if the bacteria producing the antiviral peptide

form a normal commensal bacterial strain that has a survival advantage in the pharynx. Gram-positive bacteria such as *Streptococcus* and *Lactobacilli* have a distinct advantage. *Streptococcus gordonii* has the best track record.<sup>4</sup> *S gordonii* is a commensal bacterium commonly found on healthy human oral mucosa, the upper respiratory tract, and in dental plaque with a high colonising ability. Although associated with dental caries, it is less virulent than *Streptococcus mutans* but does not lose the ability to colonise the oropharynx continuously. It forms commensal microflora in humans without causing any pathology.

(2) Peptide with anti-influenza virus function: a 20-amino-acid peptide derived from the signal sequence of fibroblast growth factor 4 has exhibited broad-spectrum antiviral activity against influenza viruses including the highly pathogenic H5N1 subtype.<sup>5</sup> This peptide prevents viral infection by binding to the viral haemagglutinin protein to block attachment of the virus to the cellular receptor *in vivo* and *in vitro*. A 100% survival was observed when BALB/c mice were infected with H5N1 A/Hong Kong/156/97 strain pre-treated with 2 mM of this peptide. In addition to the preventive effect, this peptide showed promising therapeutic value. When BALB/c mice were first infected with A/Hong Kong/156/97 and then given 2 mM of the peptide intranasally, there was 100% survival at 7 dpi, compared with 0% survival without treatment. Importantly, mice that received this peptide alone exhibited no toxicity.<sup>5</sup>

In this project, the pLEX secreting expression system was first tested with green fluorescent protein (GFP). Then an antiviral peptide gene was cloned into the pLEX vector, transforming the resulting plasmid into *S gordonii*. The expression and secretion of antiviral peptide in the culture supernatant was examined by western blot and dot blot. The protective function of the peptide

was evaluated *in vitro* by the haemagglutination inhibition (HI) assay. To verify the protection *in vivo*, mice were challenged with lethal influenza virus in the presence or absence of the engineered bacteria.

### Results

The efficiency of pLEX expression system in *S.gordonii* GP204 stain was verified by GFP report protein (Figs 1 and 2). Nevertheless, the expression and secretion of the target antiviral peptide (EB) could not be detected in the supernatant of *S.gordonii* GP204 culture by western blot or dot blot. Therefore, a series of pLEX-xEB clones was constructed to optimise expression. With the optimised EB expression system, secreted EB still could not be detected by western blot in the supernatant. The protective effect of EB expression was evaluated *in vitro* using HI

assay. EB peptides had been secreted into the culture supernatant. The secreted EB blocked influenza virus and inhibited binding of the influenza virus to turkey red blood cells (Fig 3).

The protective effect of EB-expressing *S.gordonii* against influenza virus in mice was evaluated. First, the colonisation of *S.gordonii* in mice was evaluated. Four weeks after inoculation, 75% of mice were still colonised with *S.gordonii*. To evaluate the protective effect, mice colonised with *S.gordonii* were challenged with lethal influenza virus. There was no significant difference in survival rate between the group colonised with *S.gordonii* harbouring pLEX-4EB and the control group. Further optimisation strategies of the expression system for increasing EB expression *in vivo* are necessary.

### Discussion

*S.gordonii* GP204 has been extensively studied and used to surface display or secrete various functional proteins.<sup>6</sup> We successfully verified the efficiency of the pLEX expression system in *S.gordonii* GP204 stain by GFP reporter protein. Nevertheless, when detecting EB expression in *S.gordonii* GP204, there were unexpected difficulties. Unlike GFP protein, in the supernatant and cells of recombinant bacteria, EB expression could not be detected by western blot or dot blot. This might have been because: (1) EB expression was too low to be detected. It is possible that the promoter activity of *gtfG* in pLEX may be insufficient to secrete detectable amounts of small peptide. (2) Detection method was inappropriate. The dot-blot or western blot assay may not be sensitive enough to detect such a small peptide (~2 kDa). (3) It is possible that only relatively large proteins can be secreted in this system; it is

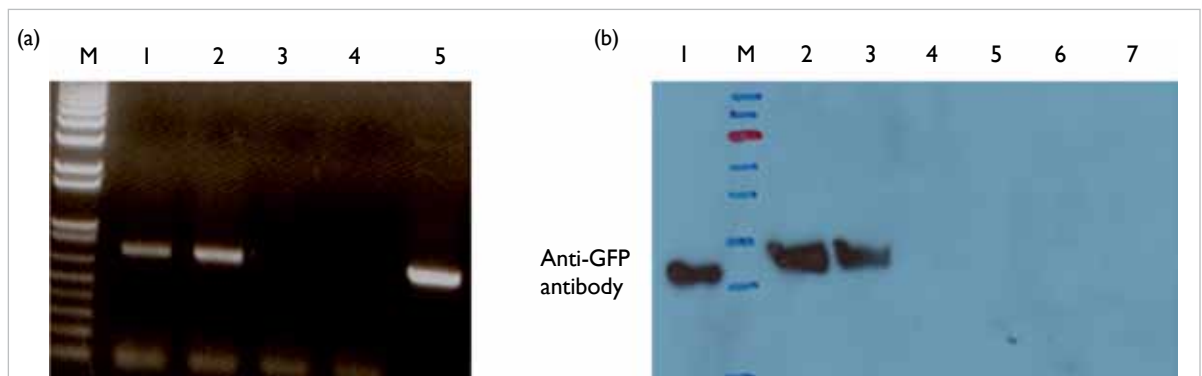
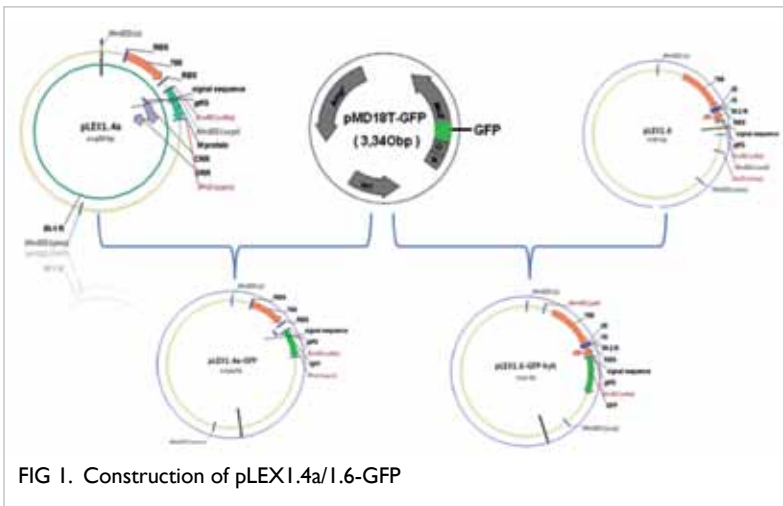
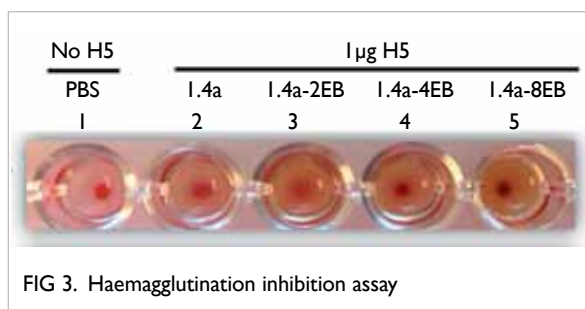


FIG 2. (a) Verification of transformation by bacteria liquid PCR: 1 denotes culture of pLEX1.4a-GFP transformed *S.gordonii* GP204, 2 Culture of pLEX1.6-GFP transformed *S.gordonii* GP204, 3 culture of blank *S.gordonii* GP204 as negative control, 4 pLEX1.6 plasmid as negative control, and 5 pLEX1.6-GFP plasmid as positive control. (b) Verification of GFP expression in culture supernatant and cells by western blot: 1 denotes cell 1 of 7207-GFP as positive control, 2 supernatant of *S.gordonii* GP204 transformed with pLEX1.4a-GFP, 3 supernatant of *S.gordonii* GP204 transformed with pLEX1.6-GFP, 4 supernatant of blank *S.gordonii* GP204 as negative control, 5 cells of *S.gordonii* GP204 transformed with pLEX1.4a-GFP, 6 cells of *S.gordonii* GP204 transformed with pLEX1.6-GFP, and 7 cells of blank *S.gordonii* GP204 as negative control.



not known if small peptides (ie 20 aa) can also be secreted by this strategy.

Therefore, our optimisation strategy was to multiply the sequence of EB. We constructed a series of pLEX-xEB-his clones to optimise the secreting expression. Likewise, western blot results detected no EB-his expression in culture supernatant. We then decided to detect the presence of EB by its protective function. This was performed *in vitro* by HI assay. The HI assay result indicated that EB peptides were likely secreted into the culture supernatant, as only the bacteria harbouring EB expressing plasmids can block influenza virus and inhibited influenza virus from binding to turkey red blood cells. The bacteria that contained the empty vector failed to block viral binding. Hence, we further evaluated the protection against influenza virus in mice. There was no significant difference in survival rate between the pLEX-4EB group and GP204 control group. We suspect that the expression of antiviral peptide was too low to completely block the influenza virus. It is possible that the amount of inoculated bacteria that could secrete antiviral peptide was insufficient, or that the efficiency of the pLEX system *in vivo* was not as high as necessary. Another possible reason was that EB peptides might have been broken down by *S. gordonii*. A minimal and optimal sequence of EB peptide has been reported to improve the antiviral efficacy and decrease the synthesis costs.<sup>7</sup> Nonetheless, it is unknown whether this minimal epitope will be better expressed in *S. gordonii*. It is also very difficult to detect and evaluate the secreting expression of small epitopes in the supernatant. Although EB is not toxic to either HeLa or Vero cells at 100 µM, toxicity of the peptide to *S. gordonii* cannot be excluded. In future, we will commercially synthesise EB peptide and evaluate its toxicity at various concentrations with *S. gordonii*.

Overall, we successfully verified the efficiency of pLEX expression system in *S. gordonii* GP204 strain by GFP reporter protein and constructed a series of engineered commensal bacteria strains. Nonetheless,

to build an effective anti-influenza bioshield, there remain a few hurdles to be overcome: (1) It is difficult to obtain high level secreting expression of EB peptide both *in vivo* and *in vitro* thus resulting in no effective protection. (2) The plasmid containing the EB peptide sequence is unstable and can be easily lost *in vivo* and may contribute to low peptide expression. (3) *S. gordonii* colonisation in mice is not stable and needs multiple inoculations supplied with appropriate antibiotics.

Although the challenge experiments did not provide efficient protection, the supernatant of the engineered bacteria did show evidence of viral inhibition. This offers hope that the strategy may work by improving the expression and colonisation efficiency. If successful, the novel bioshield can be inoculated by simple combination with nutritious foods or encapsulated. This will be more convenient and acceptable to use, and easier to administer. The bioshield can be self-administered and eliminates the use of a hypodermic needle. A bioshield against avian influenza viruses is easy to manufacture.

## Acknowledgement

This study was supported by the Research Fund for the Control of Infectious Diseases, Food and Health Bureau, Hong Kong SAR Government (#08070592).

## References

1. Chang TL, Chang CH, Simpson DA, et al. Inhibition of HIV infectivity by a natural human isolate of *Lactobacillus jensenii* engineered to express functional two-domain CD4. *Proc Natl Acad Sci U S A* 2003;100:11672-7.
2. Beninati C, Oggioni MR, Boccanera M, et al. Therapy of mucosal candidiasis by expression of an anti-idiotypic in human commensal bacteria. *Nat Biotechnol* 2000;18:1060-4.
3. Krüger C, Hu Y, Pan Q, et al. In situ delivery of passive immunity by lactobacilli producing single-chain antibodies. *Nat Biotechnol* 2002;20:702-6.
4. Sharma A, Sojar HT, Hruby DE, Kuramitsu HK, Genco RJ. Secretion of *Porphyromonas gingivalis* fimbriin polypeptides by recombinant *Streptococcus gordonii*. *Biochem Biophys Res Commun* 1997;238:313-6.
5. Jones JC, Turpin EA, Bultmann H, Brandt CR, Schultz-Cherry S. Inhibition of influenza virus infection by a novel antiviral peptide that targets viral attachment to cells. *J Virol* 2006;80:11960-7.
6. Maggi T, Spinoso M, Ricci S, Medagliani D, Pozzi G, Oggioni MR. Genetic engineering of *Streptococcus gordonii* for the simultaneous display of two heterologous proteins at the bacterial surface. *FEMS Microbiol Lett* 2002;210:135-41.
7. Jones JC, Settles EW, Brandt CR, Schultz-Cherry S. Identification of the minimal active sequence of an anti-influenza virus peptide. *Antimicrob Agents Chemother* 2011;55:1810-3.

# Oral feeding of minocycline attenuates glial activation and reductions of tau and drebrin in response to systemically injected cytokines

DCH Poon, YS Ho, CF Lau, K Chiu, RCC Chang \*

## KEY MESSAGES

1. The use of minocycline to regulate the neuropathological effects of systemically administered cytokines was studied.
2. Systemic cytokines cause glial activation, and reduce tau and drebrin in the hippocampus. Minocycline reverses these effects of cytokines, suggesting that it may be neuroprotective against cytokine storm.

Hong Kong Med J 2016;22(Suppl 4):S16-21

RFCID project number: 09080822

<sup>1</sup> DCH Poon, <sup>2</sup> YS Ho, <sup>1</sup> CF Lau, <sup>1</sup> K Chiu, <sup>1,3,4</sup> RCC Chang

*The University of Hong Kong:*

<sup>1</sup> Laboratory of Neurodegenerative Diseases, School of Biomedical Sciences

<sup>2</sup> School of Nursing, Faculty of Health and Social Sciences, The Hong Kong Polytechnic University

<sup>3</sup> Research Centre of Heart, Brain, Hormone and Healthy Aging, LKS Faculty of Medicine

<sup>4</sup> State Key Laboratory of Brain and Cognitive Sciences

\* Principal applicant and corresponding author: rccchang@hku.hk

## Introduction

Influenza leads to complications not only in the respiratory tract, but also within the central nervous system (CNS). These influenza-related neurological complications (INCs) include encephalopathy, encephalitis, and seizures, and affect up to 20% of hospitalised children diagnosed with influenza in Hong Kong. Febrile seizure is the most common type of INC.

One process that regulates INCs is the induction of cytokine storm during influenza.<sup>1</sup> A cytokine storm is an over-reactive immune response characterised by drastic elevations of many systemic inflammatory mediators. It has been suggested as the cause of multiple organ failure and high mortality during the 1918 and 2009 influenza pandemics. Infection with influenza viruses has been reported to hyper-induce an array of cytokines, ie IL-1 $\beta$ , IL-6, and TNF- $\alpha$ , IFN- $\alpha$ , and IFN- $\gamma$ , and chemokines, ie IL-8, MIG, IP-10, MCP-1, and MIP-1 $\alpha$ ,<sup>2</sup> all of which can potentially influence the brain to affect mood, behaviour, and cognition.<sup>3</sup> Both humoral and/or neural routes are believed to participate in relaying systemic cytokine responses to the brain.<sup>3</sup> We hypothesise that in the course of influenza infection, the generation of cytokine storm can lead to CNS neural and glial changes that may collectively mediate INCs.

Minocycline is a Food and Drug Administration-approved, second-generation, semi-synthetic tetracycline analogue that exerts antimicrobial, anti-inflammatory, and anti-apoptotic properties. It is well tolerated by humans in the

treatment of acne vulgaris, rheumatoid arthritis, and certain sexually transmitted diseases. Moreover, it is a strong inhibitor of microglial activity and readily penetrates the blood-brain-barrier. Its efficacy in treating various neurodegenerative disorders has been tested in animal models and clinical trials. Its neuroprotective properties have been reported in patients with cerebral ischaemia, spinal cord injury, multiple sclerosis, amyotrophic lateral sclerosis, Parkinson's disease, Huntington's disease, and Alzheimer's disease. Nonetheless, conflicting results have also been reported. We aimed to investigate whether minocycline protects against INCs by focusing on (1) the impacts of cytokine storm, which develops during influenza infection, on the brain, and (2) whether minocycline can attenuate or even reverse these changes.

## Methods

This study was conducted from October 2009 to March 2012. We injected a mixture of cytokines (IL-1 $\beta$ , TNF- $\alpha$ , IL-6, IL-8, IFN- $\alpha$ , MCP-1, MIP-1 $\alpha$ ) intraperitoneally into young male Sprague-Dawley rats to serve as a model of cytokine storm. Minocycline (25 mg/rat) was fed immediately before the injection, and the rats were sacrificed and their brains collected 1 day later to assess whether minocycline could modulate the changes in the hippocampus induced by mixed cytokines.

## Reagents and test substances

All recombinant cytokines, ie rat IL-1 $\beta$ /IL-1F2, rat TNF- $\alpha$ /TNFSF1A, rat IL-6, rat IFN- $\alpha$ , human

CXCL8/IL-8, rat CCL2/JE/MCP-1, and human CCL3/MIP-1 $\alpha$  were purchased from R&D Systems (Minneapolis [MN], USA). Minocycline hydrochloride, mouse monoclonal anti-GFAP and monoclonal anti-GAPDH antibodies, and rabbit polyclonal anti-drebrin antibody were from Sigma-Aldrich (St Louis [MO], USA). Rabbit polyclonal antibodies for p-Tau [pS396] and p-Tau [pT231], and Alexa Fluor-488 goat anti-rabbit IgG and Alexa Fluor-568 anti-mouse IgG antibodies were obtained from Invitrogen (Carlsbad [CA], USA). Rabbit polyclonal anti-Iba-1 antibody and mouse monoclonal anti-Tau-5 antibody were purchased from Wako Pure Chemical Industries (Osaka, Japan) and BD PharMingen (California, USA), respectively. Horseradish peroxidase-conjugated goat anti-rabbit and goat anti-mouse antibodies, and anti-fade fluorescent mounting medium were from DAKO (Glostrup, Denmark). The protein content assay kit and polyvinylidene fluoride membrane were obtained from Bio-Rad (Hercules [CA], USA). Enhanced chemiluminescence (ECL) detection kit was from Amersham (Buckinghamshire, UK).

### Animal procedures

All animal procedures were approved by the Committee on the Use of Live Animals in Teaching and Research of the University of Hong Kong. Briefly, male Sprague-Dawley rats (~250 g) were purchased from the Laboratory Animal Unit of the LKS Faculty of Medicine in the University of Hong Kong and housed with three rats per cage. They were maintained in a temperature-controlled room with a 12-hour light/dark cycle, and were allowed to acclimatise for 3 days before the start of the experiment. On the day of the experiment, the rats were randomly divided into four groups: control (n=6), mixed cytokines alone (n=5), minocycline alone (n=5), and mixed cytokines plus minocycline (n=5). All feeding and injection procedures were performed at 11:00 am. Minocycline hydrochloride was dissolved in distilled water to a concentration of 50 mg/mL. Rats were then orally fed with either 500  $\mu$ L water or 500  $\mu$ L of the minocycline solution (ie 25 mg/rat of minocycline), immediately followed by an intraperitoneal injection of 500  $\mu$ L phosphate buffered saline (PBS) or mixed cytokines (500 ng/kg IL-1 $\beta$ , 100 ng/kg TNF- $\alpha$ , 500 ng/kg IL-6, 500 ng/kg IL-8, 500 IU/kg IFN- $\alpha$ , 20 ng/kg MCP-1, and 10 ng/kg MIP-1 $\alpha$ , in PBS). Rats were returned to their home cage, and 24 hours later were sacrificed by an overdose of sodium pentobarbital. They were perfused with saline for 3 minutes, and brains were quickly removed and microdissected on ice. The right brain tissue was snap frozen in liquid nitrogen and stored at -80°C for western blot analysis. The left brain tissue was fixed in 4% paraformaldehyde at 4°C for 3 days before tissue processing.

### Tissue processing, immunofluorescence staining, and imaging

After fixation, brain tissue was dehydrated in a graded series of ethanol, cleared in xylene, and embedded in paraffin. It was cut into 6-micron coronal brain sections, dewaxed, and rehydrated. Antigen retrieval was performed by heating in 0.01 M citrate buffer (pH 6.0) with 0.1% Tween-20 at 95°C for 15 minutes. Subsequently, sections were washed in PBS. Non-specific binding between antibodies and tissues was blocked by 10% normal goat serum in PBS for 1.5 hours. Sections were incubated with primary antibodies for Tau-5 (1:400), drebrin (1:400), Iba-1 (1:500), and glial fibrillary acidic protein (GFAP) (1:500) at 4°C overnight, washed with PBS, then Alexa Fluor-488 or -568 added for 1.5 hours. Subsequently, sections were washed with PBS, stained with 4',6-diamidino-2-phenylindole (DAPI) for 15 minutes, washed again, and mounted with anti-fade fluorescent mounting medium. Finally, sections were examined using confocal microscopy (Figs 1 & 2) and under a Zeiss Axioplan 2 microscope with a 20X or 40X objective (Figs 3 & 4).

### Western blot analysis

Brain tissue was homogenised in ice-cold lysis buffer containing 10 mM Tris-HCl (pH 7.4), 1 mM NaCl, 20 mM Na<sub>4</sub>P<sub>2</sub>O<sub>7</sub>, 2 mM Na<sub>3</sub>VO<sub>4</sub>, 1% Triton-X-100, 10% glycerol, 0.5% deoxycholate, 0.1% SDS, 1 mM phenylmethylsulfonyl fluoride, protease inhibitor cocktail and phosphatase inhibitor cocktail, centrifuged at 14 000 g at 4°C for 30 minutes, and the supernatant collected. The protein in the cell lysates was quantified using the protein content assay kit. Afterwards, samples from the same group (n=5/6) were mixed, subjected to SDS 10% polyacrylamide gel electrophoresis at 140V, and transferred to polyvinylidene fluoride membranes. Non-specific binding on the membranes was blocked by 5% non-fat milk in TBST (TBS-containing 0.1% Tween-20) for 1 hour. Primary antibodies were diluted in TBST and incubated with the membrane as follows: p-Tau [pT231] (1:3000), p-Tau [pS396] (1:4000), Tau-5 (1:2000), drebrin (1:4000), glyceraldehyde 3-phosphate dehydrogenase (GAPDH) (1:20 000). After washing, the membranes were incubated with horseradish peroxidase-conjugated secondary antibodies for 1 hour and subsequently developed using the ECL western blotting detection kit. Densitometry measurements were made using Image J software (National Institutes of Health, USA). The band intensities were normalised against GAPDH and results were expressed as fold of control.

### Statistical analysis

Normalised band intensities were analysed by one-way ANOVA, followed by Student-Newman-

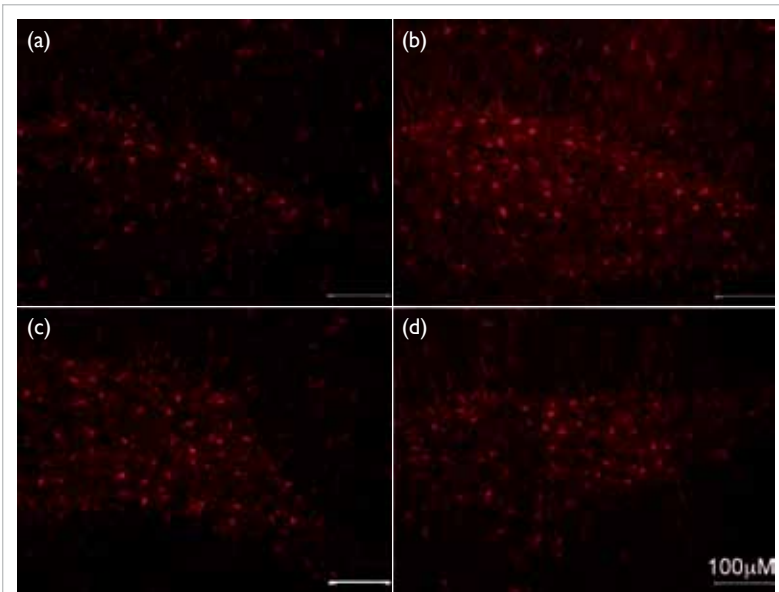


**FIG 1.** Fluorescent images of GFAP positive astrocytes 1 day post-treatment, in the dentate gyrus of rats treated with (a) control, (b) mixed cytokines, (c) 25 mg minocycline, and (d) 25 mg minocycline plus mixed cytokines. Minocycline attenuates the increase in GFAP immunoreactivity by mixed cytokines.

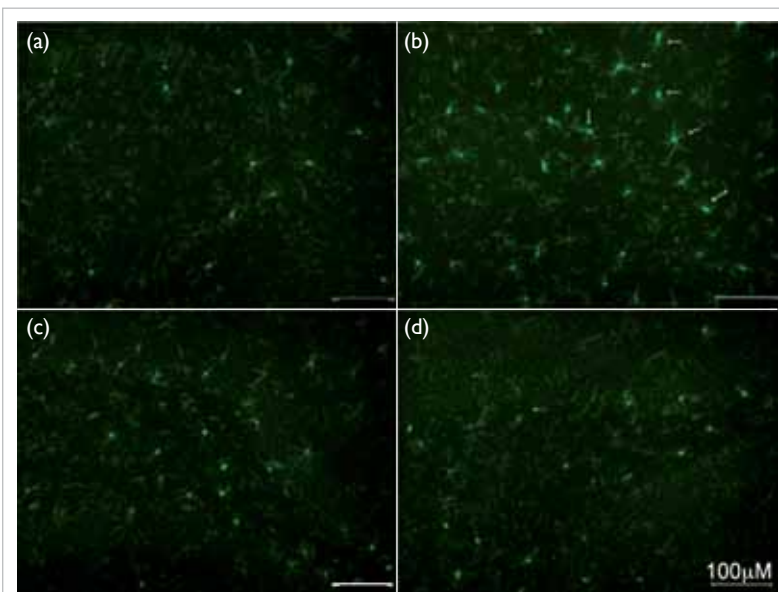


**FIG 2.** Fluorescent images of Iba-1 positive microglia 1 day post-treatment, in the dentate gyrus of rats treated with (a) control, (b) mixed cytokines, (c) 25 mg minocycline, and (d) 25 mg minocycline plus mixed cytokines. Arrows in (b) indicate activated microglia, ie hypertrophy of cell body, thickening of processes, in the mixed cytokine-treated rats. Minocycline reduces activation of microglia by mixed cytokines.

Keuls test using SigmaStat (Jandel Scientific [CA], USA). Results were considered to be significantly different if  $P < 0.05$ .

## Results

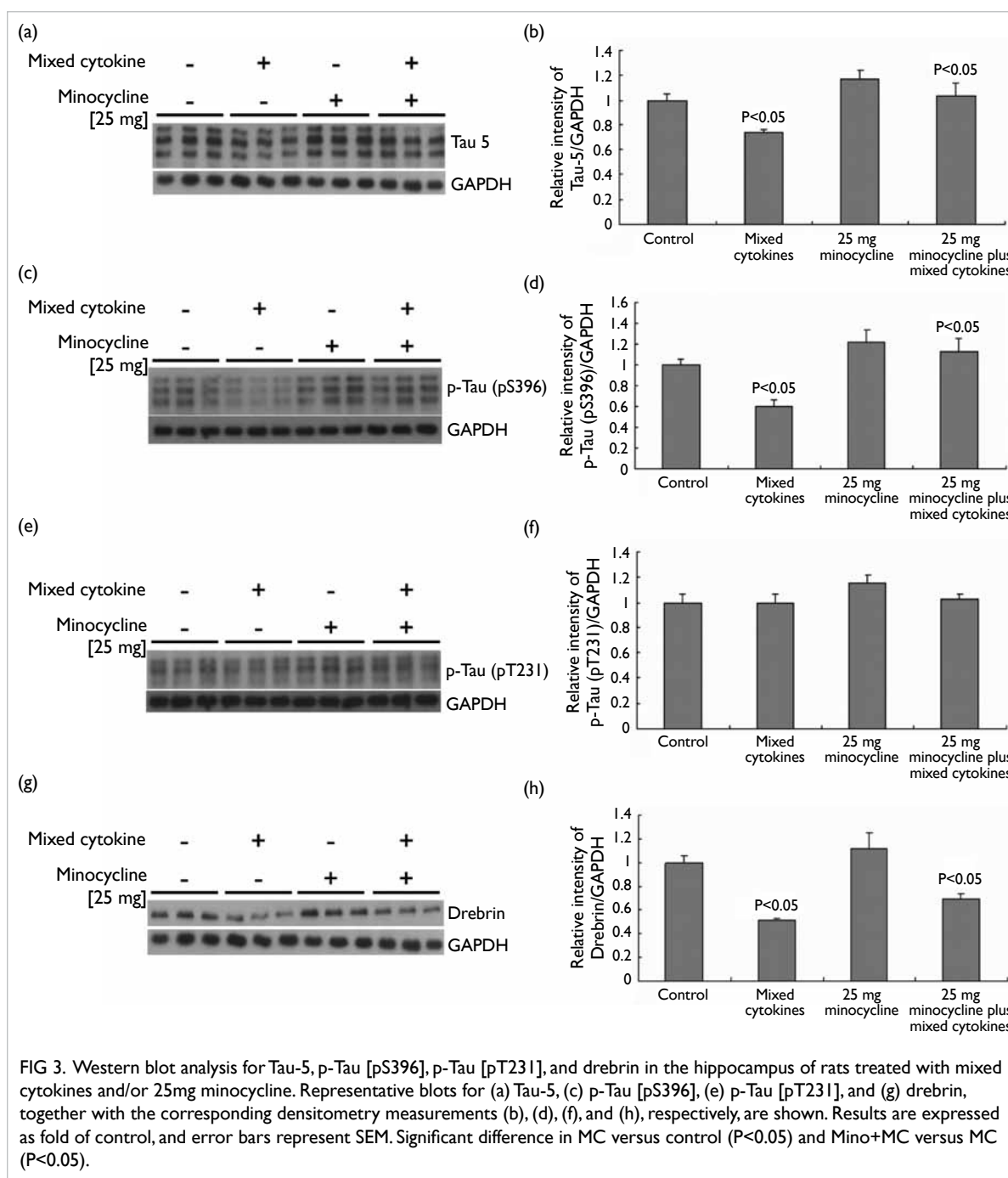
Mixed cytokines led to activation of microglia and astrocytes at the dentate gyrus, and treatment with minocycline appeared to reduce these phenomena. Moreover, mixed cytokines reduced both protein expression level and immunoreactivity of the cytoskeleton-associated proteins tau and drebrin, and decreased the phosphorylation of tau at serine-396 but precipitated no change at threonine-231. Minocycline significantly reversed, if not totally, the decrements in total tau, p-Tau (pS396), and drebrin by mixed cytokines. These results suggest that oral administration of minocycline can likely reverse the impact of cytokine storm on glia and the neuronal cytoskeleton in the brain. Future studies are encouraged to verify whether minocycline will be useful in alleviating INCs.

### Minocycline suppressed mixed cytokine-mediated glial activation

Systemic injection of mixed cytokines led to signs of astrocyte activation (ie increased GFAP immunoreactivity and astrocyte number versus the control) and microglial activation (ie cell body hypertrophy, and thickening of processes versus the control) within the dentate gyrus (Fig 1). Minocycline alone did not induce any observable differences in cell morphology or cell numbers of astrocytes and microglia (Figs 1 and 2). When rats were co-treated with mixed cytokines and minocycline, there was decreased astrocyte and microglia activation compared with the mixed cytokine group (Figs 1 and 2).

### Minocycline reversed the reduction in Tau-5 and p-Tau [pS396] immunoreactivities caused by mixed cytokines

We performed western blot analysis (Fig 3) and immunofluorescence staining (Fig 4) for Tau-5, which serves as an index for total Tau. Mixed cytokines reduced Tau-5 protein immunoreactivity to  $0.74 \pm 0.02$ -fold ( $P < 0.05$  versus control group). Although minocycline alone did not cause any change in Tau-5 protein immunoreactivity, eg  $1.17 \pm 0.07$ -fold, it did attenuate the reduction in Tau-5 mediated by mixed cytokines to  $1.03 \pm 0.1$ -fold ( $P < 0.05$  versus mixed cytokines group). Such changes in protein expression were accompanied by a similar change in Tau-5 immunoreactivity in the CA3 region. Mixed cytokines reduced Tau-5 immunoreactivity compared with that of the control. Minocycline alone did not appear to affect Tau-5 immunoreactivity, but did reduce the drop in immunoreactivity when it was co-treated with mixed cytokines. Moreover, it should be noted that in both the minocycline alone group and the co-treatment group, there was increased Tau-5 immunoreactivity



in the cell bodies of parenchymal cells.

We further verified if there was any change in the phosphorylation of Tau at serine-396 and threonine-231. Similar to the trend in Tau-5, mixed cytokines decreased the p-Tau [pS396] level to  $0.60\pm 0.07$ -fold ( $P<0.05$  versus control group). Minocycline alone did not elicit any effect, ie  $1.22\pm 0.11$ -fold, but could reverse the reduction in p-Tau [pS396] level when it was co-treated with mixed cytokines ( $1.13\pm 0.13$ -fold,  $P<0.05$  versus mixed cytokines group). There was no significant

difference in the p-Tau (pT231) level amongst all groups.

### Minocycline attenuated the decrease in drebrin protein expression and immunoreactivity induced by mixed cytokines

Mixed cytokines led to a significant decrease in the expression of drebrin (Fig 3) to  $0.51\pm 0.02$ -fold ( $P<0.01$  versus control group). Minocycline *per se* did not change expression of drebrin, ie  $1.12\pm 0.12$  fold. However, co-treatment of mixed cytokines

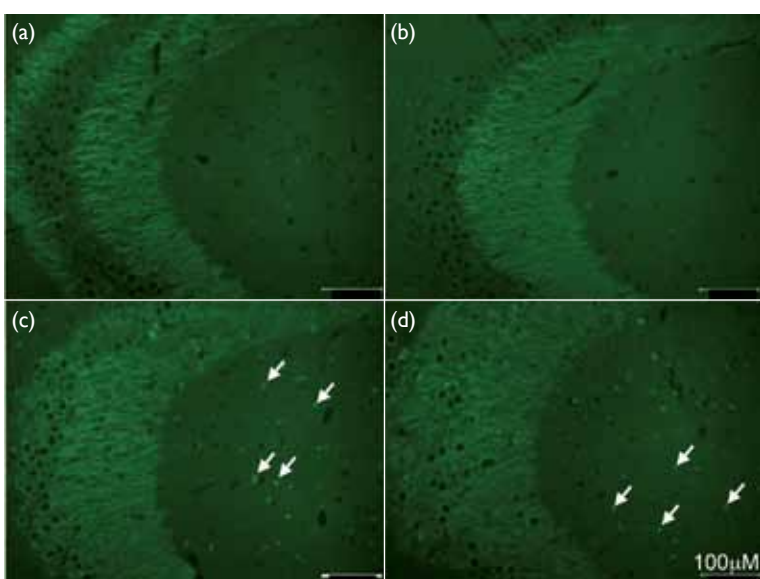


**FIG 4.** Fluorescent images of Tau-5 immunofluorescence staining, 1 day post-treatment, in the CA3 region of rats treated with (a) control, (b) mixed cytokines, (c) 25 mg minocycline, and (d) 25 mg minocycline plus mixed cytokines. Arrows indicate increased number of cells having Tau-5 immunoreactivity in the cell body of the Mino group and MC+Mino group. Minocycline reverses the drop of Tau-5 immunoreactivity by mixed cytokines.

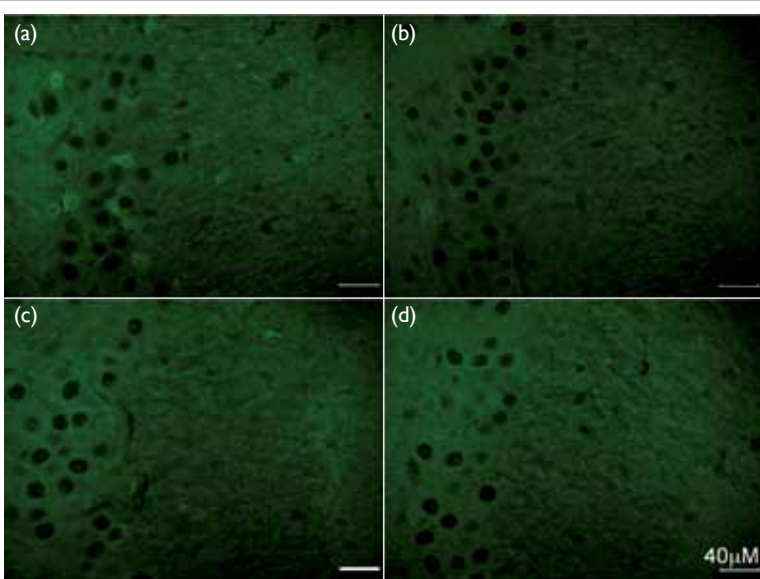


**FIG 5.** Fluorescent images of drebrin immunofluorescence staining, 1 day post-treatment, in the CA3 region of rats treated with (a) control, (b) mixed cytokines, (c) 25 mg minocycline, and (d) 25 mg minocycline plus mixed cytokines. Minocycline hinders the decrease in drebrin puncta number and immunoreactivity by mixed cytokines.

with minocycline could partially suppress the reduction of drebrin protein triggered by mixed cytokines to  $0.69 \pm 0.05$ -fold ( $P < 0.05$  versus mixed cytokines group). Such changes in drebrin protein

expression were associated with a similar pattern of immunofluorescent staining at the CA3 region (Fig 5). Mixed cytokines reduced the abundance of drebrin puncta and its immunoreactivity. Minocycline alone did not seem to alter these two parameters. When co-treated with mixed cytokines, minocycline abolished the drop in the abundance of drebrin puncta and its immunoreactivity by mixed cytokines.

## Discussion

In order to mimic cytokine storm, we injected intraperitoneally a mixture of cytokines comprised of IL-1 $\beta$ , IL-6, and TNF- $\alpha$ , IFN- $\alpha$ , IL-8, MCP-1, and MIP-1 $\alpha$ . We chose to inject these cytokines because they have demonstrated an increase in blood and in nasal fluids during influenza infection. We also used nanogram levels of cytokines because in the presence of influenza infection, these cytokines exist at concentrations of pg/ml in blood.<sup>2</sup> Based on the assumption that their *in-vivo* half-life ranges from minutes to hours, these cytokines would be able to last for hours *in-vivo* before they return to basal levels. We focused on any change that occurred within the hippocampus because damage in this region has been frequently reported in several models of seizure,<sup>4</sup> ie the most common neurological complication in patients with influenza.

Neuroinflammation is a common phenomenon that occurs in acute neurological complications, eg epilepsy, encephalitis, and encephalopathy, and in chronic neurodegenerative diseases, eg Alzheimer’s disease, Parkinson’s disease, and multiple sclerosis. Activation of astrocytes and microglia leads to production of inflammatory mediators such as cytokines, chemokines, and prostaglandins. These inflammatory mediators not only alter neurotransmitter, synaptic plasticity, neurotrophin signalling, and the cytoskeleton, but also influence mood, behaviour, and cognition.<sup>3</sup> We showed that systemic injection of mixed cytokines induced signs of astrocytic and microglial activation within the dentate gyrus. Oral feeding of minocycline attenuated this activation. These results imply that cytokine storm may cause glial activation, and may be inhibited by minocycline.

Tau protein associates with microtubules and stabilises them. In mature neurons, tau protein is predominately located along axons and is required for axonal growth and transport.<sup>5</sup> The binding of tau protein to microtubules is in turn regulated by its phosphorylation. We asked whether mixed cytokines could alter the level of total tau protein and/or its phosphorylation at the residues serine 396 and threonine 231, and if yes, could minocycline hinder such changes? To our surprise, mixed cytokines decreased the amount of total tau, as revealed by decreases in Tau-5 immunoreactivity and protein

expression. Minocycline treatment restored Tau-5 protein immunoreactivity and expression. Yet, it is notable that minocycline treatment, ie in both the minocycline group and co-treatment group, appeared to increase Tau-5 immunoreactivity in the cell bodies of parenchymal cells. Such disorganisation of tau protein into the cell body by minocycline was rather unexpected. Although the mis-sorting of tau protein into the cell body of neurons has been previously reported with beta-amyloid treatment, and it is thought to be undesirable,<sup>5</sup> we are not sure whether this indicates a negative impact of minocycline in our model, and have not validated the cell type of these cells. In addition, mixed cytokines reduced the p-Tau [pS396] level and minocycline was able to attenuate it. Based on these results, we suggest that in our model mixed cytokines may have affected the dynamics of tau protein, and minocycline may have hindered these effects.

Apart from tau protein, we also studied whether mixed cytokines altered drebrin, which is a binding protein of F-actin, the major cytoskeleton in dendritic spines.<sup>6</sup> Drebrin regulates spine plasticity: overexpression of drebrin leads to elongation of dendritic spines in mature neurons,<sup>7</sup> whereas down-regulation of drebrin expression by antisense oligonucleotides reduces the width and density of filopodia-spines in developing neurons.<sup>8</sup> Our results showed that mixed cytokines decreased both drebrin immunoreactivity at the CA3 region and protein expression. Minocycline was able to attenuate such decrements induced by mixed cytokines. Such data raise the possibility that cytokine storm could modulate synaptic plasticity and spine morphogenesis, and minocycline may remove this modulation.

Therefore, it could be seen that mixed cytokines induced activation of glia, and changes in the cytoskeleton-associated proteins tau and drebrin in the hippocampus 1 day post-treatment. An oral dose of minocycline at the time of mixed cytokine injection was able to inhibit glial activation and cytoskeleton-related changes. Although these results may suggest that minocycline can be effective in tackling glial activation and the neuronal cytoskeletal changes induced by cytokine storm, one should take into account several points before jumping to this conclusion. Firstly, minocycline was administered at the same time as mixed cytokines. In a clinical setting, a patient's cytokine storm will have been present for 1-2 days before the medical consultation. Hence, the toxicity of cytokine storm on the brain would have proceeded such that minocycline is no longer of any benefit. Secondly, rats were sacrificed 1 day post-

injection, but cytokine storm during influenza can last for up to 7 days. Hence, the experiment could be extended and include multiple injections of mixed cytokines and multiple oral doses of minocycline throughout the study period. This is particularly important because a longer cytokine storm could likely lead to more severe toxicity to the brain, and drug resistance to minocycline could develop after several doses and limit its effectiveness.

Based on these results, we believe that minocycline is probably protective against the neuropathological impact of cytokine storm. Future studies should verify whether minocycline relieves the neurological complications caused by influenza infection.

## Acknowledgements

This study was supported by the Research Fund for the Control of Infectious Diseases, Food and Health Bureau, Hong Kong SAR Government (#09080822), HKU Alzheimer's Disease Research Network under Strategic Research Theme on Healthy Aging, Seed Funding for Basic Science Research (201111159160) and Small Project Funding (201007176112).

## References

1. Sellner J, Leib SL. Flu-related neurological complications: incidence and risk factors in children. *Nat Clin Pract Neurol* 2007;3:606-7.
2. de Jong MD, Simmons CP, Thanh TT, et al. Fatal outcome of human influenza A (H5N1) is associated with high viral load and hypercytokinemia. *Nat Med* 2006;12:1203-7.
3. Dantzer R, O'Connor JC, Freund GG, Johnson RW, Kelley KW. From inflammation to sickness and depression: when the immune system subjugates the brain. *Nat Rev Neurosci* 2008;9:46-56.
4. Jung KH, Chu K, Lee ST, et al. Cyclooxygenase-2 inhibitor, celecoxib, inhibits the altered hippocampal neurogenesis with attenuation of spontaneous recurrent seizures following pilocarpine-induced status epilepticus. *Neurobiol Dis* 2006;23:237-46.
5. Zempel H, Thies E, Mandelkow E, Mandelkow EM. Abeta oligomers cause localized Ca(2+) elevation, missorting of endogenous Tau into dendrites, Tau phosphorylation, and destruction of microtubules and spines. *J Neurosci* 2010;30:11938-50.
6. Ivanov A, Esclapez M, Ferhat L. Role of drebrin A in dendritic spine plasticity and synaptic function: Implications in neurological disorders. *Commun Integr Biol* 2009;2:268-70.
7. Hayashi K, Shirao T. Change in the shape of dendritic spines caused by overexpression of drebrin in cultured cortical neurons. *J Neurosci* 1999;19:3918-25.
8. Takahashi H, Sekino Y, Tanaka S, Mizui T, Kishi S, Shirao T. Drebrin-dependent actin clustering in dendritic filopodia governs synaptic targeting of postsynaptic density-95 and dendritic spine morphogenesis. *J Neurosci* 2003;23:6586-95.

# Modulation of cell signalling by human coronavirus HKU1 S and M proteins

DY Jin \*, PCY Woo

## KEY MESSAGES

1. S proteins of both SARS-CoV and HCoV-HKU1 share a similar profile of unfolded protein response (UPR)-activating activity. They activate the production of UPR effector proteins Grp78/94 and to a lesser extent CHOP through PERK kinase.
2. S proteins of SARS-CoV and HCoV-HKU1 have distinct UPR-activating domains. Whereas the UPR-activating activity requires the central region (amino acids 201-400) of the S1 subunit in SARS-CoV, the corresponding part in the HCoV-HKU1 S protein does not induce endoplasmic reticulum stress or UPR.
3. Suppression of type I interferon (IFN) production is a unique property of SARS-CoV M protein. HCoV-HKU1 M protein does not inhibit the innate IFN response.
4. IFN antagonism of SARS-CoV M protein is ascribed to its first transmembrane domain (TM1) situated at the N terminus. TM1 targets M protein to the Golgi complex and interacts with TRAF3 and other transducer proteins to prevent the formation of a functional TRAF3-containing multi-component complex.

Hong Kong Med J 2016;22(Suppl 4):S22-4

RFCID project number: 10091192

<sup>1</sup> DY Jin, <sup>2</sup> PCY Woo

*The University of Hong Kong:*

<sup>1</sup> School of Biomedical Sciences

<sup>2</sup> Department of Microbiology

\* Principal applicant and corresponding author: dyjin@hku.hk

## Introduction

In 2003, an outbreak of severe acute respiratory syndrome (SARS) occurred in Hong Kong and spread worldwide. The SARS coronavirus (SARS-CoV) caused a highly lethal disease and disproved the concept that human coronaviruses are generally associated with mild respiratory disease. Another new coronavirus—HCoV-HKU1—that circulates commonly in the human population and causes relatively milder respiratory tract illness worldwide was also discovered.<sup>1</sup> The mechanism by which SARS-CoV and HCoV-HKU1 cause respiratory diseases of different severity remains elusive. Variations in their ability to modulate cell signalling and innate immunity might be influential.<sup>2</sup>

Human coronaviruses are enveloped and positive-stranded RNA viruses with a large genome. They hijack the endoplasmic reticulum (ER) to process their structural and non-structural proteins produced in extraordinarily large amounts. They also need to circumvent the production and function of type I interferons (IFNs), major effectors of innate antiviral immunity. We have demonstrated the capability of SARS-CoV S protein to induce ER stress and to activate the unfolded protein response (UPR).<sup>3</sup> We have also found that SARS-CoV M protein suppresses innate IFN production by impeding the formation of a functional complex of tumour necrosis factor receptor-associated factor 3 (TRAF3) - TRAF family member-associated NF- $\kappa$ B activator (TANK) - TANK-binding kinase

1(TBK1)/ inhibitor of nuclear factor  $\kappa$ B kinase subunit  $\epsilon$  (IKK $\epsilon$ ).<sup>4</sup> In the present study, we set out to determine whether HCoV-HKU1 S and M proteins homologous to their counterparts in SARS-CoV might have similar properties. We also mapped the functional domains in SARS-CoV S and M proteins that are required for their respective UPR-activating and IFN-antagonising activity.

## Methods

This study was conducted from January 2011 to December 2012. HCoV-HKU1 may be cultured in primary human ciliated airway epithelial cells.<sup>5</sup> Nonetheless, success was limited and the virus remains unculturable in most laboratories. Lack of an infectious clone of HCoV-HKU1 further hampers functional analysis. At this stage, mechanistic studies could only be performed through analysis of cloned HCoV-HKU1 S and M genes as well as their mutants. Therefore, all experiments were carried out with cultured HEK293 or 293FT cells transiently transfected with expression vectors for SARS-CoV and HCoV-HKU1 S and M proteins or their truncated mutants.

## Results

### UPR activation by SARS-CoV and HCoV-HKU1 S proteins

We have reported the activation of binding immunoglobulin protein (Grp78) and heat shock

protein 90kDa beta member 1 (Grp94) promoters by SARS-CoV S protein.<sup>2</sup> Grp78 and Grp94 are robust UPR markers. They function as molecular chaperones and are swiftly induced in the UPR. We found that the transcriptional activity driven by the Grp94 promoter was stimulated to a similar extent by S proteins of both SARS-CoV and HCoV-HKU1 (Fig 1). HCoV-HKU1 S protein activated the Grp94 promoter in a dose-dependent manner and with equal potency when compared with SARS-CoV S protein. For another comparison,  $\beta$ -galactosidase was also overexpressed. The activity of Grp94 promoter was minimally or very mildly affected by this large foreign protein. Similar results were obtained with the Grp78 promoter and to a lesser extent with the DNA damage-inducible transcript 3 (C/EBP homologous protein; CHOP) promoter. Activation of Grp78 and Grp94 promoters by S proteins required eukaryotic translation initiation factor 2-alpha kinase 3 (PERK) kinase. Thus, S proteins from both coronaviruses exhibited similar activity to induce ER stress and to activate UPR signalling.

### Definition of UPR-activating domain in S protein of SARS-CoV

SARS-CoV S protein is proteolytically processed into S1 and S2 subunits. To determine whether

the S1 (amino acids 1-770) or S2 (amino acids 771-1255) subunit is required for UPR activation by SARS-CoV S protein, we compared them side by side for activation of Grp78 and Grp94 promoters. The activity of Grp78 and Grp94 promoters was not affected by S2, but induced fully by S1. To compare with HCoV-HKU1 S protein, the cleavage of which inside cells remains uncertain, similar regions matching the S1 and S2 subunits of SARS-CoV S protein were interrogated for their ability to activate Grp78 and Grp94 promoters. Neither S1 nor S2 of HCoV-HKU1 was capable of activating these promoters. The UPR-activating domain in SARS-CoV S1 subunit was further dissected to the central region (amino acids 201-400).

### Suppression of type I IFN production by M protein of SARS-CoV, but not HCoV-HKU1

We have demonstrated that SARS-CoV M protein is capable of antagonising type I IFN production.<sup>3</sup> To assess whether HCoV-HKU1 M protein behaves similarly, we compared the two M proteins for their ability to induce IFN- $\beta$ . We used mitochondrial antiviral-signalling protein (MAVS), a mitochondrial adaptor protein that transmits the activation signal, to boost IFN production. The steady-state level of IFN- $\beta$  transcript in transfected HEK293 cells

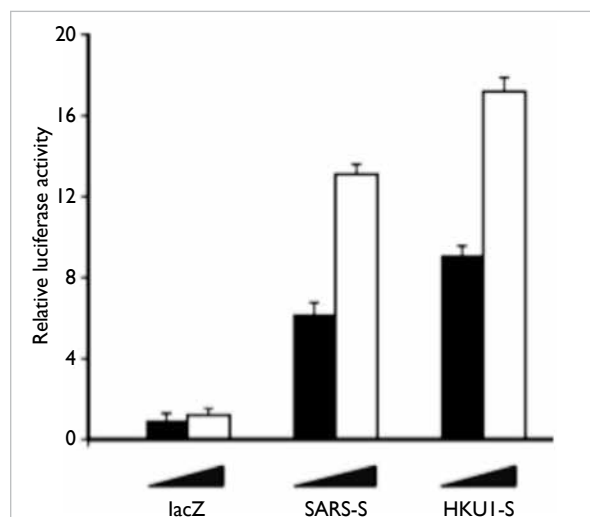


FIG 1. Activation of UPR signalling by S proteins: 293FT cells were transfected with the indicated pGrp94-Luc luciferase reporter and expression constructs. Cells were harvested 36 hours after transfection and dual luciferase assay was performed. Amounts of expression plasmids for lacZ and S proteins were progressively increased. Relative luciferase activity was derived from readouts of firefly luciferase activity normalised to readouts of *Renilla* luciferase activity. Activity recovered from cells receiving lacZ vector alone was set as 1. Results represent means from triplicate experiments with error bars indicating the SD (Reproduced with permission from the Cell and Bioscience and the Cellular and Molecular Immunology).

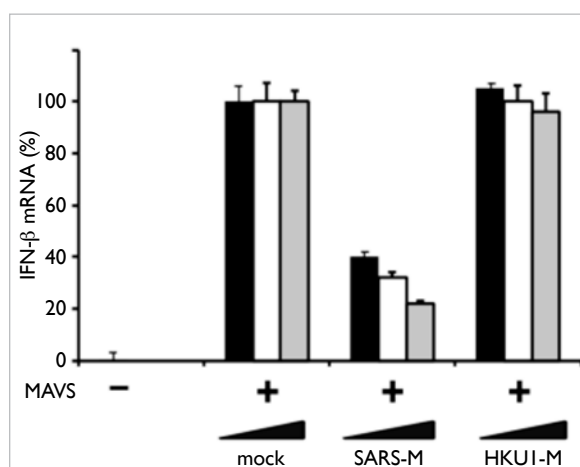


FIG 2. Inhibition of IFN- $\beta$  production by M protein of SARS-CoV (SARS-M) but not of HCoV-HKU1 (HKUI-M): HEK293 cells were transfected with the indicated plasmids and harvested at 30 hours after transfection. Real-time RT-PCR was carried out to quantify the levels of IFN- $\beta$  and glyceraldehyde 3-phosphate dehydrogenase (GAPDH) transcripts. A fixed amount of MAVS expression vector and progressively escalating amounts of SARS-M and HKUI-M expression plasmids were used. Relative expression levels of IFN- $\beta$  mRNA were derived from  $2^{-C_t(\text{GAPDH}) - C_t(\text{IFN-}\beta)}$  and normalised to levels from cells mock-transfected with empty expression vector, which were set as 100% (Reproduced with permission from the Cell and Bioscience and the Cellular and Molecular Immunology).

expressing or not expressing SARS-CoV and HCoV-HKU1 M proteins was then monitored by real-time RT-PCR. Interestingly, M protein of SARS-CoV but not of HCoV-HKU1 mitigated the IFN-inducing activity of MAVS (Fig 2). Similar results were also obtained with RIG-I and TBK1. Additional luciferase reporter assays lent further support to the notion that suppression of IFN production by M protein is specific to SARS-CoV and not seen in HCoV-HKU1.

### IFN antagonism is mediated through TM1 of SARS-CoV M protein

Three transmembrane domains (TM1: 1-38 amino acids; TM2: 51-69 residues; and TM3: 76-85 residues) followed by a cytoplasmic endodomain (86-221 amino acids) are found in SARS-CoV M protein. To map the IFN-antagonising domain in SARS-CoV M protein, a series of truncated mutants designated M1, M2, TM1', TM2' and TM3' were constructed and tested in a stepwise approach. First, the three TMs in M1 were indispensable for the suppression of IFN production by SARS-CoV M protein. Second, TM1 of the three TMs was absolutely required for IFN antagonism. Among the three mutants named TM1', TM2' and TM3', which respectively contain TM1 (amino acids 1-38), TM2 (amino acids 51-69) and TM3 (amino acids 76-85) domains fused to the endodomain for the purpose of maintaining protein stability, only TM1' was able to suppress IFN- $\beta$  promoter activity activated by RIG-I, MAVS or TBK1. Neither TM2' nor TM3' showed any IFN-antagonising activity. Since TM2, TM3 and endodomain were not required for IFN antagonism, only TM1 was essential and probably sufficient for the suppressive effect on IFN production.

### Discussion

We compared the UPR-activating and IFN-antagonising activities of S and M proteins of SARS-CoV and HCoV-HKU1. The two S proteins displayed a similar profile of UPR-activating properties with the ability to activate Grp78, Grp94 and CHOP promoters but not UPR element enhancer. The two S proteins also possessed a distinct UPR-activating domain. The S1 subunit of SARS-CoV sufficed to activate the UPR, but no UPR-modulating activity was seen in its counterpart in HCoV-HKU1. Although SARS-CoV and HCoV-HKU1 S proteins had distinct UPR-activating domains, they exerted similar modulatory effects on UPR signalling.

Our findings on the activation of UPR by SARS-CoV and HCoV-HKU1 S proteins have important implications for therapeutic intervention. Pharmaceutical UPR modulators have been developed and extensively tested for diseases including viral infection. Inhibition of PERK

kinase has a negative impact on cytomegalovirus replication, but a small-molecule UPR activator also displays broad-spectrum antiviral activity. In this regard, our analysis of the activation of UPR by S proteins might lay the foundation for further assessment of the utility of UPR modulators for the treatment of SARS and HCoV-HKU1 infection.

SARS-CoV M protein does not share its IFN-antagonising property with HCoV-HKU1 M protein. Its IFN antagonism is mediated by the TM1 domain (amino acids 1-38), which targets it to the Golgi apparatus where it associates with TRAF3 to impede the interaction with TBK1 and IKK $\epsilon$ . Our findings provide additional molecular details for suppression of IFN production by SARS-CoV M protein. Our definition of a small TM1 domain that mediates immune evasion will pave the way for rational design and development of new immunosuppressive agents. In this regard, both peptide mimetics and recombinant proteins that mimic the action of TM1 might prove useful.

### Acknowledgements

This study was supported by the Research Fund for the Control of Infectious Diseases, Food and Health Bureau, Hong Kong SAR Government (#10091192).

Results of this study have been published in: (1) Siu KL, Chan CP, Kok KH, Woo PC, Jin DY. Comparative analysis of the activation of unfolded protein response by spike proteins of severe acute respiratory syndrome coronavirus and human coronavirus HKU1. *Cell Biosci* 2014;4:3. (2) Siu KL, Chan CP, Kok KH, Chiu-Yat Woo P, Jin DY. Suppression of innate antiviral response by severe acute respiratory syndrome coronavirus M protein is mediated through the first transmembrane domain. *Cell Mol Immunol* 2014;11:141-9.

### References

1. Woo PC, Lau SK, Chu CM, et al. Characterization and complete genome sequence of a novel coronavirus, coronavirus HKU1, from patients with pneumonia. *J Virol* 2005;79:884-95.
2. Tatura AL, Baric RS. SARS coronavirus pathogenesis: host innate immune responses and viral antagonism of interferon. *Curr Opin Virol* 2012;2:264-75.
3. Chan CP, Siu KL, Chin KT, Yuen KY, Zheng B, Jin DY. Modulation of the unfolded protein response by severe acute respiratory syndrome coronavirus spike protein. *J Virol* 2006;80:9279-87.
4. Siu KL, Kok KH, Ng MH, et al. Severe acute respiratory syndrome coronavirus M protein inhibits type I interferon production by impeding the formation of TRAF3-TANK-TBK1/IKKepsilon complex. *J Biol Chem* 2009;284:16202-9.
5. Dijkman R, Jebbink ME, Koekkoek SM, et al. Isolation and characterization of current human coronavirus strains in primary human epithelial cell cultures reveal differences in target cell tropism. *J Virol* 2013;87:6081-90.

# Antibody-dependent enhancement of SARS coronavirus infection and its role in the pathogenesis of SARS

MS Yip, HL Leung, PH Li, CY Cheung, I Dutry, D Li, M Daëron, R Bruzzone, JSM Peiris, M Jaume \*

## KEY MESSAGES

1. Anti-SARS-CoV spike antibodies promote infection of primary human immune cells by SARS-CoV.
2. The antibody-dependent enhancement (ADE) infection pathway grants SARS-CoV an opportunity to infect primary human macrophages, but it does not sustain productive viral replication in the infected cells.
3. ADE of SARS-CoV infection does not alter pro-inflammatory gene expression profile of primary human macrophages.
4. Infectivity of SARS-CoV does not rely solely on the potency of target cells to bind - via Fcγ receptor II (CD32) - infectious immune complexes, but depends on the properties of the intracellular domain of the FcγRII.
5. Occurrence of ADE of SARS-CoV infection into

human primary macrophages, without alteration to their pro-inflammatory properties, advocates cautious development of SARS-CoV vaccine in humans, and provides new ways of investigation to understand the pathogenesis of SARS.

Hong Kong Med J 2016;22(Suppl 4):S25-31

RFCID project number: 09080872

<sup>1,2</sup> MS Yip, <sup>1,2</sup> HL Leung, <sup>1,2</sup> PH Li, <sup>2</sup> CY Cheung, <sup>1,2</sup> I Dutry, <sup>1,2</sup> D Li, <sup>3,4</sup> M Daëron, <sup>1,2,5</sup> R Bruzzone, <sup>1,2</sup> JSM Peiris, <sup>1,2</sup> M Jaume

<sup>1</sup> HKU-Pasteur Research Pole, The University of Hong Kong

<sup>2</sup> School of Public Health, The University of Hong Kong

<sup>3</sup> Institut Pasteur, Département d'Immunologie, Unité d'Allergologie Moléculaire et Cellulaire, Paris, France

<sup>4</sup> Inserm, Unité 760, Paris, France

<sup>5</sup> Institut Pasteur, Department of Cell Biology and Infection, Paris, France

\* Principal applicant and corresponding author: Martial.Jaume@gmail.com

## Introduction

Infection with SARS-CoV involves not only the respiratory tract but also the gastrointestinal tract and other organ systems. Several reports have highlighted the direct infection of haematopoietic cells by SARS-CoV. It is unclear how the virus gets into immune cells that do not express the SARS-CoV receptor angiotensin I converting enzyme 2 (ACE2).

Immune-mediated infections and, in particular, antibody-dependent enhancement (ADE) is known to be exploited by a variety of viruses, such as dengue virus, HIV, and animal coronavirus, as an alternative way to infect host cells.<sup>1</sup> In addition to an interaction between viral protein and host receptors, these viruses can enter cells through the binding of virus/antibody immune-complexes to Fc receptors (FcR), complement receptors, or alternatively by inducing conformational change in envelope glycoproteins that are required for virus-cell membrane fusion.<sup>1</sup>

We have demonstrated that anti-spike antibodies potentiate infection of both monocytic and lymphoid human immune cell lines with SARS-CoV Spike-pseudotyped lentiviral particles (recombinant viruses encoding a reporter gene and bearing SARS-CoV Spike proteins at the virion surface; SARS-CoVpp) and also with replication-competent SARS-coronavirus.<sup>2</sup> Because antibody-

mediated infection accounts for the altered response to infection, we hypothesised that ADE of SARS-CoV infection—by widening SARS-CoV tropism toward immune cells—would elicit a hyper-induced profile of immune mediators (cytokine/chemokines) that would impair the homeostasis of the immune system and ultimately contribute to SARS pathogenesis.

This study highlighted the occurrence of ADE of SARS-CoVpp infection in different circulating immune cell types, among which the monocytic lineage was a prime target. In addition to monocytes, infection of human macrophages was enhanced in the presence of anti-viral antibodies. Despite being increasingly susceptible to infection, macrophages did not support productive replication of the virus, or modify expression of some pro-inflammatory cytokines/chemokines upon antibody-mediated invasion. Our findings point towards the likely occurrence of ADE infection of immune cells by SARS-CoV, but the outcomes of such an alternative infection pathway on the cell functionality/homeostasis remain unclear.

## Methods

This study was conducted from October 2009 to September 2011.

### Cell lines and primary human immune cell cultures

VeroE6 (African green monkey kidney epithelial cells), Raji (Burkitt's lymphoma/B lymphoblast), parental ST486 (Burkitt's lymphoma/B lymphoblast lacking expression of FcγR) and FcγR/ST486 were cultured as previously described.<sup>2</sup>

Peripheral blood mononuclear cells (PBMCs) were prepared from human buffy coats of healthy blood donors (Hong Kong Red Cross Blood Transfusion Service). The research protocol was approved by the Institutional Review Board of the University of Hong Kong/Hospital Authority Hong Kong West Cluster (UW09-375). Monocyte-derived macrophages were generated *in vitro* using standard protocol. Briefly, mononuclear cells were isolated by a Ficoll-Paque density gradient (Pharmacia Biotech) and monocytes were enriched by plastic adherence. Alternatively, CD14<sup>+</sup> purified mononuclear cells were prepared by positive magnetic bead selection (Miltenyi biotec). Cells were then seeded on tissue culture plates in RPMI 1640 medium supplemented with 5% heat-inactivated autologous plasma, 0.6 mg/L penicillin and 60 mg/L streptomycin at 10<sup>6</sup> cells/mL (Life Technologies). The cells were replenished with fresh medium every 2 days and allowed to differentiate for 14 days. The purity of macrophages was consistently above 90%, as ascertained by immunofluorescence staining for human CD68 (macrosialin/gp110). Depending on the downstream application, macrophages were either seeded on a glass-cover slip or in an appropriate culture vessel the day before infection. All cells were maintained in a humidified atmosphere at 37°C with 5% CO<sub>2</sub> supply.

### Immunisation with recombinant spike proteins or inactivated SARS-CoV

Recombinant SARS-CoV spike protein production and immunisation procedure have been described.<sup>2</sup> Six- to 8-week-old BALB/c mice (n=4-5 per group) were immunised intraperitoneally at 3-week intervals with 2 μg of FLAG-tagged recombinant codon-optimised SARS-CoV spike full-length or injected with saline solution emulsified with 1 mg of alum. Sera were collected at day 55 post-immunisation, heat-inactivated for 30 minutes at 56°C and stored at -20°C for subsequent use.

### Production and use of lentiviral pseudotyped particles

The pseudotyped viral particles expressing a luciferase reporter gene were produced as described.<sup>2</sup> Briefly, SARS-CoV spike pseudotyped lentiviral particles (SARS-CoVpp), vesicular stomatitis virus glycoprotein pseudotyped lentiviral particles (VSVpp) or lentiviral particles lacking

expression of any viral envelope protein (Δenvpp) were obtained by transfection of HEK293T cells with an HIV-1 provirus construction (pNL4.3.Luc R-E<sup>pro</sup>) and a plasmid encoding the viral envelope protein of interest, ie SARS-CoV spike, VSV-G, or empty vector (pcDNA3.1; Invitrogen), respectively. Following a purification step on 20% sucrose cushion, the concentrated viral particles were titrated by ELISA for lentivirus-associated HIV-1 p24 protein according to the manufacturer's instructions (Cell Biolabs) and the viral stocks were stored at -80°C until use.

### Infection with SARS-CoV

Serial, 2-fold dilutions of heat-inactivated mouse serum were incubated for 1 hour at 37°C with an equal volume of live SARS-CoV (strain HKU-39849) under appropriate containment in a BSL3 laboratory (Department of Microbiology, The University of Hong Kong). Cells were infected at a multiplicity of infection (MOI) of 1 for 60 minutes at 37°C, washed and then incubated in supplemented culture medium containing appropriate dilutions of mouse serum. At the end of the experiment cells were either fixed in 4% paraformaldehyde (dissolved in phosphate-buffered saline) for immunofluorescence microscopy, or resuspended in lysis buffer (RLT buffer, RNeasy RNA Mini kit; QIAGEN) for real-time quantitative PCR and stored appropriately until use. Additionally, samples of cell culture supernatants (100 μL) harvested at different time points were mixed with 350 μL of RLT buffer and stored at -80°C until use.

### Immunofluorescence microscopy

To assess SARS-CoV infection, cells were incubated for 45 minutes with a mouse monoclonal antibody specific for the viral nucleoprotein (N), and revealed by secondary TRITC-conjugated goat anti-mouse (Zymed Laboratories). To assess SARS-CoV Spike pseudoparticle (SARS-CoVpp) infection, cells were incubated for 45 minutes with FITC-conjugated polyclonal goat anti FireFly luciferase (Rockland). Slides were assembled with DAPI-containing mounting reagent (Southern Biotech) and analysed with an AxioObserver Z1 microscope (Zeiss). Pictures from 5-10 randomly selected fields were acquired with an Axiocam MRm camera and processed with MetaMorph software (Molecular Devices).

### Real-time quantitative RT-PCR for viral gene expression

Total RNAs were extracted with an RNeasy RNA Mini kit (QIAGEN), with DNase digestion, according to the manufacturer's instructions. Extracted RNAs were stored at -80°C until use. Superscript III reverse transcriptase (Invitrogen)

and random hexamer primers (Invitrogen) or gene-specific oligonucleotides were used to convert RNAs to cDNAs. The amount of viral and host RNA was measured by real-time quantitative PCR using SybrGreen-based technology on a LightCycler 480-II instrument (Roche).

### Statistical analysis

Differences between groups were compared using the unpaired Student's t-test with a 0.05 significance level.

## Results

### Anti-spike immune serum promotes infection of primary human immune cells with SARS-CoV

Following previous observations made with human immune cell lines,<sup>2</sup> we determined whether ADE of SARS-CoV infection could occur also in primary human immune cells. To explore this hypothesis, we pre-incubated SARS-CoVpp with mouse anti-spike control serum prior to infection of PBMCs. We then examined the extent of infection by monitoring the expression of the luciferase reporter protein encoded by the SARS-CoVpp. Compared with controls, infection in the presence of heat-inactivated anti-spike serum facilitated infection of human PBMCs with SARS-CoVpp (Fig 1). In order to shed light on the identity of the ADE-infected primary immune cells, co-staining for the widely accepted myeloid marker CD68 (macrosialin/gp110) was also performed. Among the cells infected in the presence of anti-viral antibodies, over 75% were positive for CD68 (Fig 1). Because CD68 was expressed on a variety of cells other than the monocytic lineage, we highly purified CD14<sup>+</sup>-cells (ie monocytes) and assessed their susceptibility to ADE of SARS-CoVpp infection.

### The monocytic lineage is a prime target for ADE of SARS-CoV infection

As previously shown with the monocytic cell line THP-1,<sup>2</sup> primary human monocytes were susceptible to infection by SARS-CoVpp in the presence of anti-spike antibodies only. Inoculums made of SARS-CoVpp, or SARS-CoVpp pre-incubated in the presence of control serum never resulted in a detectable luciferase signal (not shown). Because in the course of the deadly feline infectious peritonitis, anti-spike antibodies have been shown to trigger massive infection of macrophages, a key event for disease pathogenesis, we also monitored occurrence of antibody-mediated SARS-CoV infection in human monocyte-derived macrophages. When human macrophages were infected in the presence of anti-spike immune-serum, detection of the luciferase reporter protein was markedly different compared

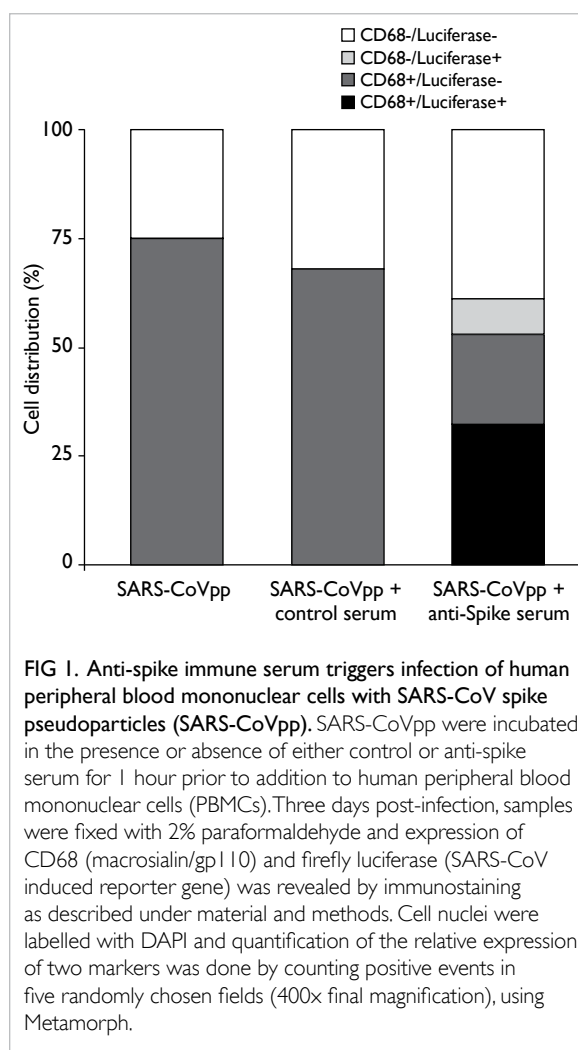


**FIG 1. Anti-spike immune serum triggers infection of human peripheral blood mononuclear cells with SARS-CoV spike pseudoparticles (SARS-CoVpp).** SARS-CoVpp were incubated in the presence or absence of either control or anti-spike serum for 1 hour prior to addition to human peripheral blood mononuclear cells (PBMCs). Three days post-infection, samples were fixed with 2% paraformaldehyde and expression of CD68 (macrosialin/gp110) and firefly luciferase (SARS-CoV induced reporter gene) was revealed by immunostaining as described under material and methods. Cell nuclei were labelled with DAPI and quantification of the relative expression of two markers was done by counting positive events in five randomly chosen fields (400x final magnification), using Metamorph.

with those infected in the presence of control serum (not shown). Of note, infection of primary macrophages with recombinant viral particles pseudotyped with the glycoprotein of the VSVpp or Δenv.pp was never modified by the presence of anti-SARS-CoV spike immune serum (not shown). These experiments indicate that anti-spike antibodies facilitate infection of SARS-CoVpp but not VSVpp or Δenv.pp into human primary macrophages.

### Antibody-mediated enhancement of SARS-CoV infection in primary macrophages leads to abortive infection

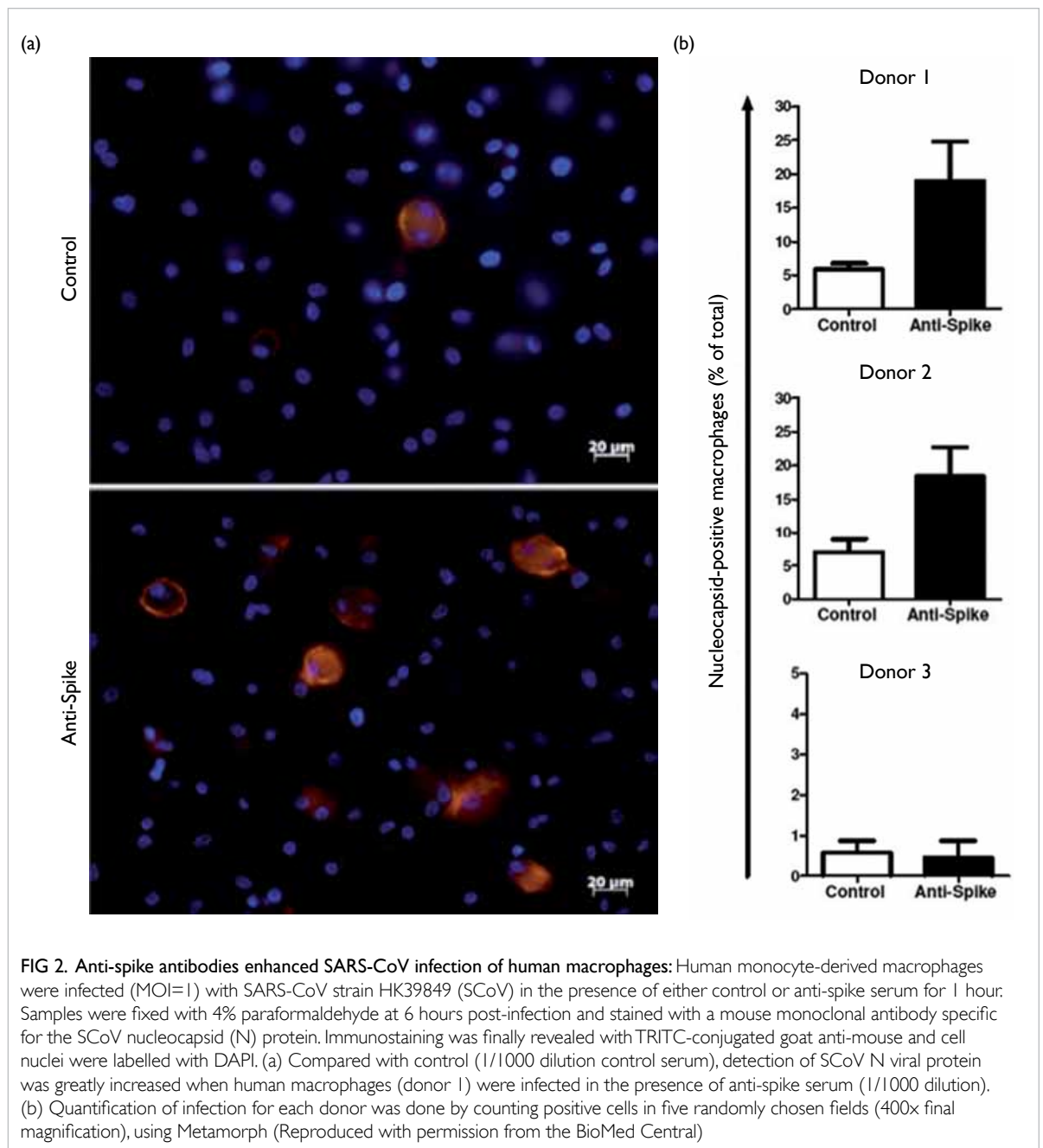
Because of the well-established roles of the macrophages in the primary response to pathogens and in the shaping of the subsequent (pathogen-specific) adaptive immune response, we investigated whether a change in tropism could also be observed during infection with replication-competent SARS-CoV.

Infection of monocyte-derived macrophages

by replication competent SARS-CoV in the presence of control serum led to modest infection. In contrast, when they were infected in the presence of anti-spike immune-serum, intracellular detection of viral nucleocapsid protein was markedly increased (Fig 2). To assess the capability of SARS-CoV to productively replicate into ADE-infected macrophage cells, we monitored the cellular viral load with real-time quantitative RT-PCR as well as the release of SARS-CoV progeny into cell culture supernatant.

Quantitative measurements of either positive (ie genomic and mRNA) or negative (ie subgenomic replicative intermediates) RNA strands

demonstrated a significant increased viral load at 6 hours post-infection in cells infected in the presence of anti-spike serum, followed by a continuing decrease in both viral RNA species with time so that no difference between groups was noted later on (not shown). Of note, there was no evidence of spreading infection to other cells (not shown). Similarly we did not detect any change in viral gene copies when we assessed the viral yield of macrophage-infected supernatants, whether incubated in the presence or absence of immune serum. Altogether these results indicate that despite the ability of SARS-CoV to exploit anti-viral antibodies to invade macrophages,



only abortive replication occurs upon infection and no infectious virus is released from the ADE-infected cells.

### **ADE infection pathway does not alter the profile of cytokine/chemokine produced by primary human macrophages**

The antibody-mediated entry route would affect functionality and cell homeostasis of ADE-infected macrophages but would not result in productive infection. Indeed, ADE infection induced the initiation of viral gene transcription, with production of viral gene intermediate species, and viral protein synthesis. Given the ability of intracellular innate immune sensors, such as the pattern recognition receptor families TLR and RLH, to detect viral gene species and the disturbance to the cell homeostasis caused by SARS-CoV viral proteins (such as 3a protein and SARS-Unique Domain), we evaluated the expression profile of some characteristic proinflammatory immune mediators and apoptosis-inducing ligands. As previously documented, infection of human monocyte-derived macrophages with SARS-CoV led to induction of several proinflammatory cytokines and chemokines, without expression of type-I interferon IFN- $\beta$  (not shown). Similarly, infection in the presence of control serum did not trigger induction of IFN- $\beta$  and similar kinetics and levels of TNF- $\alpha$ , CCL2/MCP-1, CCL3/MIP-1 $\alpha$ , and CXCL10/IP-10 were detected (Fig 3). When cells were infected in the presence of anti-SARS-CoV spike immune-serum (Fig 3), despite a 3-4 fold increase in intracellular SARS-CoV viral load (Fig 2), no change in the kinetic or in the expression of the type-I interferons and the proinflammatory cytokines/chemokines was noted. Similarly, compared with controls ADE-infection of macrophages never altered gene expression of prototypical death ligands such as TNF- $\alpha$  (Fig 3), FasL or TNF-related apoptosis-inducing ligand (not shown). Our results indicated that despite an enhanced infection of cells in the presence of anti-viral antibodies, the occurrence of ADE of SARS-CoV entry had little effect on the inflammatory response and the death ligand-induced killing activity of the macrophages.

### **The occurrence of ADE of SARS-CoV infection relies on the intracellular signalling domain of the human Fc $\gamma$ R by the target cells**

Our previous work demonstrated a major role for immune receptors, particularly Fc-gamma receptor II (Fc $\gamma$ RII) family, in triggering infection of immune cells with SARS-CoV.<sup>2</sup> Because this FcR family includes members that bind immunoglobulins/immune complexes with different affinities in addition to delivering either activating or inhibitory signals, we established a model to understand what, from

binding event to the Fc $\gamma$ RII or from internalisation/signalling cascade, played a preponderant role in the occurrence of ADE infection. Thanks to molecular mutagenesis, we established immune cell lines that expressed either a truncated form (ie lacking intracellular domain) or chimeric form (ie swapping of the intracellular domain) of Fc $\gamma$ RIIA (CD32a) and Fc $\gamma$ RIIB (CD32b), the only two receptors proved to be involved in ADE of SARS-CoVpp.<sup>2</sup> Our results indicated a prominent role of the intracellular domain over the extracellular domain of human Fc $\gamma$ RII in the occurrence of ADE of SARS-CoVpp.<sup>3</sup> All the Fc $\gamma$ RII receptors with truncation of their intracellular domain became unable to trigger ADE infection despite being able to efficiently bind immune complexes. This demonstrated that attachment of the immune-complexes to the target cells was not an event sufficient to trigger ADE of SARS-CoVpp infection (not shown).

## **Discussion**

The possibility that an immune response to pathogens may also have deleterious effects on the host homeostasis has been reported. For example, the hyper-induction of cytokines following avian influenza infection has been implicated in the severity of the disease, and infection of cells by antibody-dependent enhancement has been known to occur for several viral diseases.<sup>1</sup> In our study, anti-spike antibody potentiated infection of primary human immune cells with SARS spike-pseudotyped lentiviral particles and replication-competent SARS-coronavirus. Nonetheless in macrophages, antibody-mediated infection did not lead to productive replication of the virus, and did not induce a skewed profile of proinflammatory cytokines and chemokines.

After initiation of viral gene transcription and viral protein synthesis, a block seems to occur in the replication process ultimately ending in an abortive viral cycle without detectable release of progeny virus. Such abortive replication of SARS-CoV into macrophages has been documented,<sup>4</sup> but conversely to this previous report where 90% of the macrophages were infected with SARS-CoV in the absence of immune-serum (MOI=1-2). We detected a much lower infection yield (about 5-7%) using a similar experimental setup. Of note from three independent donors, two macrophage cultures showed evident infection ( $\geq 5\%$  infected macrophages; donor 1 and 2), whereas one displayed low permissiveness ( $< 1\%$  infected macrophages; donor 3) [Fig 2]. In the latter, addition of anti-spike antibodies did not make the macrophages more susceptible to infection, thus likely illustrating inter-individual variability of human macrophage to SARS-CoV infection.

Despite a four-fold increase in infection and initiation of viral gene transcription in the

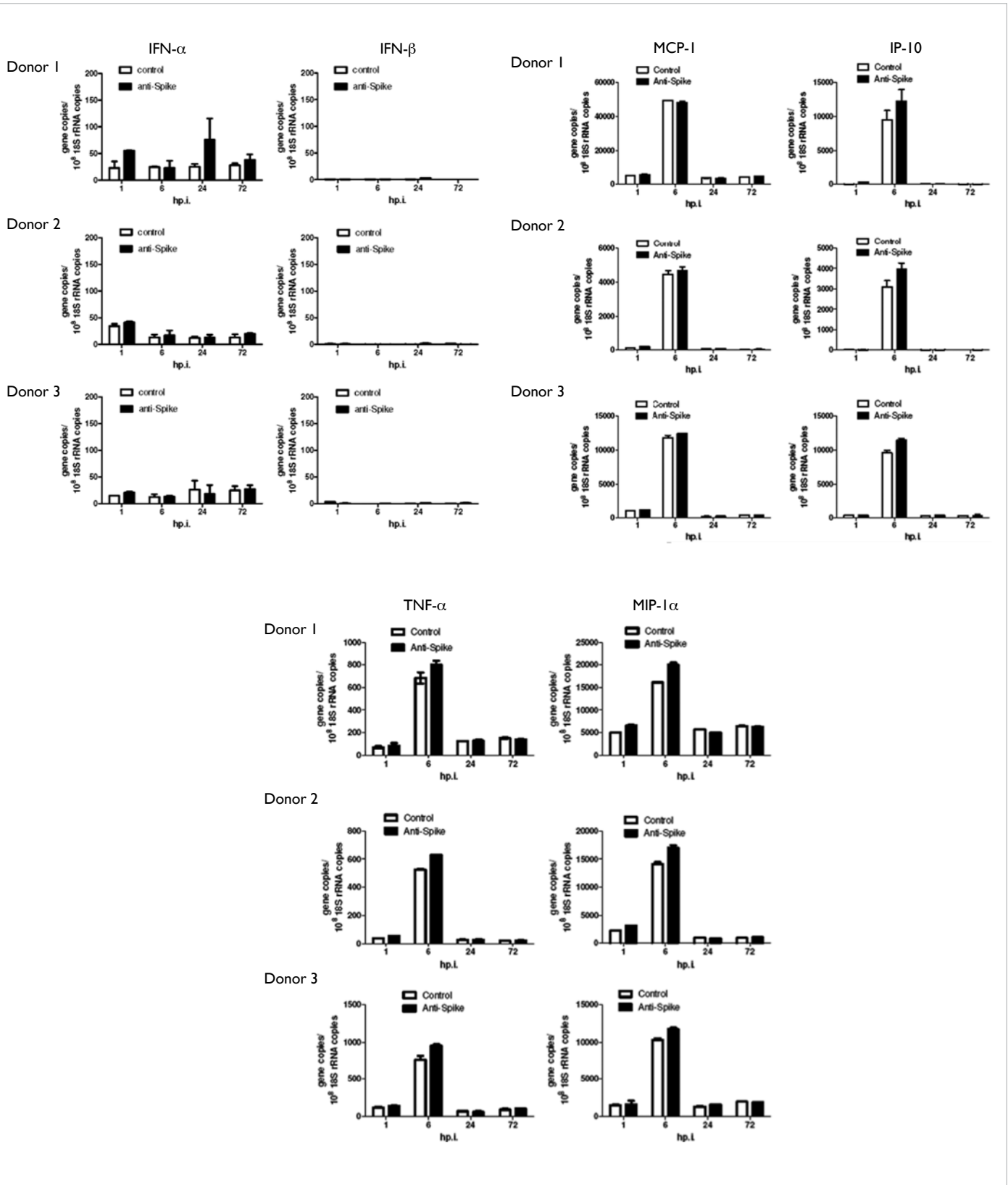


**FIG 3. Induction of cytokines/chemokines by SARS-CoV in human macrophages following antibody-mediated infection:** Human monocyte-derived macrophages were incubated for 1 hour in the absence or presence of SARS-CoV strain HK39849 (SCoV), with two-fold serial dilutions (1/1000 and 1/2000) of either control (open bars) or anti-spike (closed black bars) serum. Cells were lysed at 1, 6, 24, and 72 hours post-infection, and total RNAs were extracted for RT-PCR amplification. The mRNA levels of different cytokines and chemokines were determined by real-time quantitative RT-PCR and for the sake of clarity only one serum dilution (1/1000) is shown. In most cases, when induced, cytokines/chemokines were detected before 24 hours post-infection only. Addition of anti-spike serum, compared with control serum, did not lead to a skewed expression profile and no significant changes were seen (Reproduced with permission from the BioMed Central)

ADE-infected macrophages, no change in gene expression of some pro-inflammatory cytokines/chemokines and death ligands was detected. Although we did not thoroughly investigate the occurrence of cell death with dedicated methods, our microscopic observations did not reveal chromatin condensation or membrane blebbing of the ADE-infected macrophages up to 72 hours post infection. Considering approximately 20% of macrophages were ADE-infected, and in regard to the apparent well-being of the infected cultures with cell loss/variation in total cell number of less than 8% throughout the 3-day assay, we speculate that in macrophages, ADE of SARS-CoV infection does not trigger massive cell death.

In regard to clinical observations of poor disease outcomes in early seroconverted SARS patients,<sup>5</sup> and because ADE of other viral infections (such as Ross River Virus, feline coronavirus, poliovirus, coxsackievirus) have been shown to elicit markedly distinct responses compared with viral entry through the natural host receptor, and as immune deregulation is a hallmark of SARS, involvement of ADE mechanisms during SARS pathogenesis was worthy of investigation.

The findings of this study partially invalidated our initial hypothesis that antibody-mediation would, by widening tropism of SARS-CoV toward immune cells, elicit an altered profile of immune mediators that impair homeostasis of the immune system and ultimately contribute to SARS pathogenesis. Nonetheless, it is still intriguing to us that triggering an enhanced infection of cornerstone innate immune cells such as macrophages would have no consequences. It is true that in contrast to studies that showed cell perturbation following ADE-infection, others have documented fewer, barely discernible consequences.<sup>6</sup> Hence it is possible that ADE of SARS-CoV infection is happening without deleterious consequences to the target cells. Nonetheless, with reference to the great deal of controversy in the literature regarding the relationship between immune mediators, cell death and the pathophysiological events of SARS, our study may not have focused on the right gene candidates. Thus for future investigations, it is advised to conduct genome-wide gene expression profiling.

## Conclusion

Our results suggest the rational development of vaccination strategies in the event of a SARS-like virus outbreak, with reasonable concerns about the occurrence of severe adverse effects.

## Acknowledgments

This study was supported by the Research Fund for the Control of Infectious Diseases, Food and Health Bureau, Hong Kong SAR Government (#09080872) and by the RESPARI project of the Institut Pasteur International Network. We wish to thank our colleague Mr Lewis Siu (HKU-Pasteur Research Pole) for sharing with us his stock of SARS-CoV spike lentiviral particles. We also thank Dr Kwok Hung Chan (Queen Mary Hospital) for the gift of mouse monoclonal antibody (4D11) specific for the SARS-CoV nucleoprotein. Finally, we would like to express our deep gratitude to all members of the HKU-Pasteur Research Pole for expert advice and helpful discussions.

Results of this study have been published in: Yip MS, Leung NH, Cheung CY, et al. Antibody-dependent infection of human macrophages by severe acute respiratory syndrome coronavirus. *Virology* 2014;11:82.

## References

1. Sullivan NJ. Antibody-mediated enhancement of viral disease. *Curr Top Microbiol Immunol* 2001;260:145-69.
2. Jaume M, Yip MS, Cheung CY, et al. Anti-severe acute respiratory syndrome coronavirus spike antibodies trigger infection of human immune cells via a pH- and cysteine protease-independent FcγR pathway. *J Virol* 2011;85:10582-97.
3. Yip MS, Leung NH, Cheung CY, et al. Antibody-dependent infection of human macrophages by severe acute respiratory syndrome coronavirus. *Virology* 2014;11:82.
4. Cheung CY, Poon LL, Ng IH, et al. Cytokine responses in severe acute respiratory syndrome coronavirus-infected macrophages in vitro: possible relevance to pathogenesis. *J Virol* 2005;79:7819-26.
5. Lee N, Chan PK, Ip M, et al. Anti-SARS-CoV IgG response in relation to disease severity of severe acute respiratory syndrome. *J Clin Virol* 2006;35:179-84.
6. Kou Z, Lim JY, Beltramello M, et al. Human antibodies against dengue enhance dengue viral infectivity without suppressing type I interferon secretion in primary human monocytes. *Virology* 2011;410:240-7.

# Structure-based discovery and development of natural products as Type II JAK2 inhibitors for the treatment of hepatitis C

EDL Ma \*, CH Leung, P Chiu, YC Cheng

## KEY MESSAGES

1. Hepatitis C is a highly infectious disease that imposes a high health, social and financial burden on the population in Hong Kong and worldwide.
2. A new platform for the virtual screening of JAK2 Type II inhibitors was constructed and utilised to identify amentoflavone as a lead scaffold for the development of new inhibitors.
3. Novel natural inhibitors were developed and showed anti-JAK2 activity and anti-viral activity in cellular systems.

4. The compounds potentially represent a novel therapeutic approach to the treatment of hepatitis C, and may supplement existing regimens for hard-to-treat HCV genotypes in Hong Kong.

Hong Kong Med J 2016;22(Suppl 4):S32-6

RFCID project number: 11101212

EDL Ma, CH Leung, P Chiu, YC Cheng

Department of Chemistry, Hong Kong Baptist University, Hong Kong

\* Principal applicant and corresponding author: edmondma@hkbu.edu.hk

## Introduction

Hepatitis C virus (HCV) can cause a highly infectious liver disease. Intravenous drug users, transfusion-dependent children with haematological disease, HIV-positive patients, and hepatocellular carcinoma patients are at high risk of HCV infection, with an associated incidence of 46.0%, 16.3%, 7.9%, and 7.3%, respectively.<sup>1</sup> Worldwide, HCV infects 3 000 000 to 4 000 000 people each year and has been estimated to infect 200 million people, or 3% of the global population.

Chronic HCV disease can result in liver fibrosis and cirrhosis and finally liver damage and/or liver cancer, life-threatening oesophageal varices, and gastric varices. Existing treatment of chronic HCV disease involves a combination of pegylated interferon-alpha-2a or pegylated interferon-alpha-2b (also known as peginterferon), and ribavirin.<sup>2</sup> Around 50% of HCV genotype 1 patients, which accounts for about 80% and 60% of HCV patients in the US and in Hong Kong, respectively, do not respond to this therapy.<sup>2,3</sup>

Activation of STAT-3 by HCV non-structural proteins results in constitutive activation of STAT-3 in HCV-replicon-expressing cells. STAT-3 activity and HCV RNA production significantly decrease following treatment of HCV-infected cells with Janus kinase 2 (JAK2) inhibitor AG490.4 This demonstrates that JAK2 inhibitors are useful for inhibition of HCV translation and replication, potentially supplementing existing treatment of HCV. Although many potent JAK2 inhibitors have been developed as possible anticancer agents, none of them has been certified by the US Food and Drug

Administration.

Type II inhibitors, including imatinib (Gleevec) and sorafenib, target kinases in the inactive conformation. As the inactive forms of kinases display a wide structural and chemical heterogeneity, Type II inhibitors have the potential to achieve greater selectivity for target kinases. This project proposed to select small molecules as Type II JAK2 inhibitors from databases of natural products using ligand docking-based virtual screening methods, as a new therapeutic avenue to combat HCV infection. Ligands with high efficacy and selectivity were rapidly identified using a computer-aided approach that reduced the number of compounds for *in vitro* evaluation.

## Methods

This study was conducted from December 2011 to November 2013.

### Molecular docking and virtual screening

We used the deletion-of-loop Asp-Phe-Gly-in (DOLHPIN) protocol<sup>5</sup> to change an active 'DFG-in' structure of JAK2 (Protein Data Bank code: 2B7A) into a Type II-compatible conformation that was capable of molecular docking. We conducted *in silico* screening of 150 000 natural products and natural product-like compounds on the DOLPHIN kinase model using the internal coordinate mechanics (ICM) method [ICM-Pro 3.6-1d molecular docking software (Molsoft)] to select natural product scaffolds as Type II JAK2 inhibitors. Molecular docking was conducted using the virtual library screening (VLS) module in the Molsoft programme.

## Quantification of HCV RNA

The HCV genotype 1b subgenomic replicon cell line with a luciferase reporter (Huh-luc/neo-ET) was cultured in Dulbecco's modified Eagle's medium (DMEM) supplemented with 10% foetal bovine serum (FBS), 1 mM non-essential amino acids, and 250 µg/ml G418 (Invitrogen). The cells were seeded at a density of  $1 \times 10^5$  cells per well in a 6-well plate with the treatment of the candidate compounds or DMSO. Cells were harvested after incubation for 72 hours and subjected to RNA quantification to evaluate the effect of the candidate compounds on viral replication.

## Results

### Construction of virtual screening platform for the discovery of Type II JAK2 inhibitors using the DOLPHIN protocol

At the onset, no X-ray crystal structure of JAK2 in an inactive conformation could be used for virtual screening. We successfully changed a DFG-in structure of JAK2 into a Type II-compatible conformation that could be used for molecular docking through the DOLPHIN algorithm. The molecular model of JAK2 obtained after the DOLPHIN transformation is displayed in Fig 1.

### High-throughput virtual screening of a natural product and natural product-like database

To identify useful natural product scaffolds as Type II inhibitors of JAK2, we conducted *in silico* screening of natural products and natural product-like databases using the JAK2 model obtained by DOLPHIN through the ICM method in parallel with the molecular dynamics-based Acceryls Discovery

Studio 3.0. During the screening campaign, 150 000 natural products or natural product-like compounds were screened against our molecular model of inactive form of JAK2 obtained by the DOLPHIN algorithm, the compounds of which were from the Analyticon Discovery NATx and MEGabolite databases, the ZINC natural product database and the Hongcam natural products database. The top ten highest-scoring compounds were evaluated in an ELISA in order to determine their ability to inhibit JAK2 phosphorylation *in vitro*. From these experiments, amentoflavone **1a**, a biflavonoid from the Chinese plant *Ginkgo biloba*, was chosen as a promising candidate for further biological investigation.

### In silico design and synthesis of amentoflavone derivatives

In our preliminary molecular modelling analysis, the deletion of the DFG loop in the DOLPHIN model of JAK2 kinase showed a large hydrophobic pocket, not present in the active DFG-in form of the kinase that was partially occupied by amentoflavone **1a**. We anticipated that the presence of one or more aliphatic side chains to the biflavonoid scaffold of **1a** would lead the molecule to occupy the hydrophobic pocket vacated by the DFG loop, thus producing more potent and selective inhibitors of JAK2. According to this result, we designed >50 derivatives of amentoflavone **1a** and docked these compounds against the DFG-out model of JAK2 kinase *in silico*. We found that analogues **1b-j** with long, alkyl chains emerged as top-scoring compounds.

We synthesised the compounds **1b-j** in three steps from amentoflavone **1a** using a protection-transetherification-deprotection sequence (Fig 2). These derivatives included both monoalkylated (**1b-e**, **1h**, **1i**) and dialkylated (**1f**, **1g**) analogues,

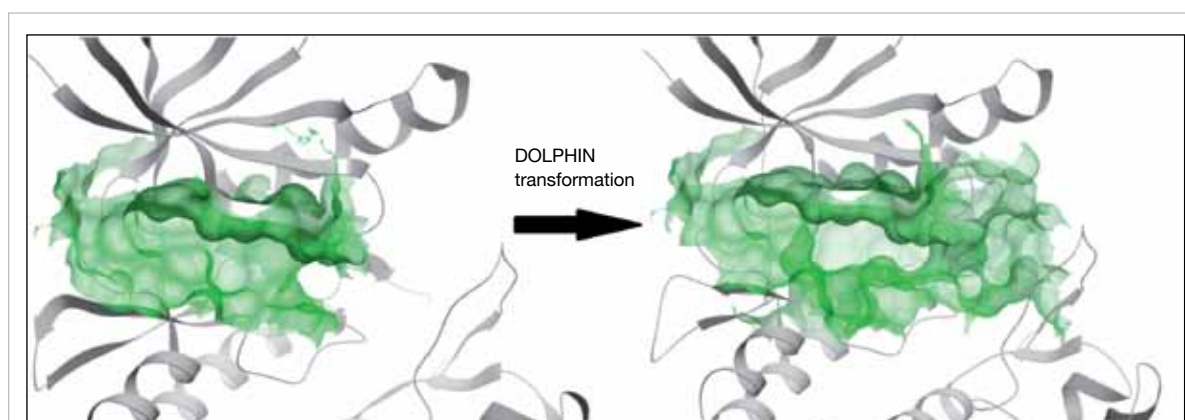


**FIG 1.** The molecular model of the inactive form of JAK2 generated using DOLPHIN: The active conformation of JAK2 (left) is converted to the inactive form (right) by removing DFG Phe and the next four residues in the sequence. The binding pocket is shown as a translucent green surface. (Reproduced with permission from the Centre National de la Recherche Scientifique (CNRS) and The Royal Society of Chemistry)

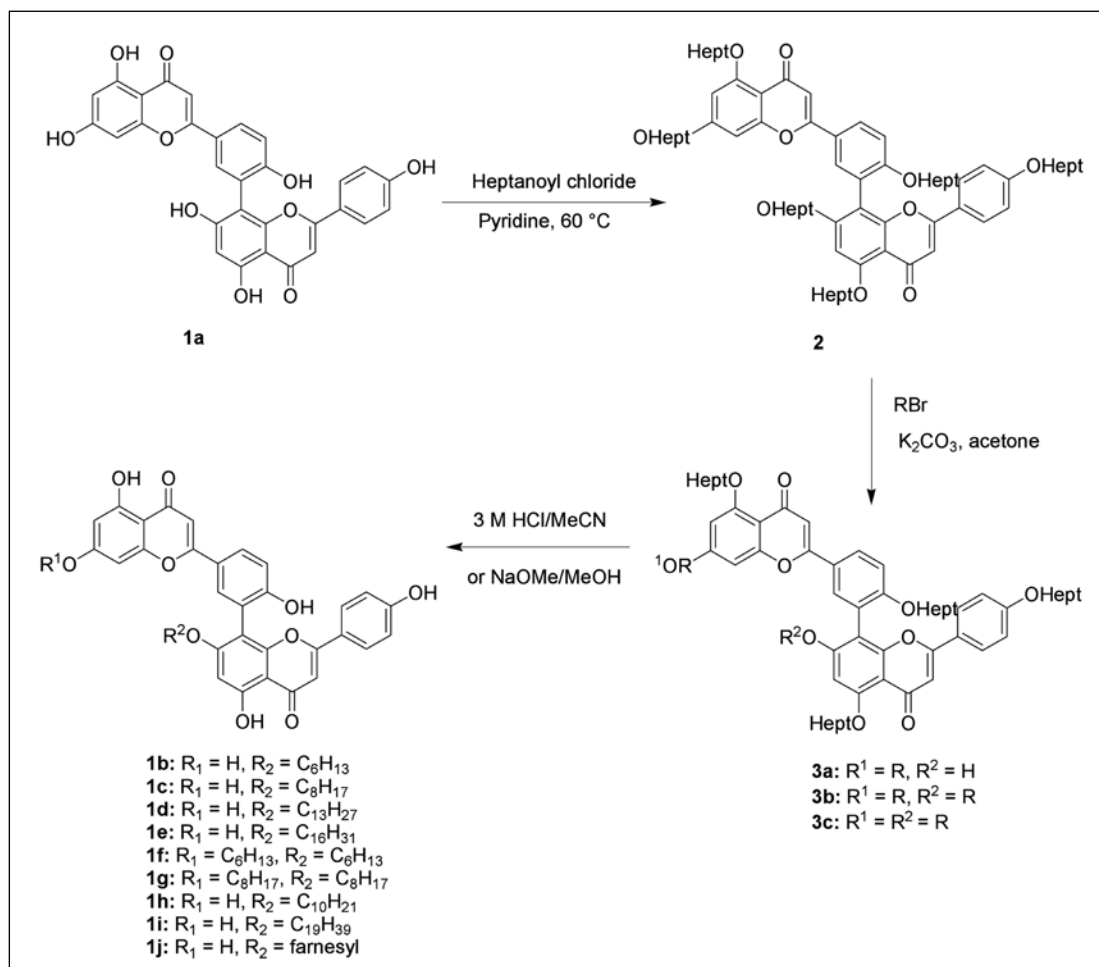


FIG 2. Synthetic procedure for the preparation of top-scoring compounds (Reproduced with permission from the Centre National de la Recherche Scientifique (CNRS) and The Royal Society of Chemistry)

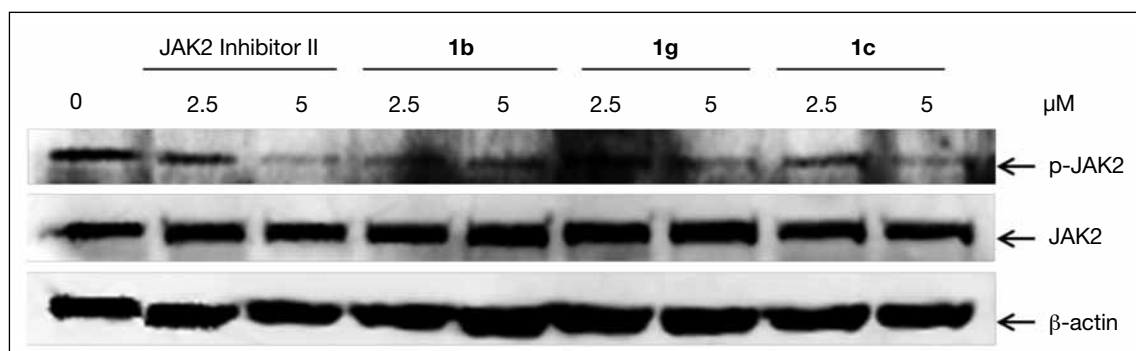


FIG 3. HEL cells were incubated with the compounds for 16 hours and protein lysates were electrophoresed and immunoblotted using anti-phospho-JAK2 Y1007/Y1008 antibody or anti-JAK2 antibody. Equal protein loading was confirmed by total  $\beta$ -actin levels. Representative gel photograph images of triplicate experiments are shown. Western blot analysis of the effect of compounds **1a**, **1c**, **1g** and JAK2 Inhibitor II on JAK2 autophosphorylation *in cellulo*. Estimated IC<sub>50</sub> values: **1c**=2.5  $\mu$ M and **1g**=5  $\mu$ M. (Reproduced with permission from the Centre National de la Recherche Scientifique (CNRS) and The Royal Society of Chemistry)

as well as an alkenyl analogue (**1j**). These novel derivatives were fully characterised by  $^1\text{H}$  and  $^{13}\text{C}$  NMR spectroscopy and high-resolution mass spectrometry.

### JAK2 inhibitory activity of top-scoring candidates in cellulo

We next evaluated the effect of the amentoflavone derivatives **1a-j** on JAK2 autophosphorylation using a Western blot assay in human erythroleukaemia cells (HEL), which harbour a V617F mutation in JAK2 leading to constitutive JAK2 activity. Among the ten compounds tested, significant inhibition of JAK2 autophosphorylation was observed for the monoalkylated analogue and **1c** and the dialkylated analogue **1g**, with estimated  $\text{IC}_{50}$  values of 2.5 and 5  $\mu\text{M}$  (Fig 3). The potencies observed for **1c** and **1g** were comparable with those of the positive control compound JAK2 inhibitor (1,2,3,4,5,6-hexabromocyclohexane). Encouragingly, these two compounds exhibited superior efficacy against JAK2 autophosphorylation in comparison with the parent compound amentoflavone **1a**, demonstrating the application of our structure-based techniques to develop more potent JAK2 inhibitors.

### Molecular modelling analysis of candidate compounds

Our molecular modelling results showed that **1c** was situated snugly in the binding pocket of the inactive form of JAK2 DOPHLIN model. The amentoflavone moiety was located at the ATP binding pocket, whereas the alkyl side chain protruded inward into the hydrophobic pocket beside the ATP binding site. The ICM binding score for **1c** to the inactive conformation of JAK2 was calculated to be  $-38.46$  kcal/mol, showing the strong binding interaction between **1c** and the binding site. Moreover, the interaction between **1c** and the active conformation of JAK2 was relatively weak ( $-13.36$  kcal/mol). These results indicate that compound **1c** may be used as a potential JAK2 Type II inhibitor.

### Anti-viral activity of the candidate compounds

We then tested the HCV anti-viral activity of selected amentoflavone analogues in the Huh-Luc/neo-ET cell line. The results demonstrated that compound **1c** led to a decrease in the HCV RNA level, with an  $\text{EC}_{50}$  value of  $3.1 \pm 0.8$   $\mu\text{M}$ . Notably, **1c** was also the most potent compound in the JAK2 autophosphorylation assay. We anticipated that the inhibition of JAK2 signalling in the infected cells was at least in part due to the HCV anti-viral activity of compound **1c**, thus causing reduced STAT-3 activity and HCV RNA production.

### Cytotoxicity evaluation of candidate compounds

The cytotoxicity of the amentoflavone analogues against HEL cells was determined by MTT assay. Most of the amentoflavone analogues were relatively non-toxic. Importantly, derivatives **1c** and **1g** showed the greatest activity against JAK2 autophosphorylation, and displayed  $\text{IC}_{50}$  values of  $>100$   $\mu\text{M}$ . This suggests that their ability to inhibit JAK2 and HCV viral activity, and thus potentially HCV viral replication, may be achieved at concentrations that are non-toxic to normal cells. This property is significant if these amentoflavone derivatives are to be further developed as therapeutic agents for the treatment of hepatitis C, as adverse side effects may be minimised.

### Discussion

To date, no protective vaccine for HCV is available. Current standard therapy for HCV infection using pegylated interferon alpha combined with ribavirin shows some side effects, such as fatigue, flu-like symptoms, and gastrointestinal symptoms, and results in a sustained virological response in only a small number of patients. Moreover, HCV genotype 1 infection, which accounts for the majority of HCV infection in Hong Kong, is resistant to conventional therapy. In recent years, combination therapy of boceprevir or telaprevir with pegylated interferon and ribavirin has shown to improve virological response rates, but anaemia and drug-drug interactions are potentially treatment-limiting adverse effects. The development of alternative HCV inhibitors is needed.

The HCV life cycle is closely related to host cell factors, and identification of inhibitors of such host factors (such as JAK2) offers an alternative approach to the development of anti-HCV compounds. A potential advantage of targeting host proteins such as JAK2 for the treatment of HCV is that the therapy would be less affected by drug resistance arising from the mutation of viral proteins.

In this project, we successfully applied the DOLHPIN protocol to convert the X-ray co-crystal structure of JAK2 in the active conformation into an inactive conformation, and screened 150 000 compounds from a natural product and natural product-like library using this model. From the result of *in vitro* testing assay of the initial hit-list, amentoflavone **1a** was selected as a promising candidate for further optimisation. After screening over 50 rationally-designed derivatives of amentoflavone **1** *in silico*, high-scoring amentoflavone derivatives **1b-j** were synthesised in three steps using efficient organic chemistry techniques. In a cellular assay, derivatives **1c** and **1g** showed potent activity against JAK2 autophosphorylation. Furthermore, compound **1c** displayed anti-viral activity in a HCV

replicon cell line. Molecular modelling analysis indicated that the compounds may be used as Type II inhibitors of JAK2. We envisage that these non-toxic JAK2 inhibitors have significant potential to be further developed as JAK2 inhibitors for the treatment of hepatitis C.

## Acknowledgement

This study was supported by the Research Fund for the Control of Infectious Diseases, Food and Health Bureau, Hong Kong SAR Government (#11101212).

Results of this study have been published in Ma DL, Chan DS, Wei G, et al. Virtual screening and optimization of Type II inhibitors of JAK2 from a natural product library. *Chem Commun (Camb)* 2014;50:13885-8.

## References

1. Leung N, Chu C, Tam JS. Viral hepatitis C in Hong Kong. *Intervirology* 2006;49:23-7.
2. Ferenci P. Peginterferon and ribavirin in HCV: improvement of sustained viral response. *Best Pract Res Clin Gastroenterol* 2008;22:1109-22.
3. Manns MP, McHutchison JG, Gordon SC, et al. Peginterferon alfa-2b plus ribavirin compared with interferon alfa-2b plus ribavirin for initial treatment of chronic hepatitis C: a randomised trial. *Lancet* 2001;358:958-65.
4. Waris G, Turkson J, Hassanein T, Siddiqui A. Hepatitis C Virus (HCV) constitutively activates STAT-3 via oxidative stress: role of STAT-3 in HCV replication. *J Virol* 2005;79:1569-80.
5. Kufareva I, Abagyan R. Type-II kinase inhibitor docking, screening, and profiling using modified structures of active kinase states. *J Med Chem* 2008;51:7921-32.

# Functional characterisation of hepatitis B viral X protein/microRNA-21 interaction in HBV-associated hepatocellular carcinoma

CH Li, SC Chow, DL Yin, TB Ng, YC Chen \*

## KEY MESSAGES

1. miR-21 overexpression is critical to promote early carcinogenesis of hepatocytes upon hepatitis B virus infection.
2. HBx-induced IL-6-STAT3 pathway upregulates miR-21 expression.
3. The high dependency of miR-21 expression on HBx is a unique viral oncogenic pathway aberrantly affecting gene expression network.
4. Inhibition of miR-21 attenuates the anchorage-independent colony formation and subcutaneous

tumour growth of non-tumour hepatocytes.

Hong Kong Med J 2016;22(Suppl 4):S37-42

RFCID project number: 11100452

<sup>1</sup> CH Li, <sup>1</sup> SC Chow, <sup>2</sup> DL Yin, <sup>1</sup> TB Ng, <sup>1</sup> YC Chen

<sup>1</sup> School of Biomedical Sciences, Faculty of Medicine, The Chinese University of Hong Kong

<sup>2</sup> Department of Internal Medicine, College of Medicine, East Tennessee State University, Johnson City, TN, USA

\* Principal applicant and corresponding author: frankch@cuhk.edu.hk

## Introduction

Hepatocellular carcinoma (HCC) associated with hepatitis B virus (HBV) infection exhibits a higher degree of aggressiveness than non-infected tumours. HBV X protein (HBx) is encoded from the HBV genome<sup>1</sup> and is involved in the pathogenic mechanism of HBV-associated HCC. It has multiple molecular functions in human hepatocytes via interactions with various transcription factors and modulates numerous cellular signalling pathways of the host.<sup>2</sup> The role of HBx protein in HCC biology has been studied, but the gene expression network affected by the viral protein is not fully understood.

HBx protein induces differential expression of microRNAs (miRNAs). Aberrant expression of miRNAs has been implicated in numerous cancer types including HCC. Nonetheless, HBV-associated miRNAs that drive the transformation of normal hepatocytes and HCC carcinogenesis are poorly studied. In addition, the mechanism by which HBx alters the expression of miRNAs is largely unexplored. In this project, we demonstrated that induction of miR-21 was dependent on HBx-activation of the IL-6-STAT3 pathway. Expression of miR-21 is essential in transforming non-tumour hepatocytes to gain the ability to form anchorage-independent colonies and in vivo tumours, and implies a critical role during early HCC development.

## Methods

This study was conducted from December 2011 to December 2013.

## Cell culture and drug treatment

A human hepatoma cell line, Hep3B, immortalised non-tumourigenic hepatocyte cells, MIHA, and 293T, were maintained under standard procedures. Cells were treated with STAT3 inhibitor, curcubitacin (Tocris, Bristol, UK), at a dose of 0.5  $\mu$ M for 72 hours, or with recombinant human IL-6 (Invitrogen) at designated doses and durations.

## Cancer-associated miRNA profiling in HBx-expressing stable cell line

MIHA cells were transfected with pcDNA3.1/myc containing COOH-terminal truncated HBx cDNA (HBx- $\Delta$ 35). After transfection, the cells were incubated with G418 (Invitrogen) for ~2 weeks. Differential expression of cancer-associated miRNA in HBx protein expressing MIHA cells was measured by Cancer MicroRNA qPCR Array with QuantiMir (System Biosciences). As an internal control, U6 primers were used for RNA template normalisation.

## Lentivirus packaging and transduction

Myc-tagged full-length human HBx (HBx-FL) and HBx- $\Delta$ 35 were cloned into a lentiviral vector coexpressing EGFP (pLIG). Lentiviral vector carrying transgene of small hairpin RNA targeting STAT3 (shSTAT3) (BLOCK-iT RNAi system) (Invitrogen) or miRZip-21 (MZIP21-PA-1) (System Biosciences) was purchased. Lentiviruses containing either myc-tagged HBx, HBx- $\Delta$ 35, shSTAT3 or miRZip-21 were packaged and transduced into MIHA cells with the presence of 8  $\mu$ g/mL polybrene (Sigma). Cells were

sorted for GFP expression by the BD FACSAria III cell sorter (BD Biosciences, New Jersey, USA) to obtain pure populations of MIHA-HBx and MIHA- $\Delta$ 35.

### Soft agar assay

Cells ( $5 \times 10^3$ ) were re-suspended in 1.5 ml 0.35% agar in DMEM, and were layered onto six wells containing solidified 0.5% agar. Colonies were allowed to grow for 4-6 weeks before being stained with crystal violet.

### Subcutaneous xenograft tumour models

All animal experiments were approved by the Animal Experimentation Ethics Committee of the Chinese University of Hong Kong. MIHA cells, MIHA-LIG, MIHA-HBx and MIHA-HBx- $\Delta$ 35 ( $2 \times 10^6$ ) were injected subcutaneously into nude mice ( $n=5$ ). Tumour volume was calculated by the equation:  $\text{volume} = (\text{length} \times \text{width}^2) / 2$ .

## Results

### miR-21 was upregulated by ectopic HBx expression in MIHA cells

We profiled cancer-associated miRNAs expression in HBx- $\Delta$ 35 overexpressing MIHA cells by Cancer MicroRNA qPCR Array with QuantiMir. MiRNAs with fold changes larger than 1.5 were considered biologically significant, and oncomiRs including miR-21 and miR-373 were upregulated while tumour suppressor miRNAs miR-126 and miR-137 were downregulated after HBx- $\Delta$ 35 overexpression (Fig 1a). To investigate the association between HBx and the miRNAs, we generated lentivirus carrying full length HBx (HBx-FL) or HBx- $\Delta$ 35 transgene to transduce MIHA cells. We showed that both HBx-FL and HBx- $\Delta$ 35 significantly promoted MIHA cell proliferation (Fig 1b). We hypothesised that HBx proteins could induce differential miRNAs expression, contributing to the altered phenotypes of non-tumour hepatocytes.

Subsequently, we validated the miRNA profiling in both HBx-FL- and HBx- $\Delta$ 35-expressing MIHA cells by qRT-PCR. MiR-21 expression was significantly increased upon ectopic HBx expression (Fig 1c), whereas miR-126, miR-137 and miR-373 showed no significant change (data not shown). To prove the presence of HBx-miR-21 pathway in HCC cells, we inhibited HBx by siRNAs in Hep3B cells that were positive for HBx expression. MiR-21 expression was significantly inhibited upon knockdown of HBx in Hep3B cells (Fig 1d). The level of other miRNAs was also measured, but knockdown of HBx failed to alter their expression (data not shown). Inhibition of miR-21 activity by miRZip-21 in HBx-FL expressing MIHA cells could upregulate a putative miR-21 target programmed cell death 4 (PDCD4) [Fig 1e]. Taken together, we illustrated that miR-21 was an

important downstream regulator of HBx proteins during HBV-mediated hepatocarcinogenesis.

### Upregulation of IL-6 by HBx protein induced miR-21 expression

We studied the association between the HBx-IL-6 pathway and miR-21 induction during early hepatocyte transformation. Overexpression of HBx-FL and HBx- $\Delta$ 35 significantly increased the expression of IL-6 in MIHA cells (Fig 1f). HBx- $\Delta$ 35 induced a remarkably higher IL-6 expression in cells compared with HBx-FL, suggesting that such variant could activate the IL-6 pathway more robustly. We further treated MIHA cells with recombinant human IL-6, and the level of miR-21 in cells was increased both time-dependently (Fig 1g) and dose-dependently (Fig 1h). Recombinant IL-6 treatment also increased both pri-miR-21 (Fig 1i) and pre-miR-21 levels (Fig 1j) time-dependently. The concurrent upregulation of primary, precursor and mature miR-21 suggested that IL-6 transcriptionally activated the transcription of the miR-21 gene in non-tumour hepatocytes, and subsequently elevated mature miR-21 level. Furthermore, knockdown of IL-6 by siRNAs significantly reduced the expression of miR-21 in Hep3B cells (Fig 1k), suggesting that IL-6 signalling was pivotal to HBx-mediated induction of miR-21 expression in HCC cells.

### Role of STAT3 in HBx-induced miR-21 expression

We further delineated the molecular pathway of IL-6-mediated miR-21 upregulation. IL-6 and STAT3 pathway is prevalent in human HCC. Nonetheless, the role of HBx proteins in regulation of the IL-6-STAT3 pathway was not clear. We showed that phosphorylated STAT3 was significantly elevated after overexpression of HBx-FL and HBx- $\Delta$ 35 (Fig 2a). Similar to the upregulation of IL-6 mRNA expression, HBx- $\Delta$ 35 induced a higher level of phosphorylated STAT3 compared with HBx-FL (Fig 2a). HBx was highly associated with activation of the IL-6-STAT3 pathway in HCC cells, as we further showed that phosphorylation of STAT3 was effectively inhibited when IL-6 was depleted by siRNAs in Hep3B cells (Fig 2b). To reveal the importance of STAT3 in HBx-induced miR-21 activation, lentiviral vector containing shSTAT3 was transduced in MIHA cells with or without HBx-FL and HBx- $\Delta$ 35 expression. Western blotting showed that the level of total STAT3 was drastically prohibited in all MIHA cell lines after lentiviral infection (Fig 2c). In turn, we measured the change in miR-21 level in the STAT3-depleted cells. As expected, upregulation of mature miR-21 was significantly attenuated in both HBx-FL and HBx- $\Delta$ 35 overexpressed MIHA cells (Fig 2d). In contrast, depletion of STAT3 in parental and control lentivirus infected MIHA cells did not alter miR-21

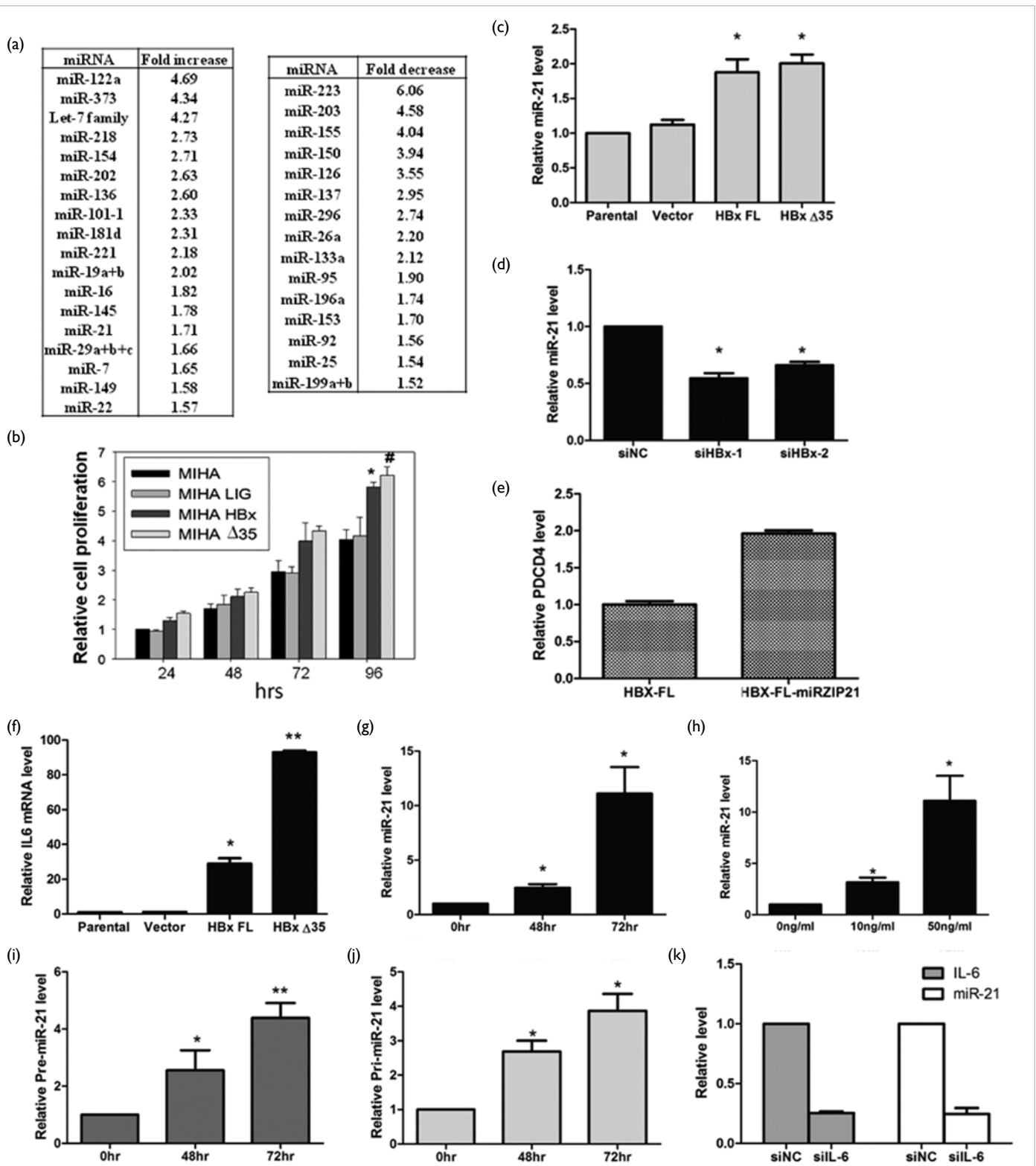


**FIG 1. Ectopic HBx expression induced miR-21 expression in non-tumour hepatocytes via IL-6 signalling.** Differential expression of cancer-associated miRNAs was measured in MIHA cells upon overexpression of HBx protein, and (a) upregulated miRNAs including miR-21 and miR-373, and downregulated miRNAs including miR-126 and miR-137 were identified. (b) Cell proliferation assay showed that ectopic expression of HBx-FL or HBx-Δ35 significantly increased the cell proliferation rate of MIHA cells compared with parental and lentivirus control cells. (c) Lentiviral overexpression of HBx-FL and HBx-Δ35 upregulated the level of miR-21 in MIHA cells. (d) Knockdown of HBx inhibited the expression of miR-21 in Hep3B cells. (e) Inhibition of miR-21 activity in HBx-expressed MIHA cells through second infection of lentivirus expressing miRZip-21 significantly increased the transcript level of PDCD4. (f) Both HBx-FL and HBx-Δ35 protein induced the expression of IL-6 in MIHA cells, while HBx-Δ35 induced a significantly higher IL-6 level compared with HBx-FL. Recombinant human IL-6 upregulated the expression of mature miR-21 in a (g) time-dependent and (h) dose-dependent manner in parental MIHA cells. (i) Precursor miR-21 and (j) primary miR-21 were upregulated with IL-6 treatment time-dependently. (k) Knockdown of IL-6 by siRNAs significantly inhibited the level of endogenous miR-21 in Hep3B cells. (Reproduced with permission from Elsevier)

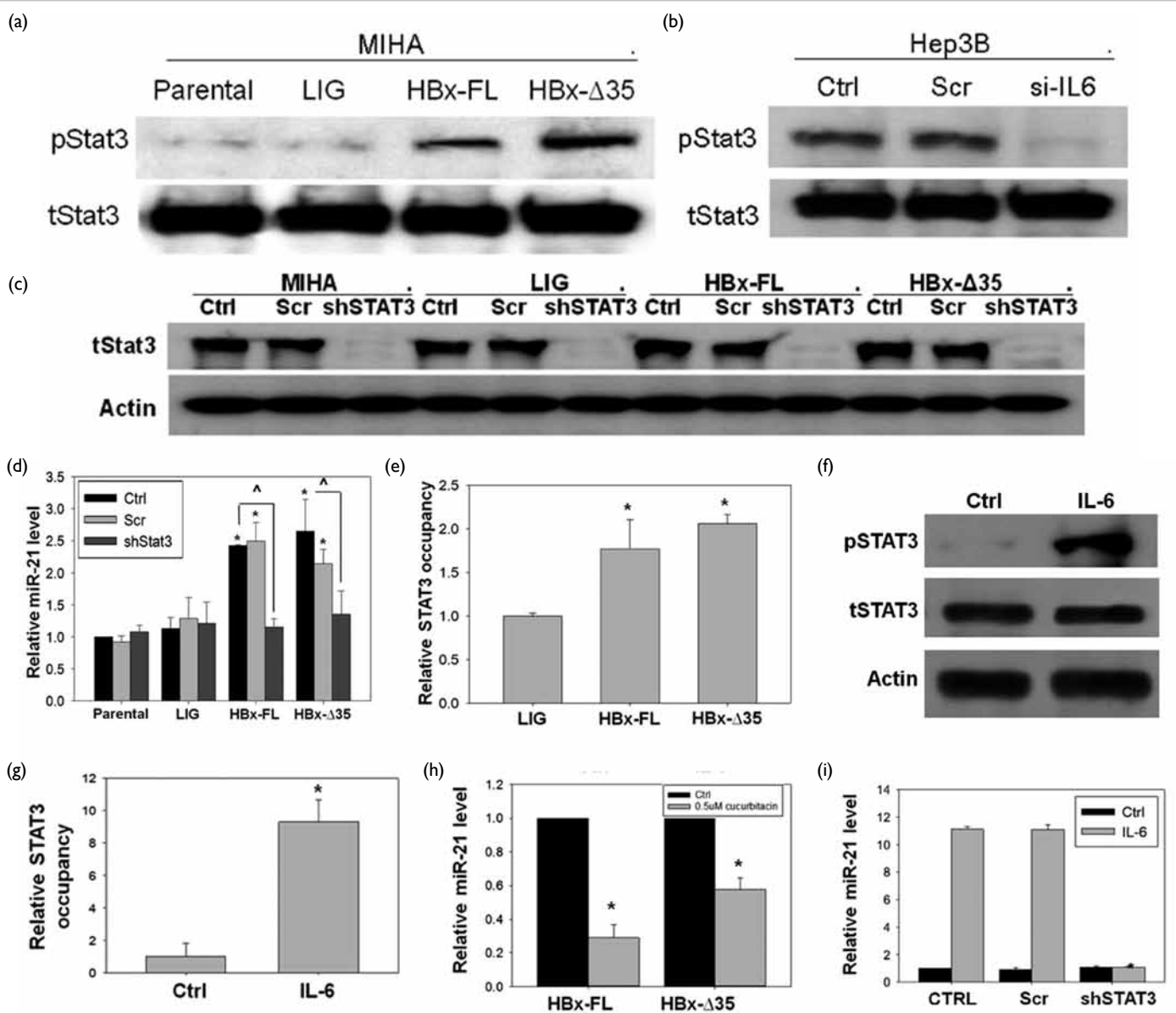


**FIG 2. Role of STAT3 in HBx-induced miR-21 expression:** (a) Phosphorylation of STAT3 was promoted in MIHA cells expressing HBx-FL and HBx-Δ35. (b) Knockdown of IL-6 by siRNAs inhibited the phosphorylation of STAT3 in Hep3B cells. (c) shRNAs targeting STAT3 were transduced in whole panel of MIHA cell lines, and the protein expression of STAT3 was knocked down. (d) While ectopic expression of HBx induced the expression of mature miR-21, simultaneous inhibition of STAT3 by shRNAs prohibited the expression of miR-21. (e) ChIP assay showed that about two-fold of miR-21 promoter was occupied by STAT3 in the presence of HBx-FL or HBx-Δ35 in MIHA cells. (f) STAT3 was activated by IL-6 in parental MIHA cells whereas total STAT3 expression was not influenced. (g) IL-6 treatment was able to induce an eight-fold increase in phosphorylated STAT3 occupancy at miR-21 promoter. (h) Upregulation of miR-21 by HBx-FL and HBx-Δ35 was attenuated when STAT3 was inhibited by STAT3 inhibitor cucurbitacin in MIHA cells. (i) The promotional effect on miR-21 level in MIHA cells by recombinant IL-6 treatment was lost when STAT3 was silenced by shRNAs. (Reproduced with permission from Elsevier)

expression (Fig 2d). This implied that the regulation of miR-21 by STAT3 in non-malignant hepatocytes was dependent on HBx, which proved that aberrant miR-21 expression was driven by HBx-IL-6-STAT3 signalling.

**Phosphorylation of STAT3 enhanced miR-21 promoter occupancy**

Chromatin immunoprecipitation (ChIP) analysis revealed a significant increase in STAT3 occupancy

in the miR-21 promoter upon ectopic expression of HBx-FL or HBx-Δ35 (Fig 2e). Western blotting analysis revealed an increase in STAT3 phosphorylation after treatment with recombinant IL-6 in MIHA cells (Fig 2f), and ChIP analysis showed that exposure of IL-6 to MIHA cells significantly enriched STAT3 proteins at the promoter of miR-21 gene (Fig 2g).

To further demonstrate the importance of STAT3 activity in the HBx-miR-21 pathway, a selective JAK/STAT3 signalling pathway inhibitor,

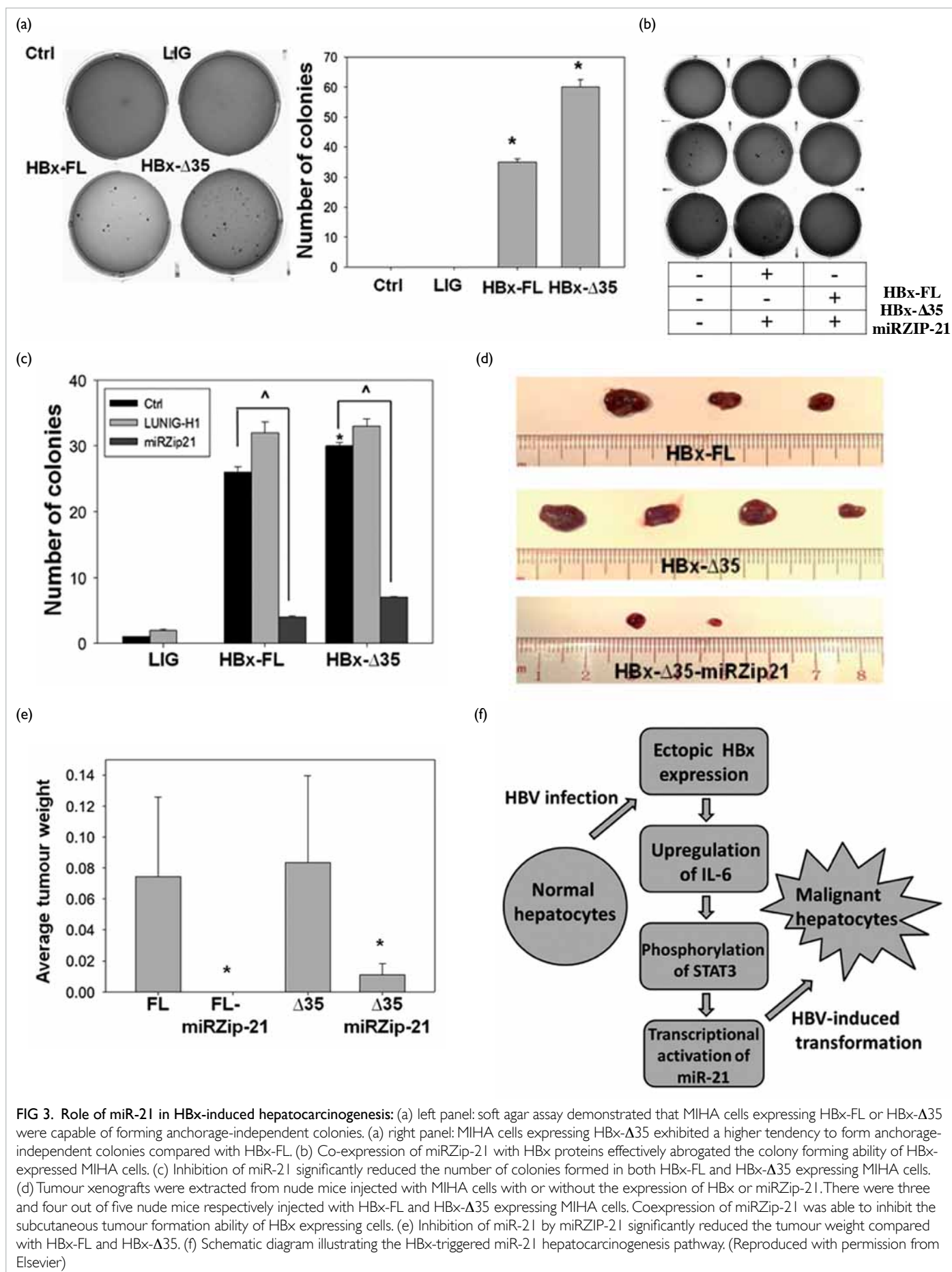


**FIG 3. Role of miR-21 in HBx-induced hepatocarcinogenesis:** (a) left panel: soft agar assay demonstrated that MIHA cells expressing HBx-FL or HBx-Δ35 were capable of forming anchorage-independent colonies. (a) right panel: MIHA cells expressing HBx-Δ35 exhibited a higher tendency to form anchorage-independent colonies compared with HBx-FL. (b) Co-expression of miRZip-21 with HBx proteins effectively abrogated the colony forming ability of HBx-expressed MIHA cells. (c) Inhibition of miR-21 significantly reduced the number of colonies formed in both HBx-FL and HBx-Δ35 expressing MIHA cells. (d) Tumour xenografts were extracted from nude mice injected with MIHA cells with or without the expression of HBx or miRZip-21. There were three and four out of five nude mice respectively injected with HBx-FL and HBx-Δ35 expressing MIHA cells. Coexpression of miRZip-21 was able to inhibit the subcutaneous tumour formation ability of HBx expressing cells. (e) Inhibition of miR-21 by miRZIP-21 significantly reduced the tumour weight compared with HBx-FL and HBx-Δ35. (f) Schematic diagram illustrating the HBx-triggered miR-21 hepatocarcinogenesis pathway. (Reproduced with permission from Elsevier)

cucurbitacin I, was applied to deactivate STAT3 in HBx-FL and HBx-Δ35 overexpressed MIHA cells. HBx-induced miR-21 expression in MIHA-HBx and MIHA-Δ35 was attenuated in the presence of the STAT3 inhibitor at 48 hours of treatment (Fig 2h). In addition, while exposure of recombinant IL-6 significantly increased the level of miR-21 in parental MIHA cells, such treatment failed to activate the expression of miR-21 when STAT3 was constitutively inhibited by shRNAs (Fig 2i). Taken together, STAT3 was the key transcriptional factor activated during HBx-induced transformation, which led to the active transcription of miR-21.

### Role of miR-21 in HBx-induced hepatocarcinogenesis

By soft agar assay, overexpression of both full length HBx and HBx-Δ35 was able to induce anchorage-independent colony formation of MIHA cells, whereas neither parental MIHA cells nor the lentiviral control MIHA-LIG cells could form colonies (Fig 3a). MIHA cells expressing HBx-Δ35 could generate twice as many colonies as those expressing full length (Fig 3a). HBx-Δ35 possessed a greater ability to transform non-tumour hepatocytes compared with its full length counterpart.

In order to characterise the role of miR-21 in HBx-induced cell proliferation, MIHA cells were co-infected with lentivirus carrying miRZip-21 transgene. Soft agar assay was conducted after infection of the panel of MIHA cells with lenti-CTRL or lenti-miRZip-21. The colony forming capability of HBx-FL and HBx-Δ35 expressing MIHA cells was inhibited by miRZip-21 (Figs 3b and 3c). Moreover, MIHA cells expressing HBx and HBx-Δ35 proteins were injected subcutaneously into nude mice (n=5). Cells expressing HBx-FL developed tumours in three out of five mice, whereas those expressing HBx-Δ35 developed tumours in four out of five mice (Fig 3d). More importantly, no tumours were found in mice injected with cells coexpressing HBx-FL and miRZip-21. Inhibition of miR-21 also effectively abrogated the effect of HBx-Δ35 to induce tumour formation, in which only two out of five mice developed tumours with obviously reduced tumour volume and weight (Figs 3d and 3e).

### Discussion

We aimed to identify HBx-induced miRNAs that have an important role during early HCC development. Overexpression of miR-21 occurred as soon as the hepatocytes were infected with HBV. Among various upstream pathways that regulate miR-21, the IL-6-STAT3 signalling pathway is closely related to cellular transformation and oncogenesis in HCC. High levels of IL-6 are found in patients with HBV infection and HBV-associated HCC.<sup>3</sup> HBx-induced miR-21 expression was highly dependent

on activation of the IL-6-STAT3 pathway, which demonstrated the specificity of miR-21 induction by HBx. Apart from overexpressing HBx in non-tumour hepatocytes, silencing IL-6 in HBx protein expressing HCC cell line Hep3B could result in a reduction in miR-21 level, which consolidated the interactions between HBx, IL-6-STAT3 and miR-21.

Our results from soft agar assay and xenograft assay suggest that HBx-induced miR-21 is pivotal in the transformation of non-tumour hepatocytes. More importantly, as inhibiting miR-21 with miRZIP-21 inhibited tumour xenograft growth, there is high therapeutic value to targeting miR-21 in HBV-associated HCC. Inhibition of miR-21 effectively prohibited MIHA cells from formation of both anchorage-independent colony and *in vivo* subcutaneous tumour, which suggests abrogation of the transformation of non-tumour hepatocytes.

Taken together, miR-21 was a critical downstream effector of HBx that drove the tumorigenesis of non-tumour hepatocytes. Ectopic HBx expression triggered the IL-6 pathway, promoted the phosphorylation and activation of transcriptional factor STAT3, and induced the expression of miR-21. Our *in vitro* and *in vivo* studies supported that miR-21 exhibited phenotypical change of the non-tumour cells during HBx-mediated hepatocarcinogenesis. Inhibiting miR-21 or attenuating its activation pathways (ie IL6-STAT3) could be promising when developing novel therapies for HBV-associated HCC. Given the important association between HBx and miR-21 in early HCC development, targeting miR-21 may also provide a novel means to prevent the development of HCC in HBV carriers.

### Acknowledgement

This study was supported by the Research Fund for the Control of Infectious Diseases, Food and Health Bureau, Hong Kong SAR Government (#11100452).

Results of this study have been published in Li CH, Xu F, Chow S, et al. Hepatitis B virus X protein promotes hepatocellular carcinoma transformation through interleukin-6 activation of microRNA-21 expression. *Eur J Cancer* 2014;50:2560-9.

### References

1. Kremsdorf D, Soussan P, Paterlini-Brechot P, Brechot C. Hepatitis B virus-related hepatocellular carcinoma: paradigms for viral-related human carcinogenesis. *Oncogene* 2006;25:3823-33.
2. Caselmann WH, Koshy R. Transactivators of HBV, signal transduction and tumorigenesis. In: Caselmann WH, Koshy R, editors. *Hepatitis B virus: molecular mechanisms in disease and novel strategies for therapy*. London: Imperial College Press; 1998:161-81.
3. Coskun U, Bukan N, Sancak B, et al. Serum hepatocyte growth factor and interleukin-6 levels can distinguish patients with primary or metastatic liver tumors from those with benign liver lesions. *Neoplasma* 2004;51:209-13.

# Gender disparity of hepatocellular carcinoma: role of hepatitis B virus X protein and androgen receptor

YT Chiu, IOL Ng \*

## KEY MESSAGES

1. The natural COOH-terminal truncated HBx was more frequently detected in hepatocellular carcinoma (HCC) in male than female patients.
2. There was no significant clinicopathological correlation with the HBx status or remarkable changes in androgen receptor (AR) expression in the presence of different truncated HBx mutants compared with full-length HBx.
3. Lower expression of AR was associated with

more aggressive tumour phenotype and a higher metastatic potential of HCC.

Hong Kong Med J 2016;22(Suppl 4):S43-7  
RFCID project number: 12111092

YT Chiu, IOL Ng

Department of Pathology, The University of Hong Kong

\* Principal applicant and corresponding author: iolng@hku.hk

## Introduction

Hepatocellular carcinoma (HCC) is especially prevalent in Hong Kong due to prevalent hepatitis B virus (HBV) infection. HBV-associated HCC has a male predominance, with a male-to-female ratio of about 4-5:1. This is in contrast to HCV-associated HCC that has a male-to-female ratio of 1.5-2:1. HBV is a partially double-stranded DNA virus containing four overlapping open reading frames. Among them, the X gene is most frequently integrated into the host genome naturally. Naturally integrated X gene is frequently found to be deleted at the 3'-end, leading to COOH-terminal truncated HBx protein.

In our previous study, we showed that in HBV-positive patients with HCC, full-length HBx (HBxFL) was detected in all non-tumourous livers (n=51). However, HBxFL (HBx 1-154 amino acids) was found in only 53% of the tumours, whereas natural COOH-truncated HBx (HBx 1-130 amino acids) was found in the remaining 47%. The presence of natural COOH-truncated HBx significantly correlated with the presence of venous invasion ( $P < 0.01$ ), a hallmark of metastasis, suggesting COOH-truncation of HBx plays a significant role in enhancing cell invasiveness and metastasis in HCC.<sup>1</sup> In addition, HBx mutants with different COOH-truncated length cause HCC by altering intracellular distribution and consecutive modulation of the important proliferative STAT/SOCS signalling, indicating a role of various shorter HBx mutants in tumorigenesis.<sup>2</sup> The mislocalisation of HBx truncated mutants can be explained in part by the finding that HBx protein contains a functional nuclear export sequence from amino acids 89 to 100.<sup>3</sup> Therefore, the COOH-terminal truncated form of HBx has been demonstrated to play a tumorigenic role in HCC and its oncogenicity may vary according to the truncated length.

Among male HBV carriers, the risk of HCC development is significantly increased in those with higher androgen receptor (AR) activity. HBV infection may, therefore, particularly cooperate with male-specific AR signalling to accelerate hepatocarcinogenesis. Moreover, HBx has been shown to enhance AR transcriptional activity through GSK-3 $\beta$  kinase pathways.<sup>4</sup> However, no report has shown a correlation between AR signalling and COOH-terminal truncated HBx protein.

In this study, we hypothesised that HBx cooperated with male-specific AR signalling to enhance hepatocarcinogenesis, and natural HBx truncated mutants had different effects on this AR signalling. The prevalence of natural COOH-terminal truncated HBx mutants (HBx  $\Delta$ C1 and HBx  $<$  $\Delta$ C1) was slightly higher in male than female with HCC, but no significant clinicopathological association was observed with the expression of COOH-terminal truncated HBx mutants in HCCs. The COOH-terminal truncated HBx mutants were not associated with the mRNA expression of AR in the same HCC specimens, but the mRNA expression of AR showed a significant correlation with the metastatic potential, cellular differentiation and staging of HCC.

## Methods

This study was conducted from April 2013 to April 2014.

### Patient samples

A total of 99 pairs of human HCCs from patients who underwent liver resection for HCC between 1992 and 2001 at Queen Mary Hospital, Hong Kong, were selected. All these 99 patients (77 men and 22 women) aged 19 to 74 years were positive for serum hepatitis B surface antigen (HBsAg). All specimens

were snap-frozen in liquid nitrogen and kept at -80°C. Frozen sections were cut from HCC blocks separately and stained for histological examination to ensure a homogenous cell population of tissues.

**RNA extraction and reverse-transcriptase polymerase chain reaction**

Total RNA was isolated using TRIZOL reagent (Invitrogen, Carlsbad [CA], USA) following the manufacturer’s instructions. cDNA was synthesised by using Gold RNA PCR Core Kit (Applied Biosystems, Foster City [CA], USA) following the manufacturer’s instructions.

**Semi-quantitative PCR**

For semi-quantitative PCR, the reaction was set up using AmpliTaqGOLD enzyme (Applied Biosystems, Carlsbad [CA], USA) and carried out with Takara PCR Thermal Cycler. PCR products were detected by 1.5% ethidium bromide-agarose gel electrophoresis at 100V for 15 minutes and visualised on a gel documentation system. The primers for PCR were as follows: HBx ATG: 5’-CCC AAG CTT ATG GCT GCT AGG CTG TGC T-3’; HBx full length (HBxFL): 5’-CGA ATT CTT AGG CAG AGG TGA AAA AGT TG-’; HBx ΔC1: 5’-CGA ATT CTT ACT TTA ATC TAA TCT CCT CCC C-3’; HBx <ΔC1: 5’-CTT ATG TAA GAC CTT GGG CAA CAT-3’

**Quantitative real-time PCR**

The reaction was set up using SYBR Green Real-Time PCR Master Mixes (Applied Biosystems) and was carried out with Applied Biosystems 7900 HT Fast Real-Time PCR System (Applied Biosystems) according to the manufacturer’s protocol. All reactions were performed in triplicate and the expression of targeted gene relative to hypoxanthine guanine phosphoribosyl transferase was determined using 2<sup>-ΔCT</sup> method. The primer sequences for real-time PCR were as follows: AR F: 5’-CTC ACC AAG CTC CTG GAC TC-3’; AR R: 5’-GAA AGG ATC TTG GGC ACT TG-3’; HPRT F:5’-CTTTGCTGACCTGCTGGATT-3’; HPRT R:5’-CTGCATTGTTTTGCCAGTGT -3’.

**Results**

**The prevalence of natural COOH-terminal truncated HBx mutants (HBx ΔC1 and HBx <ΔC1) was slightly higher in HCCs from male than female patients**

The HCCs were screened for the presence of COOH-terminal truncated HBx mutants, ΔC1 (HBx 1-130 amino acids) and <ΔC1 (HBx 1-95 amino acids). The expression pattern of the truncated HBx mutants between male and female patients was compared. Among the 99 HCC samples, the natural COOH-terminal truncated HBx mutants (HBx ΔC1

and HBx <ΔC1) were more frequently detected in HCCs in males than females (44% vs 37%, Fig 2). The frequency of HBx ΔC1 in HCCs in males was similar to that in females (30% vs 32%), but a more remarkable difference was observed for HBx <ΔC1 mutants (14% vs 5%, Fig 1). These indicated that the COOH-terminal truncated HBx mutants that are shorter than ΔC1 may be found more frequently in male HCCs and may be more associated than HBx ΔC1 with the male predominance in HCC.

**The expression of COOH-terminal truncated HBx mutants in human HCCs showed no significant clinicopathological or survival correlation**

To examine whether the presence of natural COOH-terminal truncated HBx mutants was associated with a particular tumour biological behaviour and consequent prognosis, the expression of full-length HBx and truncated HBx mutants was correlated with different clinicopathological features and survival rates in the 99 HCC patients. The presence of COOH-terminal truncated HBx mutants (ie the group with either HBx ΔC1 or HBx<ΔC1) did not show any significant correlation with the clinicopathological features (Fig 2a). In addition, there was no significant

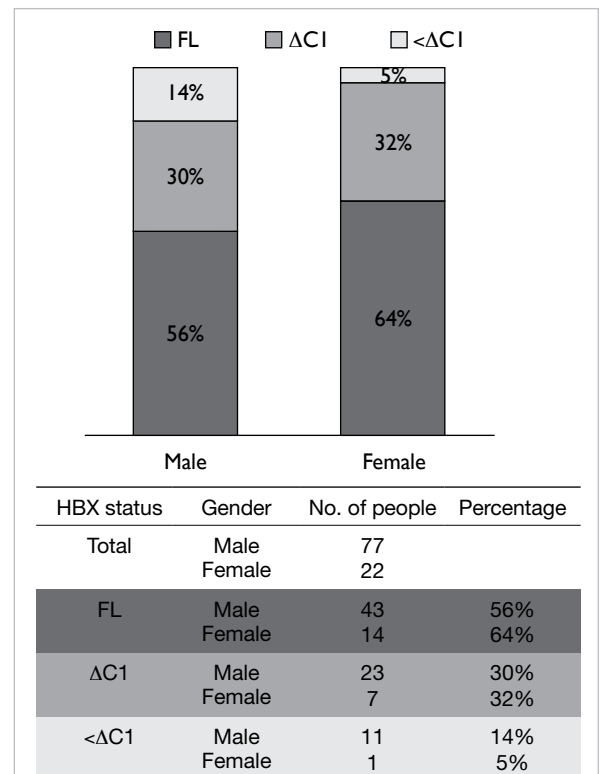
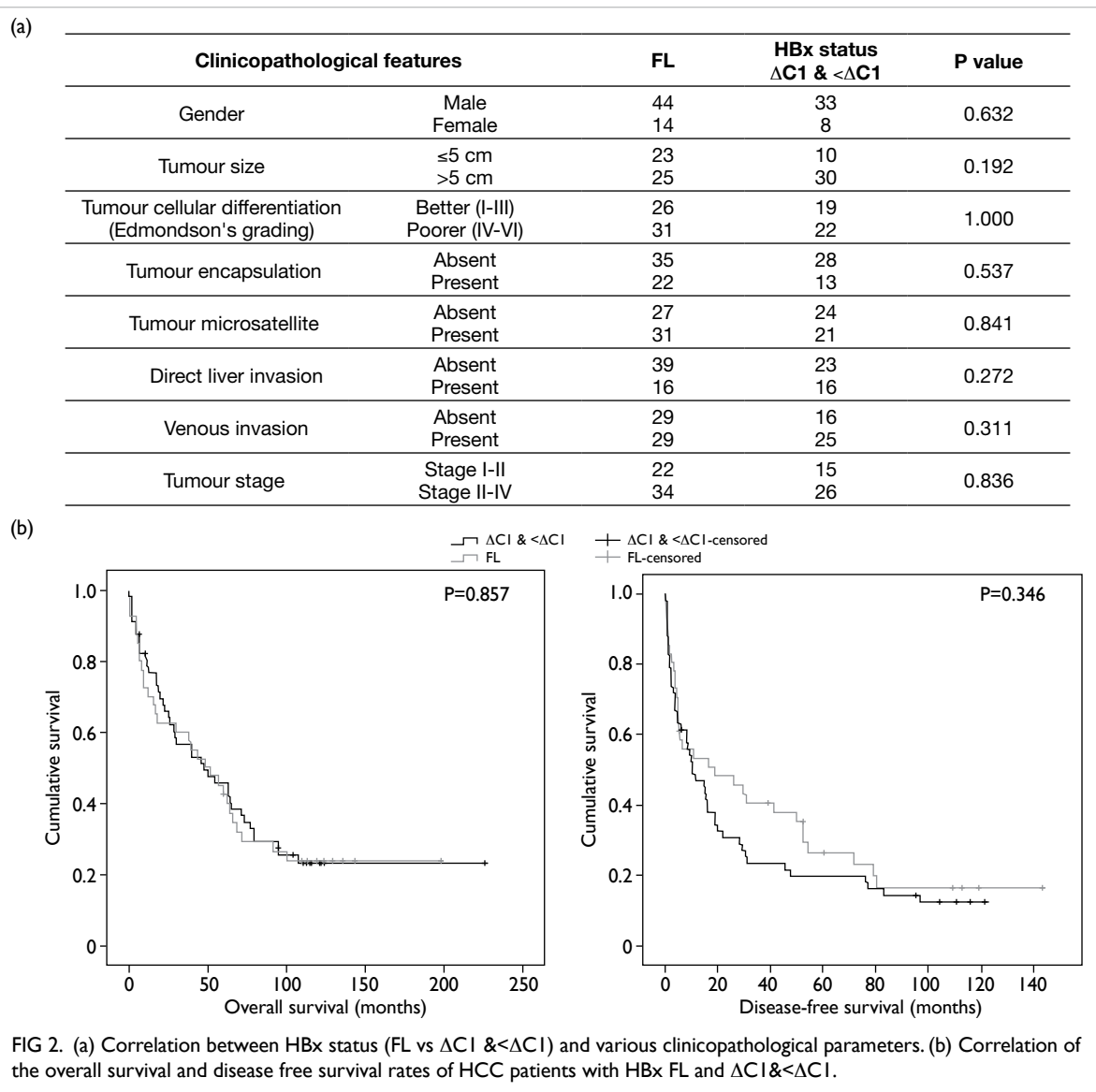


FIG 1. The frequency of presence of HBx FL and COOH-terminal truncated HBxΔC1 and Δ<C1 in male and female HBV-associated HCCs (n=99). Presence of HBx FL and COOH-terminal truncated HBx mutants was detected by conventional PCR. The frequency of COOH-truncated mutants was higher in male than female HCC patients.



difference between the presence of HBx mutants and the disease free or overall survival (Fig 2b). This demonstrated that the presence of COOH-terminal truncated HBx mutants might not be associated with tumour biological behaviour.

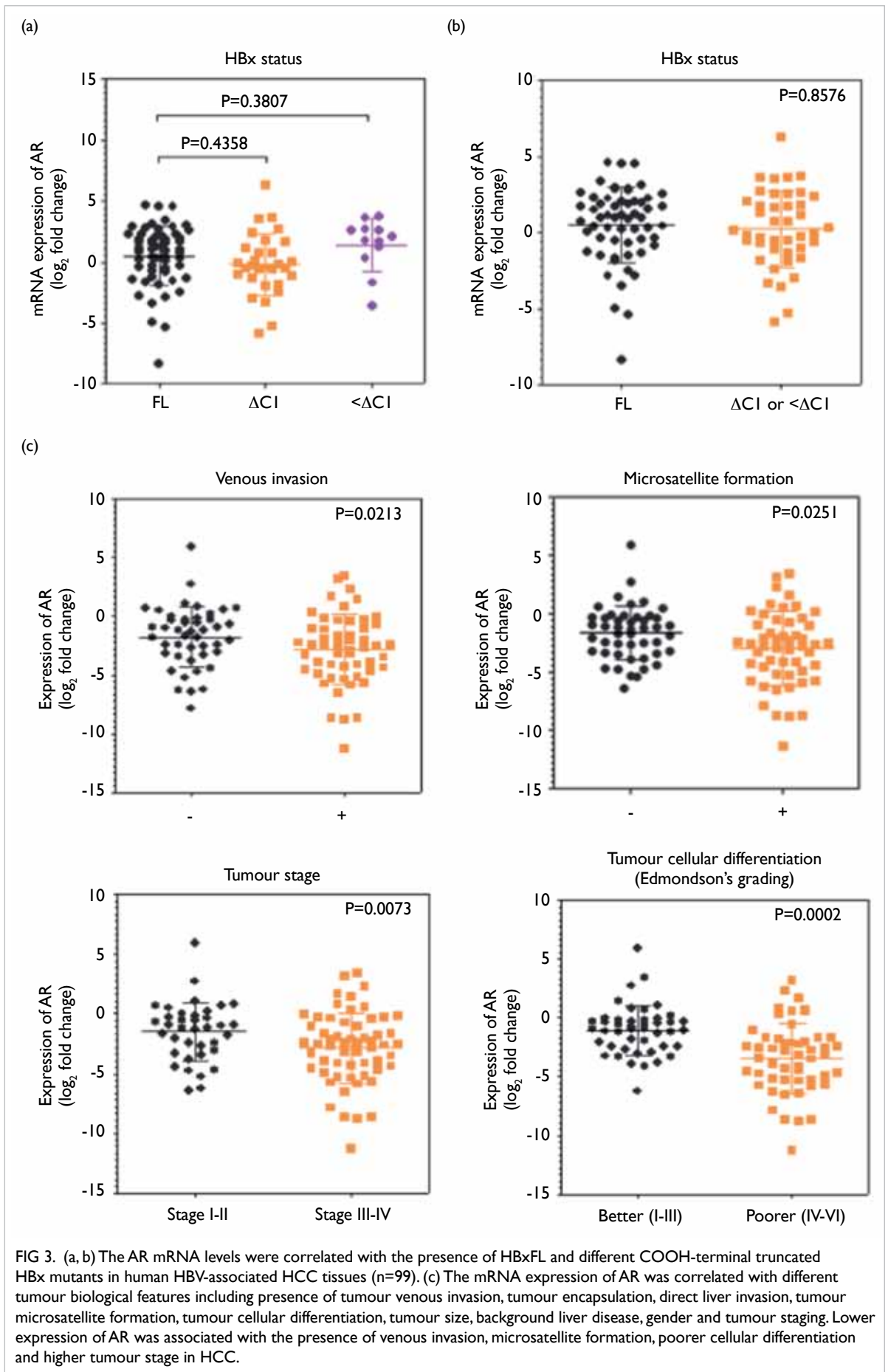
**The COOH-terminal truncated HBx mutants had no significant correlation with the mRNA expression of AR in the same HCC specimens**

To investigate the effect of different COOH-terminal truncated HBx mutants on the mRNA expression level of AR, the expression level of AR was examined and correlated with the presence of COOH-terminal truncated HBx mutants in the 99 HCCs. There was no significant difference between the mRNA levels of AR and the presence of COOH-terminal truncated HBx mutants or the full-length HBx (Fig 3a). Although there was a trend of association between the presence of HBx $\Delta C1$  and downregulation of AR (P=0.4358), the mRNA levels of AR were not

significantly different upon further stratification of the HBx mutants into HBx $\Delta C1$  and HBx $<\Delta C1$  (Fig 3b). These indicated that the COOH-terminal truncated HBx mutants, either HBx  $\Delta C1$  or HBx $<\Delta C1$ , may not regulate mRNA expression of AR.

**The mRNA expression of AR showed a significant correlation with the metastatic potential, cellular differentiation and staging of HCC**

To evaluate the association of the mRNA expression of AR with a particular tumour biological behaviour and prognostic significance in HCC, the mRNA levels of AR correlated with different clinicopathological features. Lower expression of AR in the HCC was associated with the presence of tumour venous invasion (P=0.0213), tumour microsatellite formation (P=0.0251), poorer tumour cellular differentiation (P=0.0002) and higher tumour stage (P=0.0073) [Fig 3c]. This correlation



study demonstrated that lower expression of AR was associated with a higher metastatic potential and more aggressive tumour phenotype in HCC.

## Discussion

The frequency of natural COOH-terminal truncated HBx (HBx  $\Delta$ C1 and HBx< $\Delta$ C1) was higher in HCCs of male than female patients (44% vs 37%). More importantly, when the mutants were stratified into the group with HBx< $\Delta$ C1 only and the other one with HBx FL or HBx  $\Delta$ C1, the frequency of HBx mutants in male and female HCCs (14% vs 5%) was even more obvious. With a higher frequency of HBx< $\Delta$ C1 in HCCs of males and the differential regulatory roles of shorter truncated HBx mutants in HCC due to nuclear mislocalisation,<sup>2</sup> these imply that HBx<C1 may play a role in hepatocarcinogenesis in male HCC patients and may contribute in part to the male predominance of HCC. Nonetheless, the underlying mechanisms require further investigation. In addition, the expression status of HBx in the HCCs showed no significant correlation with any clinicopathological features or patient survival. This might have been a result of technical limitations in examining HBx gene truncation, where the co-existence of HBx FL and COOH-terminal truncated mutants in the same specimen cannot be detected by conventional PCR. The HCC tumours with HBx FL detected might also harbour HBx $\Delta$ C1 and/or HBx< $\Delta$ C1, and this may influence the comparison among groups of various parameters.

Full-length HBx protein has been shown to enhance AR transcriptional activity through modulation of c-Src and GSK-3 $\beta$  kinase pathways.<sup>5</sup> In addition, HBx protein enhances AR-responsive gene expression depending on androgen level.<sup>6</sup> Therefore, the regulatory roles of full-length HBx on AR activity are well demonstrated. In the present study, we examined the consequence of COOH-terminal truncated HBx on AR transactivation. The results showed no significant correlation between the presence of X truncation and mRNA expression of AR in HCCs when compared with the full-length HBx, suggesting that COOH-truncated HBx mutants may not exert a more potent activation on AR than the full-length HBx. Nevertheless, a lower expression of AR was associated with more aggressive tumour behaviour. This finding was consistent with that in other studies that report hepatic AR suppression of HCC metastasis through modulation of cell migration and anoikis,<sup>7</sup> enhanced cell adhesion and decreased cell migration via modulating  $\beta$ 1-integrin-AKT signalling in HCC cells.<sup>8</sup> In contrast to our results, several reports found that the activation and overexpression of AR promoted cell invasion and migration in HCC and tumour staging.<sup>9</sup> Therefore, the potential roles of AR in hepatocarcinogenesis remain elusive and warrant further investigation.

## Conclusion

The HBx truncated mutants are more frequent in HCCs of males than females, and this may implicate a role of HBx truncated mutants in the male predominance of HCC. Nonetheless, the correlation study of the presence of HBxC1 or HBx< $\Delta$ C1 and the different clinicopathological features of HCC patients and the mRNA levels of AR implied that HBx truncated mutants alone may not exert a significant effect on the tumour biological behaviour or induce a more potent transactivation of AR than HBxFL. AR may play a role in hepatocarcinogenesis, in which lower expression of AR is associated with more aggressive tumour phenotype and a higher metastatic potential of HCC.

## Acknowledgement

This study was supported by the Research Fund for the Control of Infectious Diseases, Food and Health Bureau, Hong Kong SAR Government (#12111092).

## References

1. Sze KM, Chu GK, Lee JM, Ng IO. C-terminal truncated hepatitis B virus x protein is associated with metastasis and enhances invasiveness by C-Jun/matrix metalloproteinase protein 10 activation in hepatocellular carcinoma. *Hepatology* 2013;57:131-9.
2. Bock CT, Toan NL, Koeberlein B, et al. Subcellular mislocalization of mutant hepatitis B X proteins contributes to modulation of STAT/SOCS signaling in hepatocellular carcinoma. *Intervirology* 2008;51:432-43.
3. Forgues M, Marrogi AJ, Spillare EA, et al. Interaction of the hepatitis B virus X protein with the Crm1-dependent nuclear export pathway. *J Biol Chem* 2001;276:22797-803.
4. Yang WJ, Chang CJ, Yeh SH, et al. Hepatitis B virus X protein enhances the transcriptional activity of the androgen receptor through c-Src and glycogen synthase kinase-3 $\beta$  kinase pathways. *Hepatology* 2009;49:1515-24.
5. Wu MH, Ma WL, Hsu CL, et al. Androgen receptor promotes hepatitis B virus-induced hepatocarcinogenesis through modulation of hepatitis B virus RNA transcription. *Sci Transl Med* 2010;2:32ra35.
6. Chiu CM, Yeh SH, Chen PJ, et al. Hepatitis B virus X protein enhances androgen receptor-responsive gene expression depending on androgen level. *Proc Natl Acad Sci U S A* 2007;104:2571-8.
7. Ma WL, Hsu CL, Yeh CC, et al. Hepatic androgen receptor suppresses hepatocellular carcinoma metastasis through modulation of cell migration and anoikis. *Hepatology* 2012;56:176-85.
8. Ma WL, Jeng LB, Lai HC, Liao PY, Chang C. Androgen receptor enhances cell adhesion and decreases cell migration via modulating  $\beta$ 1-integrin-AKT signaling in hepatocellular carcinoma cells. *Cancer Lett* 2014;351:64-71.
9. Zhang Y, Shen Y, Cao B, Yan A, Ji H. Elevated expression levels of androgen receptors and matrix metalloproteinase-2 and -9 in 30 cases of hepatocellular carcinoma compared with adjacent tissues as predictors of cancer invasion and staging. *Exp Ther Med* 2015;9:905-8.

## AUTHOR INDEX

|            |        |            |    |
|------------|--------|------------|----|
| Bruzzone R | 10, 25 | Leung CH   | 32 |
| Chan M     | 7      | Leung HL   | 25 |
| Chang RCC  | 16     | Li CH      | 37 |
| Chen YC    | 37     | Li D       | 25 |
| Cheng YC   | 32     | Li PH      | 25 |
| Cheung CY  | 25     | Ma EDL     | 32 |
| Chiu K     | 16     | Ma HL      | 10 |
| Chiu P     | 32     | Nal B      | 10 |
| Chiu YT    | 43     | Ng IOL     | 43 |
| Chow SC    | 37     | Ng TB      | 37 |
| Daëron M   | 25     | Nicholls J | 7  |
| Dutry I    | 25     | Peiris JSM | 25 |
| Guan Y     | 4      | Poon DCH   | 16 |
| Ho YS      | 16     | Poon LLM   | 10 |
| Huang JD   | 13     | Smith GJD  | 4  |
| Jaume M    | 25     | Woo PCY    | 22 |
| Jin DY     | 22     | Yin DL     | 37 |
| Kien F     | 10     | Yip MS     | 25 |
| Kwong D    | 7      | Yuen KY    | 13 |
| Lau CF     | 16     | Zheng BJ   | 13 |

### Disclaimer

The reports contained in this publication are for reference only and should not be regarded as a substitute for professional advice. The Government shall not be liable for any loss or damage, howsoever caused, arising from any information contained in these reports. The Government shall not be liable for any inaccuracies, incompleteness, omissions, mistakes or errors in these reports, or for any loss or damage arising from information presented herein. The opinions, findings, conclusions and recommendations expressed in this report are those of the authors of these reports, and do not necessarily reflect the views of the Government. Nothing herein shall affect the copyright and other intellectual property rights in the information and material contained in these reports. All intellectual property rights and any other rights, if any, in relation to the contents of these reports are hereby reserved. The material herein may be reproduced for personal use but may not be reproduced or distributed for commercial purposes or any other exploitation without the prior written consent of the Government. Nothing contained in these reports shall constitute any of the authors of these reports an employer, employee, servant, agent or partner of the Government.

Published by the Hong Kong Academy of Medicine Press for the Government of the Hong Kong Special Administrative Region. The opinions expressed in the *Hong Kong Medical Journal* and its supplements are those of the authors and do not reflect the official policies of the Hong Kong Academy of Medicine, the Hong Kong Medical Association, the institutions to which the authors are affiliated, or those of the publisher.